INVESTIGATION OF PATHOPHYSIOLOGY AND THERAPEUTIC STRATEGIES IN PMM2-CDG MODEL ZEBRAFISH

by

ABIGAIL ELIZABETH CLINE

(Under the Direction of Richard Steet)

ABSTRACT

Congenital Disorder of Glycosylation PMM2-CDG results from mutations in PMM2, which encodes the phosphomannomutase that converts mannose-6-P to mannose-1-P. Patients have wide-spectrum clinical abnormalities associated with impaired protein N-glycosylation. Though widely proposed that PMM2 deficiency depletes mannose-1-P, a precursor of GDP-mannose, and consequently suppresses lipid-linked oligosaccharide (LLO) levels needed for N-glycosylation, these deficiencies have not been demonstrated in patients or any animal model. In order to explore the developmental and biochemical consequences of PMM2 deficiency, we generated and characterized a morpholino-based PMM2-CDG model in zebrafish. Morphant embryos had developmental abnormalities consistent with PMM2-CDG patients, including craniofacial defects and impaired motility associated with altered motor neurogenesis within the spinal cord. Significantly, global N-linked glycosylation and LLO levels were reduced in *pmm2* morphants. Although insufficient to reduce mannose-1-P and GDP-mannose levels, Pmm2 depletion unexpectedly caused accumulation of mannose-6-P, shown earlier to promote LLO cleavage *in vitro*. In *pmm2* morphants, the free glycan by-products of LLO cleavage

increased nearly two-fold. Suppression of the mannose-6-P synthesizing enzyme, mannose phosphate isomerase, within the *pmm2* background normalized mannose-6-P levels and certain aspects of the craniofacial phenotype, and abrogated *pmm2*-dependent LLO cleavage. Overexpression of *pmm1* mRNA, a homologous enzyme to PMM2, within the *pmm2* background not only increased phosphomannomutase activity, but also corrected abnormal phenotypes and deficient glycosylation profiles noted in *pmm2* morphants. In summary, we employed the first zebrafish model of PMM2-CDG to uncover novel cellular insights not possible with other systems, including a mannose-6-P accumulation mechanism for under-glycosylation.

INDEX WORDS: N-linked glycosylation, lipid-linked oligosaccharide, free oligosaccharide, mannose-6-phosphate, zebrafish, Congenital Disorders of Glycosylation, phosphomannomutase 2, phosphomannomutase1, mannophosphoisomerase, Fluorophore Assisted Carbohydrate Electrophoresis

INVESTIGATION OF PATHOPHYSIOLOGY AND THERAPEUTIC STRATEGIES IN PMM2-CDG MODEL ZEBRAFISH

by

ABIGAIL ELIZABETH CLINE

B.A., Wake Forest University, 2008

A Dissertation Submitted to the Graduate Faculty of The University of Georgia in Partial Fulfillment of the Requirements for the Degree

DOCTOR OF PHILOSOPHY

ATHENS, GEORGIA

2012

© 2012

Abigail Cline

All Rights Reserved

INVESTIGATION OF PATHOPHYSIOLOGY AND THERAPEUTIC STRATEGIES IN PMM2-CDG MODEL ZEBRAFISH

by

ABIGAIL ELIZABETH CLINE

Major Professor:	Richard Steet
Committee:	Michael Tiemeyer Michael Pierce Jim Lauderdale

Electronic Version Approved:

Maureen Grasso
Dean of the Graduate School
The University of Georgia
December 2012

DEDICATION

First, I would like to dedicate this thesis as well as my entire graduate studies to everyone who has helped me along the way. To all of my peers, my friends, and my family who have been patient with me through my struggles, my doubts, and my decisions. There were many times I felt like giving up on my goals, on science, and on myself. I could not have gotten this far without the safety net that they have provided for me.

Secondly, I would like to dedicate this present body of work to those who find themselves walking a long, hard road to their goals. Though others may take an easier route, it is the uphill journey that will shape you. If I had known at the beginning how much I have struggled, hurt, and endured to be here, I don't know if I ever would have started. If I think of how far I've come and how far I still have to go, I may not finish. Instead, I take comfort in the differences I have made, the service I have given, and the people I have helped. It's not supposed to be easy, and that's why it feels so good.

ACKNOWLEDGEMENTS

First I would like to thank this wonderful department for admitting a confused Latin graduate who thought science sounded fun. Sometimes I thought I was let into this program by accident, that somehow my application got switched during the interviews, so I struggled and worked in this department to show them that they didn't make a mistake. I hope I have given back to this department at least a fraction of what it has given me. The support from the faculty, the graduate coordinators, and my fellow graduate students has helped me during my time here and I would not have finished if it had not been for all of you.

Secondly, I would like to thank my wonderful lab. I knew during my rotation that this lab was where I could see myself for the next 5 years and that these people are those I could proudly work beside. To Jarrod, thank you for being like a big brother and watching out for me even when I didn't want you to. You truly demonstrate what a real scientist is and your love of science is contagious. To Aaron, thank you for being such an understanding friend. To Megan, I wish you luck and fortune in your future research! To Jennifer, thank you so much for raising the fish and managing the fish dungeon. I hope I can keep it up to the very high standards that you've set. Thank you to La Fiesta for their delicious margaritas, their endless basket of chips, and their one crazy waitress. I really am grateful for the lab environment that we have and I hope that we will always be known as the best lab on the third floor.

To Rich and Heather, thank you so much for letting me join this lab. Again, I'm not completely sure why you decided to take a chance on a Latin major, but I hope it was an investment that came back in full. I have learned so much from both of you in terms of science

and life that I know you have made a permanent mark. I still would not choose another lab if I had to do this all over again. Thank you for tolerating my eccentricities, my migraines, and my various hair colors.

To Mark Lehrman and Ningguo Gao, thank you so much for running the FACE analysis! Every email from you was like Christmas. I couldn't wait to see what the results were after I mailed you my samples.

Finally, to my family and friends who have helped me through the difficult times and the easy ones as well. To my family for supporting me through graduate school, even when you didn't know what I was working on. To my mom and dad, thank you for your help even though all you knew was that it involved fish and science. Also, thank you in advance for supporting me through medical school. I will try to make it up to you when you retire. To my friends, both here in Athens and those out of state. We've helped each other along this road for so long already that we shouldn't stop now. Even if I'm in a different city in a year, I will always be there for you whenever you need me.

TABLE OF CONTENTS

Page

LIST OF TABLES

Page

LIST OF FIGURES

Page

CHAPTER 1: LITERATURE REVIEW AND INTRODUCTION

N-linked Glycosylation- Biosynthesis and Biological Function

Overview of Glycosylation

Protein glycosylation represents a form of post-translational modification that has been identified throughout the entire phylogenetic spectrum, ranging from archaea and eubacteria to eukaryotes. The prevalence of these modifications throughout evolution suggests that protein-linked oligosaccharides play essential biological roles.[1] Glycosylation is one of the most widespread and complex forms of protein modifications. It is believed that more than half of all eukaryotic proteins are glycosylated and that an estimated 1% of all mammalian genes are involved in glycosylation.[2-4] Sugar moieties directly affect chemical properties of proteins by affecting their stability, solubility, and polarity. Furthermore, sugar modifications are necessary for a vast array of biological processes including protein quality control, directed transport, and biological activity. As such, oligosaccharyl modifications play important roles in biological processes such as growth, differentiation, organ development, and signal transduction. The defining characteristic of peptide-linked oligosaccharides is the formation of the sugar-amino acid bond. This bond determines the nature of the carbohydrate chain that influences the protein's biological activity. Protein-linked oligosaccharides compromise two major classes: O-linked glycosylation and N-linked glycosylation. This thesis will focus on N-glycosylation,

which is a β-glycosylamine linkage of GlcNAc to Asn. This linkage is the most widely distributed carbohydrate-peptide bond and facilitates the attachment of various complex and high mannose oligosaccharides on proteins that have confirmed biological importance. [5-7]

Overview of N-Linked Glycosylation Pathway and Nucleotide Sugar Synthesis

N-linked glycosylation is an essential co-translational process that begins in the Endoplasmic Reticulum (ER) and involves the transfer of a preassembled glycan onto polypeptides that contain the protein sequence Asn-X-Ser/Thr.[8] The synthesis of the N-glycan occurs on the cytoplasmic face of the ER, while the transfer of the N-glycan occurs on the lumenal side of the ER (**Figure 1.1**). Sequential addition of monosaccharide sugars from sugar donors present on both the cytoplasmic and lumenal side of the ER form the N-glycan precursor, $Glc_3Man_9GlcNAc_2$-PP-Dol. Before they can be incorporated into the growing oligosaccharide chain, sugar precursors must be generated. For example, mannose, which is either derived from diet or conversion of glucose, must be modified to form mannose-6-phosphate (Man-6-P) to serve as a precursor to GDP-Man. Generation of Man-6-P occurs either by a hexokinase directly phosphorylating mannose entering the cell or by mannophosphoisomerase (MPI) converting fructose-6-phosphate to Man-6-P. Next, phosphomannomutase 2 (PMM2) isomerizes Man-6-P to Man-1-P, which serves as the precursor to GDP-Man (**Figure 1.2**). GDP-Man is the mannosyl donor to the growing oligosaccharide chain on the cytoplasmic face of the ER, while dolichol-P-mannose (DPM) is the mannosyl donor in the ER lumen. Generation of DPM occurs from GDP-Man and dolichol-P (Dol-P) on the cytoplasmic face of the ER before it is flipped into the ER lumen.[9] On both the cytoplasmic and lumenal side of the ER, nucleotide sugars are essential donors to the growing oligosaccharide.

Assembly of the Lipid-Linked Oligosaccharide

The transfer of GlcNAc-P from UDP-GlcNAc to the lipid linked precursor Dol-P initiates N-glycan formation. As shown in **Figure 1.1**, a second GlcNAc and five mannose residues subsequently transfer in a stepwise manner from UDP-GlcNAc and GDP-Man, respectively, to generate $Man_5GlcNAc_2$-P-P-Dol on the cytoplasmic side of the ER. Prior to its addition to a polypeptide, this oligosaccharide translocates across the ER membrane bilayer so that the glycan faces the lumen of the ER. Proteins termed "flippases" are predicted to catalyze this process. Although flippases continue to remain elusive, yeast *RFT1* has been implicated in the process of translocation. [10] Once inside the ER lumen, biosynthesis of the oligosaccharide continues with the transfer of monosaccharide sugars from nucleotide sugar donors. Dol-P-Man donors transfer four mannose residues to further extend the glycan to Man_9-$GlcNAc_2$-P-P-Dol. Finally, three glucose residues from Dol-P-Glucose donors complete the processing to generate Glc_3Man_9-$GlcNAc_2$-PP-Dol. This fourteen sugar lipid linked oligosaccharide (LLO) is now ready for transfer to an asparagine of the accepting proteins by the oligosaccharyltransferase (OST).[9] In the lumen of the ER, the OST transfers the LLO from the dolichol pyrophosphate donor to selected asparagine side chains located by a Asn-X-Sher/Thr consensus within the polypeptide sequence.[11] The OST has been shown to primarily transfer full length LLO as it has no affinity for truncated oligosaccharides.[12, 13] Upon transfer of the LLO by the OST, Dol-P-P is released and recycled back to Dol-P for reuse in future rounds of glycosylation. [14]

Glycan processing in the Endoplasmic Reticulum

After attachment to a nascent polypeptide, ER glucosidases and mannosidases sequentially process the N-glycan to generate high-mannose intermediates which function in protein folding, quality control, and degradation. Glycosylation contributes to the folding process via interactions with ER chaperones that recognize specific features of the glycan.[15, 16] As the protein folds, the three glucose residues are removed from the glycan to signal that the glycoprotein is available for export from the ER to the Golgi complex.[9] Due to the fact that all glycoproteins are initially modified uniformly, processing of glycans in the ER results in limited diversity. However, once they reach the *medial* Golgi, glycoproteins undergo a wide array of distinct modifications that introduce structural differences in the glycans. The uniformity of early glycan structure coincides with its role in protein folding, quality control, sorting, and transport. These are the preliminary roles that N-glycans have in the early secretory pathway.[15] If there is early inhibition of glycosylation, the most common effect is the aggregation of misfolded proteins that failed to reach a functional state.[7, 16, 17]

Cellular Responses to Misfolded Proteins

Oligosaccharides have a direct effect on the protein folding process.[18] Previous studies have shown N-linked glycans promote more compact protein structures by altering conformational preferences close to the glycosylation site.[15] Similarly, disruptions in glycosylation through tunicamycin treatment result in improper folding of proteins and activation of ER stress. Since glucosylated N-glycans signal the quality control of protein folding, N-glycosylation is critical for the proper folding of glycoproteins.[15] The inability of a protein to fold properly results in ER-Associated Protein Degradation (ERAD).[7, 9, 19] This degradation pathway is shared by misfolded and mutant proteins as it serves to ensure quality control of

newly synthesized glycoproteins.[19, 20] ERAD identifies glycoproteins that fail to fold properly after several cycles of binding to calnexin and calreticulin.[20, 21] Misfolded proteins are retro-translocated into the cytoplasm, where they are tagged by ubiquitin and subsequently degraded by the proteosome.[22-24] If ERAD is unable to cope with the disruption of protein folding, the accumulation of misfolded proteins in the ER activates a cellular response that functions to maintain homeostasis and normal protein flux in the ER. This response is known as the unfolded protein response (UPR) and it serves two goals: to restore normal function of the ER by temporarily stopping protein translation, and to activate signaling pathways that increase molecular chaperones involved in protein folding. The transcriptional upregulation of genes encoding ER chaperones and folding enzymes increases the folding capacity of the ER and serves as an indicator of ER stress. In certain cases, the activation of the UPR may be insufficient to overcome ER stress and the accumulation of misfolded proteins may lead to cell death.[19] If the UPR succeeds, the aggregate of misfolded proteins is removed and normal function of the ER is restored.

Later Processing Steps in N-Glycosylation

After proper folding, newly synthesized glycoproteins destined for the secretory pathway are transported from the ER to the Golgi by a cytosolic coat protein complex known as COP II that initiates the budding process from the ER membrane.[25] Once the vesicle has successfully released its cargo into the lumen of the *cis* face of the Golgi apparatus, additional mannose residues may be removed from the glycan to generate more complex structures.[9] In the *medial* Golgi, N-acetylglucosaminyltransferase (GlcNAcT-1) initiates biosynthesis of hybrid and complex N-glycans by transferring GlcNAc to $Man_5GlcNAc_2$. The subsequent removal of two

mannose residues and a second addition of GlcNAc results in the precursor for all biantennary, complex N-glycans. If mannose residues remain intact after the first addition of GlcNAc, then hybrid glycans are generated.[9] Glycoproteins targeted for areas of the cell other than the ER or Golgi apparatus are moved towards the *trans* face to a complex network of membranes and vesicles. Here, glycoproteins are sorted and shipped to their destinations by their placement into specific vesicles, a process that depends on the molecular marker they carry.

This division of synthesis and processing between the ER and the Golgi complex allows for efficient utilization of the oligosaccharides' functions. In addition to protein folding, oligosaccharides also function as molecular signals to target glycoproteins to their distinct sub-cellular locations. N-glycans often serve as "tags" that allow lectins and modifying enzymes to establish order among the variety of glycoproteins. These interactions allow the ER and Golgi to monitor the time spent in the ER, folding status, and the final destination of glycoproteins.[15] Defects in enzymes involved in biosynthesis and transport of N-glycans have given significant insight into the functions of oligosaccharides. These defects often result in genetic disorders that have only recently been characterized in humans. One such set of disorders, the Congenital Disorders of Glycosylation (CDGs), emphasize the essential early processing steps of the LLO.

.

Congenital Disorders of Glycosylation Result from Defects in N-Glycosylation

The vast number of human disorders that result from mutations in genes associated with glycosylation illustrates the importance of glycosylation. The Congenital Disorders of Glycosylation (CDG) comprise a group of genetic disorders in which N-glycan assembly, modification, or trafficking is altered. CDGs are caused by mutations in genes of proteins involved in oligosaccharide biosynthesis that result in defective enzyme activity and

subsequently abnormal glycosylation.[26, 27] Originally, CDGs were divided into two groups: CDG-I included all disorders involved in the assembly of the N-glycan in the ER, while CDG-II included all other disorders of N-glycosylation, O-glycosylation, and glycolipid biosynthesis. The 15 genes associated with CDG type I are marked in red in **Figure 1.1**. Because almost 50 CDG subtypes have been identified spanning a variety of genotypes, the nomenclature has been simplified by focusing on the name of the mutated gene followed by the abbreviation "CDG". [28]

Defects in genes involved in N-glycosylation result in CDGs, and it's believed all genes involved in N-glycosylation are likely associated with a yet unidentified CDG.[29, 30] In yeast, mice, and presumably humans, complete absence of N-glycan synthesis is embryonic lethal. Therefore, all currently identified human CDG defects are the result of hypomorphic mutations, not complete loss of function.[31] The clinical severity of these symptoms varying immensely, but most of these disorders lead to psychomotor retardation, neuromuscular problems, coagulopathies , liver fibrosis, and dysmorphic features such as inverted nipples and subcutaneous fat pads.[32] The variability in clinical severity often makes diagnosing CDGs very difficult. Originally, the analysis of the more severe clinical phenotypes led to the discovery of most CDG types. As the understanding of phenotypic variability continues to expand, it is becoming increasingly clear that milder symptoms should be considered in the diagnosis of CDGs.[30] Even though the majority of identified CDG mutations affect genes involved in oligosaccharide biosynthesis, it is currently unclear to what degree clinical phenotypes result from hypoglycosylation of specific glycoproteins.

Isoelectric Focusing of Serum Transferrin

Many CDG patients have been identified by abnormal glycosylation of serum glycoproteins.[33] Patients exhibiting defective N-glycosylation often have undersialylation of serum glycoproteins such as transferrin. Serum transferrin normally has two N-glycans, which are terminated with a negatively-charged sialic acid. The N-glycan profile of transferrin is detected by isoelectric focusing using blood samples from patients.[34, 35] The glycosylation pattern of serum transferrin distinguishes between defects in N-glycosylation site occupancy and defects of N-glycan trimming and elongation. These two groups of defects had previously been defined as CDG type I and CDG type II, respectively. CDG type I patients lack sialic acid residues on transferrin because they have unoccupied glycosylation sites. This is due to defects in any of the steps required for the assembly of the LLO in the ER. This produces a structurally incomplete LLO, which results in hypoglycosylation of glycoproteins and incomplete intermediates. In CDG type II patients, both glycosylation sites of transferrin are occupied, but the structure of the glycan is altered due to defects in the processing steps of the N-glycan in the Golgi.[9, 33] Isoelectric focusing is a convenient method for testing patients that has paved the way for the identification of several defects on N-glycosylation. Two CDGs associated with a type I pattern have been well characterized at the enzymatic level: phosphomannomutase (PMM) and phosphomannose isomerase (MPI).

Defective PMM2 Activity Results in PMM2-CDG

PMM2-CDG is caused by an inherited mutation in the phosphomannomutase 2 (PMM2) gene. PMM2 is a cytosolic enzyme that catalyzes the isomerization of Man-6-P to Man-1-P, which is the precursor to GDP-mannose (**Figure 1. 2**), which serves as the mannose donor to the LLO on the cytoplasmic face of the ER. The LLO must receive four mannose residues on the

cytoplasmic face of the ER before it translocates into the ER lumen. The isomerization of Man-6-P to Man-1-P is the first committed step in the synthesis of the activated mannose donors GDP-mannose and Dol-P-mannose.[36] As shown in **Figure 1.2**, a deficiency in PMM2 is believed to reduce the amount of Man-1-P, thereby reducing the amount of GDP-mannose. A decrease in GDP-mannose has been predicted to inhibit maturation of the oligosaccharide.[36, 37] Low PMM activity can be detected in fibroblasts, leukocytes, aminocytes and liver tissues of PMM2-CDG patients. [38] Studies using [^{3}H] mannose in PMM2-CDG fibroblasts have shown reduced incorporation of radioactivity into Man-1-P, GDP-Man, and nascent glycoproteins. The formation of full length LLO was also affected, with an accumulation of immature intermediates (typically $Man_{3-6}GlcNAc_2$-P-P-Dol).[36, 39-41] Thus, phenotypes seen in PMM2-CDG patients have been attributed to limited pools of mature LLO coupled with accumulation of immature LLOs, which are themselves poor OST substrates.[42]

Abnormal Glycosylation of Glycoproteins of PMM2-CDG Patients

Serum glycoproteins from PMM2-CDG patient samples have been shown to be abnormally glycosylated. Specifically, studies have shown that PMM2-CDG patients have hypoglycosylated liver-derived serum glycoproteins and liver proteins.[43, 44] Several groups have investigated serum from patients and have reported hypoglycosylation of transport proteins[43-48], decreased activity of coagulation and anticoagulation factors [47-51], irregular levels of hormones[52, 53],and increased activity of lysosomal enzymes [54-57]. Most glycoprotein concentrations or enzyme activities in serum are decreased. Others are increased (e.g. several lysosomal enzyme activities[54]), or normal (transferrin, immunoglobulins[49]). Analysis of glycoproteins in cerebrospinal fluid has also shown hypoglycosylated isoforms of

beta-trace protein.[58] A recent study also showed that intercellular cell adhesion molecule 1 (ICAM-1) is hypoglycosylated in PMM2-CDG patient fibroblasts. ICAM-1 was reduced in fibroblasts from 31 CDG patients compared with normal controls. In PMM2-CDG cells, complementation with PMM2 partially corrected ICAM-1 hypoglycosylation restoring its presence on the plasma membrane.[59] On the other hand, a few studies have shown that some membrane bound and secreted N-glycoproteins are fully glycosylated in fibroblasts or lymphoblastoid cells from PMM2-CDG patients. [60, 61] Also, studies have shown that normal glycosylation was detected among extrahepatic glycoproteins, leading investigators to conclude that the defect in N-glycosylation of proteins is tissue-dependent in PMM2-CDG.[62]

Molecular Genetics of the PMM2-CDG

With over 800 identified patients and an incidence rate of about 1 in 50,000, PMM2-CDG is the most common CDG. PMM2-CDG occurs world-wide and affects both sexes equally.[35, 38, 63, 64] It is inherited in an autosomal recessive manner and linkage analysis has localized the human gene to chromosome 16p13.[65, 66] There are currently 103 known lesions in PMM2-CDG, most of which are missense mutations.[29, 67] The most common mutation, R141H, is found in 1 out of 80 individuals in most human populations.[68] While homozygosity for the R141H allele has not been identified , patients homozygous for the relatively frequent F119L mutation were found, as well as one patient homozygous for the D65Y mutation.[69]. This suggests that the R141H mutation may not be compatible with life because it completely abolishes PMM2 activity, which is essential for embryogenesis.[69, 70] Although there are no known mutations in the catalytic domain of PMM2, several mutations have been found to cause decreased substrate or cofactor binding. Other mutations affect protein stability, which itself

reduces catalytic activity.[29] Most PMM2-CDG patients presenting a severe clinical picture have 0-10% of normal PMM activity in fibroblasts.[26, 38, 71] Some patients exhibit a moderate clinical picture with 25% normal enzymatic activity, while heterozygous patients can be asymptomatic with just 50% activity.[72] Currently no genotype-phenotype correlation has been found, but patients with higher residual activity tend to have milder phenotypes.[73, 74] These studies suggest that there is a necessary threshold for PMM activity. If PMM activity is sufficient, no phenotypes are seen; however, as enzyme levels fall below the necessary PMM level, phenotypic presentation becomes increasingly severe. Northern analysis of human tissues shows PMM2 is highly expressed in pancreas and liver, organs which both produce a large amount of secreted proteins. The gene is also expressed in kidney and placenta, and, to a lesser extent, in skeletal muscle, heart, and brain.[67]

Clinical Presentation of PMM2-CDG

Diagnosis of PMM2-CDG can be made in the first days of life. PMM2-CDG patients exhibit three main features: a moderate to severe neurological disease, dysmorphia, and a variable involvement of organs. The neurological clinical features include developmental delay, epilepsy, ataxia, and psychomotor retardation characterized by IQ ranges from 40 to 70 and delays in language.[42] Also frequently observed in patients are symptoms of coagulopathy, hypotonia, cardiomyopathy, and liver problems such as hepatomegaly and hepatic fibrosis.[42, 75, 76] Skeletal deformities range from facial dysmorphia described as high nasal bridge and prominent jaw, long limbs with short torsos, and skeletal dysplasia, which is characterized by flattening of all vertebrae.[77-79] During infancy, there are variable feeding problems that result in failure to thrive and require nasogastric tube feeding or feeding via gastrostomy.[80] Within

the first five years of life, patients have a 20% mortality rate due to organ failure, cardiac insufficiency, or severe infections.[32, 77, 81] This is most frequently found in cases with low residual PMM2 activity, emphasizing the essential role of N-glycosylation.[77] After infancy, retinis pigmentosa, joint contractures, and stroke-like episodes (in ~ 50% of cases) develop.[82, 83] Children have severely delayed motor development and walking without support is rarely achieved.[26] Adults are usually wheelchair bound with peripheral neuropathy and mental retardation.[81] Patients exhibit endocrine dysfunction that includes hyperglycemia-induced growth hormone release, hyperprolactinemia, insulin resistance, and hyperinsulinemic hypoglycemia.[84, 85] Clinical variability is not only seen in patients with the same PMM2 genotypes, but even between affected siblings and monozygotic twins, suggesting additional impact of both environmental and genetic factors. [86-88] The severe consequences of reduced PMM2 activity are puzzling, since another PMM gene, PMM1, was identified.[89]

PMM1 is Homologous to PMM2

Though two highly conserved PMM genes have been identified in the mammalian genome, the physiological role of PMM1 remains elusive. No disorder has been associated with defects in PMM1 even though defective PMM2 activity leads to PMM2-CDG.[89-91] Human PMM1 is localized to chromosome band 22q13, while PMM2 is localized to chromosome 16p13. Since genetic linkage studies indicate that PMM2-CDG locus maps to chromosome 16p13, mutations in PMM1 could not harbor the primary defect in PMM2-CDG patients.[66, 89] PMM1 has 65% sequence identity with PMM2, but is postnatally restricted to the brain and lungs in mammals while PMM2 remains ubiquitously expressed.[90] Though the subcellular

localization and the catalytic abilities are quite similar, PMM1 does not seem to compensate for reduced PMM2 activity within PMM2-CDG patients.[92]

Pmm1 Knockout Mouse Model

A knockout mouse deficient in Pmm1 activity is viable, develops normally, and has no obvious phenotypic alterations. Furthermore, lectin histochemistry of these mice did not demonstrate any obvious altered glycosylation patterns in tissues. Though Pmm1was found to be downregulated in adult mouse tissues, its presence in tissues such as liver, kidney and brain coincide with tissues most severely affected in PMM2-CDG. [77] The presence of Pmm1 in these tissues suggests that Pmm1 cannot compensate for Pmm2 under *in vivo* conditions. Pmm2 showed similar levels in Pmm1 knockout and wild type mice, leading investigators to suggest that Pmm1 is not involved in protein glycosylation.[92] Though to fully exclude this option, Pmm1 deficiency and Pmm1 overexpression in a Pmm2-null background would have to be analyzed. Though the role of PMM1 has not yet been elucidated, PMM1 has been implicated in processes other than protein glycosylation.

PMM1 Is Similar, Not Identical to PMM2

Unlike PMM2, human PMM1 has been shown to have both PMM and phosphoglucomutase activity. *In vitro*, PMM1 converts glucose-6-P and mannose-6-P at equal rates, whereas PMM2 converts glucose-6-P 20 times more slowly than mannose-6-P. Also, Fructose-1,6-bisphosphate stimulates PMM1 to form mannose-1,6-bisphosphate from fructose-1,6-bisphosphate and Man-1-P, though no such effect was seen on PMM2. [84]Studies have also shown that PMM1 corresponds to the brain inosine monophosphate (IMP)-sensitive glucose-1,6-

bisphosphate. In the ischemic brain, PMM1 degrades glucose-1,6-bisphosphate upon stimulation by IMP.[93] In contrast, PMM2 is insensitive to IMP and has extremely low glucose-1,6-bisphosphatase activity. Thus, PMM1 encodes a PMM that shows different substrate specificity and kinetics, potentially suggesting a different physiological role for PMM1 than PMM2.

Although PMM1 and PMM2 share the same PMM activity, it is not known whether PMM1 is involved in the nucleotide sugar synthesis pathway of N-glycosylation because no disorder has been associated with it. However, defects in another enzyme involved in the same nucleotide sugar synthesis, mannoisomerase phosphate (MPI), results in MPI-CDG.

Reduced MPI Activity Results in MPI-CDG

MPI-CDG is caused by a mutation in the mannose phosphate isomerase (*mpi*) gene. MPI isomerizes Fructose-6-phosphate to Man-6-P, which is subsequently modified by PMM2 (**Figure 1.2**).[94] MPI links glycolysis to protein glycosylation by isomerizing Fructose-6-P to Man-6-P because Fructose-6-P is used in the glycolytic pathway. While complete loss of MPI is embryonic lethal, several patients have been identified with defective MPI activity. MPI-CDG, like PMM2-CDG, produces immature LLO and unoccupied N-glycosylation sites on glycoproteins.[33] Defective MPI activity leads to decreased pools of Man-6-P, resulting in decreased GDP-mannose available for LLO assembly. Approximately 25 patients have been diagnosed with MPI-CDG. Initial designation was assigned following measurement of MPI activity in patients' fibroblasts or leukocytes.[95] So far, eighteen different mutations have been identified, which comprise a group of 15 point mutations, two frame-shift mutations, and one splicing defect.[94-98] Also, contrasting PMM2-CDG, seven of the missense mutations identified in MPI-CDG patients map to the predicted catalytic domain.

Clinical Presentation of MPI-CDG and Therapy

MPI-CDG patients typically have 3-20% residual PMI activity.[99, 100] Unlike PMM2-CDG, MPI-CDG patients do not exhibit neurological symptoms. A possible explanation for this may be that during embryonic development, mannose found in the mother's plasma serves as an endogenous therapy.[101] MPI-CDG patients most frequently exhibit gastrointestinal and liver problems, such as diarrhea, vomiting, protein-losing enteropathy, hepatic fibrosis, and, in some cases, hypoglycemia and coagulopathy.[94] Currently, MPI-CDG is one of only two CDGs with a therapy option.

Patients with MPI-CDG are treated by oral mannose supplementation. Exogenously supplied mannose is thought to be taken up by the cell and phosphorylated by hexokinase, which directly yields Man-6-P and bypasses the defective isomerase step.[39] A typical oral dose of 1gram mannose per kilogram body weight per day is given to the patients.[39] This therapy has proved to be effective in MPI-CDG patients and all clinical features except hepatic fibrosis resolve when patients are given mannose supplements.[94, 102] Mannose supplementation has also been proven to correct the impaired glycosylation of serum transferrin and other serum glycoproteins.[39] Because mannose supplementation was shown to be so effective in MPI-CDG patients, it was thought that mannose supplementation might also be useful in PMM2-CDG patients. Since PMM2 is responsible for the conversion of Man-6-P to Man-1-P, it was thought by increasing the amount of substrate available for PMM2 glycosylation profiles of PMM2-CDG patients might improve.

Mannose Supplementation Did Not Correct Abnormal Phenotypes in PMM2-CDG Patients

Initial *in vitro* studies suggested that mannose supplementation might improve glycosylation in CDG-Ia patients. In these studies, PMM2 deficient fibroblasts were treated with [^{3}H] mannose pulse labeling of LLOs and glycoproteins. To increase labeling of cellular glycoconjugates, low glucose concentrations were used in culture media. In these conditions mannose supplementation resulted in corrected LLO and normal glycosylation.[36, 39-41] Unfortunately, though it was successful in fibroblasts, mannose supplementation showed no measurable improvement in either patients' symptoms or serum hypoglycosylation.[103, 104] Since MPI activity remains normal in PMM2-deficient patients, one likely explanation for the failure of mannose therapy is the Man-6-P generated following the mannose supplementation may have been rapidly isomerized by MPI to Fructose-6-P.[101] These increased pools of Fructose-6-P would be directed towards glycolysis, so that any accumulation of Man-6-P would be utilized by the glycolytic pathway.

An alternative explanation for the failure of mannose therapy in PMM2-CDG patients is that in the absence of PMM2, Man-6-P levels might accumulate and inhibit the glycosylation pathway.[103] This is supported by a study in which PMM2-CDG patients were given mannose supplements, and serum glycoproteins (transferrin, α1-antitrypsin, antithrombin, and thyroxine-binding globulin) were analyzed. In response to the mannose treatment, the mean serum concentrations of these glycoproteins tended to decrease, and the abnormal isoforms of these glycoproteins became more prominent and/or additional abnormal isoforms appeared.[103]

Researchers speculated that Man-6-P levels may be inhibiting the glycosylation pathway through an unknown mechanism.[18, 105]

In a 2005 study, PMM2-CDG fibroblasts that were grown in physiological levels of glucose showed that increased concentrations of Man-6-P specifically cleaved the mature LLO species, resulting in release of free intact glycan. The authors concluded that the release of LLO led to futile cycling of N-glycan biosynthesis, impaired by GDP-mannose and PMM2 deficiency. This decrease in mature LLO species might also decrease protein N-glycosylation. Thus, increasing Man-6-P levels in PMM2deficient cells could deplete mature LLO and exacerbate hypoglycosylation.[18, 105] The context and purpose of this mechanism for LLO hydrolysis was further developed in a recent study, which linked ER stress to elevated Man-6-P levels.[106] Researchers showed that viral infection activated ER stress, which in turn stimulated glycogenolysis. Since glycogen was found to be the origin for Man-6-P, glycogenolysis increased Man-6-P levels, which would then cleave the LLO pyrophosphate linkage. This stress-signaling pathway is believed to respond to viral stress by depleting host LLOs required for N-glycosylation of virus-associated polypeptides.[106] Though the Man-6-P activated enzyme remains unknown, the OST is a strong candidate.

Although mannose supplementation failed to correct deficient glycosylation in PMM2-CDG patients, it did uncover a novel mechanism affecting the LLO biosynthesis. This stress-signaling pathway helped expose potential pitfalls in treating PMM2-CDG patients. This potential mechanism should be taken into account for possible therapeutic strategies.

PotentialTherapies to Treat CDGs

Cellular, genetic, and metabolic options have been considered for treatment of CDG patients, but each of the current approaches has short comings. Many of the therapeutic strategies

considered rely on enzyme replacement, such as introduction of PMM2 producing stem cell populations or gene therapy to provide DNA encoding normal PMM2 enyme. While stem cell therapy may hold promise in treating other disorders, in the case of PMM2 stem cell replacement may be difficult due to the ubiquitous and cell autonomous nature of protein glycosylation. Though enzyme activity could be increased by gene therapy, human trials are unlikely to be approved given the inherent risks and very small patient population.[107] PMM2 gene therapy could correct glycosylation defects by providing DNA encoding normal enzymes, but it is not considered practical because of variable accessibility to cells, especially those in the central nervous system.[101] In many diseases, enzyme replacement therapy has been successful in providing normal active enzyme, but it is difficult in cases that require crossing the blood-brain barrier. Furthermore, reintroduction of recombinately produced PMM2 would require cytoplasmic targeting.[107]

PMM2 Activators and Enhancers

In light of the fact that PMM2-CDGs are usually the result of hypomorphic mutations, several groups have explored ways to activate or enhance either expression or activity of the mutant PMM2. Insulin is the only reported activator of PMM2, and a two-fold increase in PMM2 activity was seen in insulin-treated Cos7 cells. This increase in PMM2 activity did not involve transcription, as *pmm2* transcription levels were not found to be increased in insulin-treated cells. [108] Currently, there are no small molecule activators of PMM2, but PMM2 represents an excellent candidate for a small molecule screen. The simple coupled enzymatic assay using MPI, phosphoglucose isomerase, and glucose-6-P dehydrogenase could easily be adapted for use in a high through-put compound screen. A small molecule could potentially pass

the blood brain barrier, but potential allosteric or conformational-dependent activators must be confirmed on normal and mutant forms of PMM2. One caveat of this approach is the possibility that individual activators may not be useful due to the wide variability in PMM2 mutant isoforms. Also, activation would depend on whether the mutation affects enzyme stability, substrate binding, or transcription.[101]

Man-1-P Prodrugs May Bypass the Defect

Due to difficulties associated with gene replacement or enzyme enhancement, another option is to circumvent the enzyme completely. One way to do this is to increase endogenous Man-1-P levels directly in cells. Since Man-1-P is not membrane permeable, several groups have attempted to chemically synthesize Man-1-P analogs, collectively known as pro-drugs, that can be converted to Man-1-P after entering the cell.[109, 110] One such analog to Man-1-P, C-II, was made membrane permeable by covering the phosphate with acetoxymethyl groups and protecting OH-groups with acetyl esters or ethylcarbonate.[109] This compound successfully increased GDP-Man and corrected the LLO deficiency of several glycosylation deficient fibroblast cell lines. [109] Though this study validated the theoretical concept of bypassing PMM2 defects with Man-1-P analogs, C-II is currently too unstable and toxic to be clinically useful. Since C-II's half-life in serum is only 2.5 minutes, extremely high concentrations are required to get sufficient diffusion through the cell membrane. At the effective dosage, C-II is toxic and negatively affects protein synthesis and cell viability.[109] Additional Man-1-P prodrugs, which contain an additional phosphodiester-linked mannose residue bearing a phenyl or benzyl group, also improved permeability and increased intracellular Man-1-P. These compounds had minimal toxicity after 16 hours based on release of lactate dehydrogenase. [111]

Despite promising results *in vitro*, the lack of valid animal models for PMM2-CDG has impedes *in vivo* assessment of these potential therapeutic compounds.

Substrate Flux Therapies in CDG patients

The goal of a therapy for PMM2-CDG patients is to increase substrate flux through the glycosylation pathway. In theory, substrate flux may be altered either by increasing PMM2 activity, increasing mannose uptake, increasing the Man-6-P pools themselves, or favoring glycosylation over glycolysis. Substrate flux therapies have been effective in treating MPI-CDG, where exogenous mannose bypasses the deficient step and drives substrates through the glycosylation pathway. Therefore, we postulate that by increasing the flux of metabolic precursors into the depleted glycosylation pathways, LLO levels should be corrected and normal glycosylation should occur. While the developmental defects in that occur *in utero* will not be reversed by these therapies, even small improvements in the patients' lives make the pursuit of a therapy worthwhile. Substrate flux therapies hold promise in treating not only PMM2-CDG, but also other types of CDGs. For example, DPM1-CDG results in a deficiency of Dol-P-Man, which leads to altered mannosylation of the LLO inside the ER lumen. By increasing substrate flux through the Dol-P-Man pathway, we may be able to correct LLO levels.

Dolichol Phosphate Mannose Synthase (DPM1) Mutations Result in DPM1-CDG

DPM1-CDG, like PMM2-CDG, causes altered mannosylation of the LLO during N-glycosylation due to defective processing of sugars that serve as mannose donors. DPM1-CDG is caused by mutations in the catalytic subunit (DPM1) of dolichol phosphate mannose synthase (DPM synthase) in the ER.[112] DPM synthase produces DPM from GDP-Man and Dol-P on

the cytoplasmic face of the ER. To serve as the donors for the last four mannose residues for the N-glycan precursor, DPM translocates to the ER lumen.[113] DPM1-CDG is also expected to respond to mannose because it is already known that increased Man-1-P flux increases GDP-Man, a substrate in DPM synthesis, and corrects glycosylation defects in patient cells.[109] DPM also serves as a mannose donor in other glycosylation pathways, such as GPI anchor formation, O-mannosylation, and C-mannosylation.[113] At present, DPM is the only known mannose donor in the lumen of the ER, so defective DPM synthesis could potentially affect all four glycosylation pathways in which it is utilized.

A recent study presented a patient that had a CDG with muscular dystrophy, a clinical feature seen in patients with defective O-mannosylation.[114] Sequencing of the DPM synthase revealed a mutation in DPM3, the stabilizing unit that tethers DPM1 to the ER membrane. This mutation decreased DPM synthase activity, which may have led to deficient O-mannosylation. GPI-anchor biosynthesis and C-mannosylation pathways were not found to be altered, which indicates that residual DPM levels were sufficient for normal GPI-anchor formation and C-mannosylation. The patient seems to be on the very mild end of the clinical spectrum of DPM-CDG patients, and this was attributed to the mutation being in the stabilizing unit DPM3, and not the catalytic unit DPM1.[114] It has been suggested that the main clinical features of DPM1-CDG (seizures, developmental delay, and congenital visual loss) could be explained by an overlap with deficient O-mannosylation and GPI anchor synthesis.[114, 115] Therefore, testing substrate flux therapeutic options in DPM1-CDG may provide a chance to affect the other glycosylation pathways in addition to N-glycosylation.

Current Challenges to CDG Therapies

Since the only information regarding glycosylation from CDG patients is restricted to sera, leukocytes, or fibroblasts, insight into tissue-specific disease pathology is limited. Therefore, animal models may provide the only way to study the effects of hypoglycosylation in an entire organism. A current challenge to CDG research is the lack of available animal models in which to both study pathology and test potential therapies. As mentioned previously, complete knockdown of any Type I CDG genes is embryonic lethal in humans and mice.[70] Therefore any animal models for Type I CDGs would need to be hypomorphic mutants. Organ specific knockout expression (e.g. floxed alleles) may not be useful in models due to the ubiquitous expression of PMM2 in patients, although it would allow for specific insights into a tissue's response to PMM2 knockdown. Knock-in of PMM2 mutations may offer hope, but animals with phenotypes would have to be generated while avoiding embryonic or post-natal lethality. Utilization of PMM2 shRNAi molecules could give 80-90% reduced enzyme activity and allow integration into 2-4 cell embryos via lentiviral constructs. However, these constructs frequently integrate into multiple sites on different chromosomes, complicating the creation of a stable knockdown line.[116] Nevertheless, such experiments may provide information on the pathology of PMM2-CDG. Mouse models were developed for PMM2-CDG using a knockout strategy, though they showed variable effects in mimicking pathology seen in patients.

PMM2-CDG Mouse Models

In a constitutive knockout mouse model for PMM2-CDG generated by targeted disruption of the *Pmm2* gene, heterozygous mutant mice appeared normal in development, gross anatomy, and fertility. In contrast, embryos homozygous for the *Pmm2*-null allele were obtained in embryonic development at days 2.5 to 3.5, corresponding to the onset of transcription in

fertilized oocytes. These results confirmed the important roles of Pmm2 and glycoproteins in the early development in mice. [70] Complete loss of Pmm2 activity leads either to implantation failure or to embryonic death prior to implantation, further supporting the conclusion that complete loss of Pmm2 is not compatible with life.[70]

To overcome the early lethality of the Pmm2 knockouts, two types of hypomorphic Pmm2-deficient mouse lines were generated.[117] One line contained a knock-in of R137H allele that is analogous to the R141H mutation found in human PMM2-CDG patients, and the second line contained a knock-in of the F118L allele that is analogous to F122L, a synthetic mutation in the human protein that is predicted from X-ray crystallography to lead to a very mild loss of Pmm2 enzymatic activity. [118] Using these lines, researchers generated mice with respective homozygous *Pmm2*$^{R137H/R137H}$ and *Pmm2*$^{F118L/F118L}$, or compound heterozygous *Pmm2*$^{R137H/F118L}$ genotypes. Researchers found that no *Pmm2*$^{R137H/R137H}$ mice were recovered from matings of heterozygous parents, which was consistent with R141H homozygosity not being found in humans. [69] In contrast, *Pmm2*$^{F118L/F118L}$ mice were indistinguishable from wild type siblings and histological examinations yielded no pathological findings. The PMM activity in *Pmm2*$^{F118L/F118L}$ mice was 42% that of wild type siblings, indicating that residual Pmm2 activity in these mice is sufficient to prevent hypoglycosylation and subsequent pathological phenotypes. The compound *Pmm2*$^{R137H/F118L}$ offspring were also not recovered, suggesting embryonic lethality associated with this genotype between ED 9.5 and 10.5.

Histological examinations of recovered embryos revealed morphological defects, including breakdown of myocardial tissue, reduction in neural epithelium compaction, and massive organ-associated hemorrhaging. Pmm enzyme assays revealed *Pmm2*$^{R137H/F118L}$ mice had Pmm activity that was 11% of wild type siblings, a level similar to that found in PMM2-CDG

patients. The lower Pmm2 activity level in these mice resulted in hypoglycosylation of glycoproteins, leading to embryonic lethality. To test whether mannose supplementation may rescue the *Pmm2*$^{R137H/F118L}$ mice, heterozygous *Pmm2*$^{+/F118L}$ female mice received oral mannose treatment one week before mating to ensure that the mannose concentrations in maternal blood, and therefore embryonic exposure to mannose, would be stable throughout gestation. After mannose treatment two-fold higher serum mannose concentrations were in the dams when compared to untreated controls. Mannose supplementation successfully rescued *Pmm2*$^{R137H/F118L}$ embryos and allowed them to survive beyond weaning. Histological examination and glycosylation patterns of rescued embryos revealed no differences between wild type and *Pmm2*$^{R137H/F118L}$ mice. PMM activity in compound heterozygous embryos rescued with mannose remained at 11% of wild type embryos, indicating that mannose rescue did not increase Pmm2 activity.[117]

Mannose supplementation was successful in rescuing Pmm2 deficient mice, even though mannose supplementation in PMM2-CDG patients had no measureable improvement on phenotypes or isoelectric focusing patterns of serum transferrin, despite increased serum mannose concentrations in patients. The variability of mannose supplementation in mice was further seen in the mouse models for CDG-Ib.[119]

MPI-CDG Mouse Model

A constitutive knockout mouse model for MPI was generated by gene trap technology that led to complete loss of enzymatic activity. These mice had 0.01% MPI activity compared with the Mpi +/+ mice and showed growth retardation, abnormalities in heart formation, and placental hyperplasia. Loss of MPI did not affect embryonic glycan production in the Mpi -/-

mice as shown by normal lectin staining. Despite normal glycosylation, embryos died around E11.5 at the transition of mid to late gestation. Contrary to expectations, providing females with water that contained 10% mannose before mating and during development accelerated the embryonic lethality in the Mpi -/- mice.[119] This effect was due to the complete enzymatic block of Mpi. Since mannose is phosphorylated to Man-6-P when taken into the cell, toxic levels of Man-6-P accumulate due to MPI's inability to isomerize it to Fructose-6-P, which is used in glycolysis. The increased mannose concentration in mice depleted ATP not only through a futile cycle of Man-6-P de- and rephosphorylation, but also through inhibition of glycolytic enzymes. This effect had previously been described in honeybees as well as rats, and occurs in cells that have HK:PMI activity ratio greater than 7, where most cells typically have ratios of 2-3.[120, 121] In humans, the intracellular metabolism through MPI prevents Man-6-P accumulation and toxicity, even with increased mannose concentration.[122]

Though the mouse models for Type I CDGs have shown variable effects, the Freeze lab has currently generated a viable MPI hypomorphic mouse strain. These mice have 3-16% MPI activity in various organs, and they show hepatointestinal symptoms that are similar to MPI-CDG patients. Nevertheless, new animal models are needed to model Type I CDGs and to test potential therapies. One such animal model that holds promise is the zebrafish system.

Zebrafish - Advantages, Techniques, and Models for Glycosylation Disorders

The Zebrafish System

Due to the problems associated with mouse models, the zebrafish system may have certain advantages over other animal models that make it ideal for modeling Type I CDGs.

Zebrafish are vertebrate organisms with a high degree of genetic similarity to both humans and mice. Additionally, total glycome analysis suggests that zebrafish generate the full spectrum of expected glycoforms including oligomannosyl types of N-glycans, as well as complex types with additionally β4-galactosylated, Neu5Ac/Neu5Gc monosialylated Lewis x termini.[123] This suggests that zebrafish synthesize similar types of N-glycans to humans and mice. Zebrafish develop externally and multiple aspects of early embryogenesis are well studied. The external development process allows for analysis of their early development and the ability to directly test potential therapies in developing embryos.[124] By 24 hours post fertilization (hpf) , all organ systems are in place and are able to be visualized.[125] By 6days post fertilization (dpf), a complex circulatory system and counterparts of most mammalian organs have developed. Additionally, zebrafish exhibit highly consistent developmental behaviors such as response to stimuli and swimming behaviors that allow for further phenotypic classification. These characteristics in combination with their large clutch sizes make zebrafish a useful model for genetic studies.

Use of Morpholinos Allow for Tunable Gene Knockdown in Zebrafish

Although not yet amenable to homologue recombination and gene knock-outs, antisense morpholinos provide an alternate reverse genetic appraoch to reduce gene expression. Morpholinos are antisense oligonucleotides that contain a six-membered morpholine ring instead of a ribose or deoxyribose ring. The oligonucleotides link through undercharged phosphorodiamidate groups instead of anionic phosphates to eliminate ionization, leaving the backbone uncharged. This uncharged backbone is unrecognized by enzymes or signaling proteins, is stable to nucleases, and does not trigger an innate immune response through Toll-like

receptors. Furthermore, morpholino's length (~25 bases) and RNase H-independence allow for greater specificity and stability in transcript targeting. Thus the morpholino avoids degradation, inflammation, and interferon induction, which are problems encountered with other antisense based gene knock down reagents[126].

Morpholinos allows for tunable gene knockdown that may be analogous to hypomorphic mutations.[127] Gene knockdown is achieved by preventing cells from making the targeted protein, by disruption of either translation or mRNA splicing. Translation blocking morpholinos prevent the ribosome initiation complex from proceeding through the ATG, thereby blocking protein translation of the target transcript. Splice blocking morpholinos block proper spliceosome formation of mRNA by binding to an exon/intron junction, thereby preventing splicing. Improper splicing can result in RNA degradation or splice variants of the transcript of interest through intron retention or exon skipping.

The degree of morpholino knockdown can be assessed using enzyme activity assays or RT-PCR; however, RT-PCR can only be used in conjunction with a splice blocking morpholino because of the alterations to the transcript. In order to control for off target effects, mRNA encoding the same gene of interest is coinjected with the splice blocking morpholino. Since the mRNA has already been properly spliced, the splice blocking morpholino should not be able to bind. Thus, translation of the processed mRNA replaces production of the protein that was knocked down by the morpholino. Coinjection of a splice blocking morpholino and mRNA should result in rescued morphants that are closer to a control phenotype.

Taking these aspects into consideration, the zebrafish model system holds promise in modeling genetic disorders. The external embryogenesis, testing potential therapies, and tunable knockdown of protein expression have made zebrafish an attractive animal system for many

researchers. Emerging studies from multiple groups have demonstrated the utility of zebrafish as models of defective glycosylation disorders, either through use of morpholinos or through mutant screens.

Zebrafish Mutants of Glycosylation Disorders

The importance of multiple glycosylation pathways in early development is underscored by the several zebrafish glycosylation mutants that are abnormally affected. These include zebrafish that exhibit defective glycosaminoglycans (GAGs) biosynthesis, hypoglycosylation of α-dystroglycan, and impaired Man-6-P biosynthesis in the lysosomal targeting pathway.[128-130] Abnormal synthesis of glycosylation precursors also has been studied in zebrafish, as found in the *slytherin* mutant.

The *slytherin* (*srn*) mutant bears a missense mutation in GDP-mannose 4,6 dehydratase (GMDS), the rate-limiting enzyme in the biosynthesis of GDP-fucose. These mutants demonstrated that defects in protein fucosylation lead to defects in neuronal differentiation, maintenance, axon branching, and synapse formation. These phenotypes correspond to clinical phenotypes seen in FUCT1-CDG, which is characterized by mental retardation, slowed growth, and severe immunodeficiency due to lack of fucosylated glycoproteins. Analogous to Drosophilia mutants within the same pathway, several of these phenotypes were shown to be both Notch-dependent and Notch-independent.[131] These Notch receptors bear both N- and O-linked fucosylated glycans that, if altered, can affect propagation of downstream signaling. [132] These *srn* mutants prove to be a useful tool in guiding future analyses in human FUCT1-CDG patients and contribute further understanding of the mechanisms in this disorder.

Another zebrafish model that also affects sugar precursors in glycosylation pathways is the glutamine-fructose-6-phosphate transaminase 1 (GFPT1) morphant. GFPT1 catalyzes the transfer of an amino group from glutamine onto fructose-6-phosphate, yielding glucosamine-6-phosphate (GlcN-6-P) and glutamate. This reaction is the first and rate-limiting step of the hexosamine biosynthesis pathway, which is the obligatory source of essential amino sugars for glycoprotein, glycolipid, and proteoglycan synthesis.[133] Patients with mutations in GFPT1 have been identified with Congenital Myasthenic Syndrome (CMS), a rare autosomal disease that is characterized by a recognizable pattern of weakness of shoulder and pelvic muscles, sparing of ocular or facial muscles, and neurophysiologic signs of neuromuscular junction (NMJ) dysfunction. Because no CMS patients carried two null mutations and because glycosylation is essential for cell survival, researchers expected that GFPT1 mutations in patients create hypomorphic alleles. Thus, researchers successfully knocked down expression of the zebrafish GFPT1 ortholog gfpt1 by injection of antisense morpholinos. Morphants displayed altered tail morphology, impaired touch and swimming responses, abnormal muscle morphology, and delayed NMJ development. The morphants' similarity to patients' phenotypes may show another level of genetic evidence and could confirm that GFTP1 is required for normal NMJ formation.[134]

In addition to their use for analyses of early development, zebrafish have emerged as valuable organisms in disease modeling and pharmacological studies. A recent study used zebrafish embryos to test whether MLS0315771, an MPI inhibitor, would provide more Man-6-P for glycosylation and possibly benefit PMM2-CDG patients.[135] Since Man-6-P is the common substrate of PMM2 and MPI, only a small proportion is left for glycosylation since the majority is catabolized by MPI to be used in glycolysis. Therefore, if MPI activity was decreased and less

Man-6-P was isomerized to Fructose-6-P for glycolysis, more Man-6-P might be available for the deficient glycosylation pathway. To test this reasoning, researchers used MLS0315771 in various PMM2-CDG cell lines to divert Man-6-P away from glycolysis and towards glycosylation. Inhibition of MPI was shown to divert Man-6-P towards glycosylation and improve N-glycosylation in some PMM2-CDG fibroblasts; however, the efficacy of treatment depended on the residual activity and type of mutations. To determine whether MLS0315771 could modulate mannose flux in a whole organism, zebrafish embryos were labeled with [^{3}H] mannose in the absence and presence of MLS0315771. Labeled glycoproteins increased four-fold in the presence of MLS0315771, which corresponds to 55% MPI inhibition.[135] This study demonstrated that small molecules are able to modulate metabolic flux in favor of glycosylation *in vivo*.

Zebrafish Model for MPI-CDG

Zebrafish have also been proven an effective system for modeling CDGs. Recently, a morpholino-based zebrafish model was generated to study MPI-CDG.[136] The morphant fish consistently yielded 13% residual Mpi enzyme activity, which is within the range of MPI activity noted in MPI-CDG patients' fibroblasts. [94, 95, 97] The morphant MPI fish displayed several biochemical features of MPI-CDG patients, such as depletion n overall LLO and Man-6-P pools. The *mpi* morphants also displayed several phenotypes including increased mortality and decreased liver size. Mannose supplementation, the clinically-validated therapy for MPI-CDG patients, successfully rescued the biochemical and phenotypic defects caused by MPI deficiency. Researchers also sought to define the timeframe when mannose addition was the most effective at rescuing *mpi* morphants. They found that the presence of mannose for only the first 24 hours

was sufficient at rescuing MPI deficiency, resulting in morphants indistinguishable from controls. This finding suggests not only that MPI is crucial to early developmental events, but also that absence of mannose supplementation early in development may have long term effects.[136] This MPI-CDG model implies that zebrafish may be useful for modeling other CDGs and disorders of glycosylation.

Thesis Overview

Using the zebrafish system, we have generated a PMM2-CDG model to further study the pathology of deficient glycosylation. With this model, we established and characterized the phenotypes and biochemical parameters of the morphant zebrafish. We also evaluated the efficacy of strategies designed to modulate flux through the N-glycosylation pathway. Using these approaches, we assessed phenotypic and biochemical recovery in the morphant zebrafish. The broader impact of the project was to validate the premise that enhancing metabolic flux through a minor pathway may improve pathology and normalize metabolites.

REFERENCES

1. Spiro, R.G., *Protein glycosylation: nature, distribution, enzymatic formation, and disease implications of glycopeptide bonds.* Glycobiology, 2002. **12**(4): p. 43R-56R.
2. Apweiler, R., H. Hermjakob, and N. Sharon, *On the frequency of protein glycosylation, as deduced from analysis of the SWISS-PROT database.* Biochim Biophys Acta, 1999. **1473**(1): p. 4-8.
3. Petrescu, A.J., et al., *Statistical analysis of the protein environment of N-glycosylation sites: implications for occupancy, structure, and folding.* Glycobiology, 2004. **14**(2): p. 103-14.
4. Lowe, J.B. and J.D. Marth, *A genetic approach to Mammalian glycan function.* Annu Rev Biochem, 2003. **72**: p. 643-91.
5. Spiro, R.G., *Glycoproteins.* Adv Protein Chem, 1973. **27**: p. 349-467.
6. Montreuil, J., *Primary structure of glycoprotein glycans: basis for the molecular biology of glycoproteins.* Adv Carbohydr Chem Biochem, 1980. **37**: p. 157-223.
7. Varki, A., *Biological roles of oligosaccharides: all of the theories are correct.* Glycobiology, 1993. **3**(2): p. 97-130.
8. Kornfeld, R. and S. Kornfeld, *Assembly of asparagine-linked oligosaccharides.* Annu Rev Biochem, 1985. **54**: p. 631-64.
9. al, A.V.e., *Essentials of Glycobiology*2009, Cold Springs Harbor, NY: Cold Spring Harbor Laboratory.
10. Helenius, J., et al., *Translocation of lipid-linked oligosaccharides across the ER membrane requires Rft1 protein.* Nature, 2002. **415**(6870): p. 447-450.
11. Dempski, R.E., Jr. and B. Imperiali, *Oligosaccharyl transferase: gatekeeper to the secretory pathway.* Curr Opin Chem Biol, 2002. **6**(6): p. 844-50.
12. Karaoglu, D., D.J. Kelleher, and R. Gilmore, *Allosteric regulation provides a molecular mechanism for preferential utilization of the fully assembled dolichol-linked oligosaccharide by the yeast oligosaccharyltransferase.* Biochemistry, 2001. **40**(40): p. 12193-206.
13. Kelleher, D.J., D. Karaoglu, and R. Gilmore, *Large-scale isolation of dolichol-linked oligosaccharides with homogeneous oligosaccharide structures: determination of steady-state dolichol-linked oligosaccharide compositions.* Glycobiology, 2001. **11**(4): p. 321-33.
14. Schenk, B., F. Fernandez, and C.J. Waechter, *The ins(ide) and out(side) of dolichyl phosphate biosynthesis and recycling in the endoplasmic reticulum.* Glycobiology, 2001. **11**(5): p. 61R-70R.
15. Helenius, A. and M. Aebi, *Intracellular functions of N-linked glycans.* Science, 2001. **291**(5512): p. 2364-9.
16. Hammond, C., I. Braakman, and A. Helenius, *Role of N-linked oligosaccharide recognition, glucose trimming, and calnexin in glycoprotein folding and quality control.* Proceedings of the National Academy of Sciences, 1994. **91**(3): p. 913-917.

17. Paulson, J.C., *Glycoproteins: what are the sugar chains for?* Trends in Biochemical Sciences, 1989. **14**(7): p. 272-276.
18. Lehrman, M.A., *Stimulation of N-linked glycosylation and lipid-linked oligosaccharide synthesis by stress responses in metazoan cells.* Crit Rev Biochem Mol Biol, 2006. **41**(2): p. 51-75.
19. Rasheva, V.I. and P.M. Domingos, *Cellular responses to endoplasmic reticulum stress and apoptosis.* Apoptosis, 2009. **14**(8): p. 996-1007.
20. Ellgaard, L. and A. Helenius, *Quality control in the endoplasmic reticulum.* Nat Rev Mol Cell Biol, 2003. **4**(3): p. 181-91.
21. Parodi, A.J., *Role of N-oligosaccharide endoplasmic reticulum processing reactions in glycoprotein folding and degradation.* Biochem J, 2000. **348 Pt 1**: p. 1-13.
22. Plemper, R.K. and D.H. Wolf, *Retrograde protein translocation: ERADication of secretory proteins in health and disease.* Trends in Biochemical Sciences, 1999. **24**(7): p. 266-270.
23. Bonifacino, J.S. and A.M. Weissman, *Ubiquitin and the control of protein fate in the secretory and endocytic pathways.* Annu Rev Cell Dev Biol, 1998. **14**: p. 19-57.
24. Kopito, R.R., *ER quality control: the cytoplasmic connection.* Cell, 1997. **88**(4): p. 427-30.
25. Schekman, R. and L. Orci, *Coat proteins and vesicle budding.* Science, 1996. **271**(5255): p. 1526-33.
26. Jaeken, J. and G. Matthijs, *Congenital disorders of glycosylation.* Annu Rev Genomics Hum Genet, 2001. **2**: p. 129-51.
27. Freeze, H.H. and M. Aebi, *Altered glycan structures: the molecular basis of congenital disorders of glycosylation.* Curr Opin Struct Biol, 2005. **15**(5): p. 490-8.
28. Jaeken, J., et al., *CDG nomenclature: time for a change!* Biochim Biophys Acta, 2009. **1792**(9): p. 825-6.
29. Haeuptle, M.A. and T. Hennet, *Congenital disorders of glycosylation: an update on defects affecting the biosynthesis of dolichol-linked oligosaccharides.* Human Mutation, 2009. **30**(12): p. 1628-1641.
30. Hennet, T., *Diseases of glycosylation beyond classical congenital disorders of glycosylation.* Biochim Biophys Acta, 2012.
31. Schachter, H. and H.H. Freeze, *Glycosylation diseases: quo vadis?* Biochim Biophys Acta, 2009. **1792**(9): p. 925-30.
32. Leroy, J.G., *Congenital disorders of N-glycosylation including diseases associated with O- as well as N-glycosylation defects.* Pediatr Res, 2006. **60**(6): p. 643-56.
33. Hülsmeier, A.J., P. Paesold-Burda, and T. Hennet, *N-Glycosylation Site Occupancy in Serum Glycoproteins Using Multiple Reaction Monitoring Liquid Chromatography-Mass Spectrometry.* Molecular & Cellular Proteomics, 2007. **6**(12): p. 2132-2138.
34. Jaeken, J., et al., *Sialic acid-deficient serum and cerebrospinal fluid transferrin in a newly recognized genetic syndrome.* Clinica Chimica Acta, 1984. **144**(2–3): p. 245-247.
35. Stibler, H. and J. Jaeken, *Carbohydrate deficient serum transferrin in a new systemic hereditary syndrome.* Arch Dis Child, 1990. **65**(1): p. 107-11.
36. Körner, C., L. Lehle, and K. von Figura, *Abnormal synthesis of mannose 1-phosphate derived carbohydrates in carbohydrate-deficient glycoprotein syndrome type I fibroblasts with phosphomannomutase deficiency.* Glycobiology, 1998. **8**(2): p. 165-171.

37. Rush, J.S., et al., *Mannose supplementation corrects GDP-mannose deficiency in cultured fibroblasts from some patients with Congenital Disorders of Glycosylation (CDG).* Glycobiology, 2000. **10**(8): p. 829-35.
38. Van Schaftingen, E. and J. Jaeken, *Phosphomannomutase deficiency is a cause of carbohydrate-deficient glycoprotein syndrome type I.* FEBS Lett, 1995. **377**(3): p. 318-20.
39. Panneerselvam, K. and H.H. Freeze, *Mannose corrects altered N-glycosylation in carbohydrate-deficient glycoprotein syndrome fibroblasts.* J Clin Invest, 1996. **97**(6): p. 1478-87.
40. Powell, L.D., et al., *Carbohydrate-deficient glycoprotein syndrome: not an N-linked oligosaccharide processing defect, but an abnormality in lipid-linked oligosaccharide biosynthesis?* J Clin Invest, 1994. **94**(5): p. 1901-1909.
41. Krasnewich, D.M., et al., *Abnormal synthesis of dolichol-linked oligosaccharides in carbohydrate-deficient glycoprotein syndrome.* Glycobiology, 1995. **5**(5): p. 503-10.
42. Grunewald, S., *The clinical spectrum of phosphomannomutase 2 deficiency (CDG-Ia).* Biochim Biophys Acta, 2009. **1792**(9): p. 827-34.
43. Harrison, H.H., et al., *Multiple serum protein abnormalities in carbohydrate-deficient glycoprotein syndrome: pathognomonic finding of two-dimensional electrophoresis?* Clinical Chemistry, 1992. **38**(7): p. 1390-2.
44. Henry, H., et al., *Microheterogeneity of serum glycoproteins and their liver precursors in patients with carbohydrate-deficient glycoprotein syndrome type I: Apparent deficiencies in clusterin and serum amyloid P.* Journal of Laboratory and Clinical Medicine, 1997. **129**(4): p. 412-421.
45. Gu, J., et al., *Oligosaccharide structures of immunoglobulin G from two patients with carbohydrate-deficient glycoprotein syndrome.* Glycoconjugate Journal, 1994. **1**(4): p. 247-252.
46. Seta, N., et al., *Diagnostic value of Western blotting in carbohydrate-deficient glycoprotein syndrome.* Clinica Chimica Acta, 1996. **254**(2): p. 131-140.
47. Yuasa, I., et al., *Carbohydrate-deficient glycoprotein syndrome: electrophoretic study of multiple serum glycoproteins.* Brain and Development, 1995. **17**(1): p. 13-19.
48. Van Geet, C. and J. Jaeken, *A unique pattern of coagulation abnormalities in carbohydrate-deficient glycoprotein syndrome.* Pediatr Res, 1993. **33**(5): p. 540-1.
49. Stibler, H., U. Holzbach, and B. Kristiansson, *Isoforms and levels of transferrin, antithrombin, alpha(1)-antitrypsin and thyroxine-binding globulin in 48 patients with carbohydrate-deficient glycoprotein syndrome type I.* Scand J Clin Lab Invest, 1998. **58**(1): p. 55-61.
50. Stibler, H., et al., *Complex functional and structural coagulation abnormalities in the carbohydrate-deficient glycoprotein syndrome type I.* Blood Coagulation & Fibrinolysis, 1996. **7**(2): p. 118-126.
51. Iijima, K., et al., *Hemostatic studies in patients with carbohydrate-deficient glycoprotein syndrome.* Thrombosis Research, 1994. **76**(2): p. 193-198.
52. de Zegher, F. and J. Jaeken, *Endocrinology of the carbohydrate-deficient glycoprotein syndrome type 1 from birth through adolescence.* Pediatr Res, 1995. **37**(4 Pt 1): p. 395-401.

53. Ohzeki, T., et al., *Carbohydrate-deficient glycoprotein syndrome in a girl with hypogonadism due to inactive follicle stimulating hormone.* Horm Metab Res, 1993. **25**(12): p. 646-8.
54. Barone, R., et al., *Lysosomal enzyme activities in serum and leukocytes from patients with carbohydrate-deficient glycoprotein syndrome type IA (phosphomannomutase deficiency).* J Inherit Metab Dis, 1998. **21**(2): p. 167-72.
55. Ohno, K., et al., *The carbohydrate deficient glycoprotein syndrome in three Japanese children.* Brain Dev, 1992. **14**(1): p. 30-5.
56. Jaeken, J., H. Stibler, and B. Hagberg, *The carbohydrate-deficient glycoprotein syndrome. A new inherited multisystemic disease with severe nervous system involvement.* Acta Paediatr Scand Suppl, 1991. **375**: p. 1-71.
57. Stibler, H., J. Jaeken, and B. Kristiansson, *Biochemical Characteristics and Diagnosis of the Carbohydrate-deficient Glycoprotein Syndrome.* Acta Pædiatrica, 1991. **80**: p. 21-31.
58. Grünewald, S., et al., *β-Trace protein in human cerebrospinal fluid: a diagnostic marker for N-glycosylation defects in brain.* Biochimica et Biophysica Acta (BBA) - Molecular Basis of Disease, 1999. **1455**(1): p. 54-60.
59. HE, P., et al., *Identification of intercellular cell adhesion molecule 1 (ICAM-1) as a hypo-glycosylation marker in congenital disorders of glycosylation cells.* Journal of Biological Chemistry, 2012.
60. Marquardt, T., et al., *Carbohydrate-deficient glycoprotein syndrome (CDGS)--glycosylation, folding and intracellular transport of newly synthesized glycoproteins.* Eur J Cell Biol, 1995. **66**(3): p. 268-73.
61. Bergmann, M., et al., *Abnormal surface expression of sialoglycans on B lymphocyte cell lines from patients with carbohydrate deficient glycoprotein syndrome I A (CDGS I A).* Glycobiology, 1998. **8**(10): p. 963-972.
62. Dupré, T., et al., *Defect in N-glycosylation of proteins is tissue-dependent in Congenital Disorders of Glycosylation Ia.* Glycobiology, 2000. **10**(12): p. 1277-1281.
63. Di Rocco, M., et al., *Carbohydrate-deficient glycoprotein syndromes: the Italian experience.* J Inherit Metab Dis, 2000. **23**(4): p. 391-5.
64. Eeg-Olofsson, K.E. and J.A.N. Wahlstrom, *Genetic and Epidemiological Aspects of the Carbohydrate-deficient Glycoprotein Syndrome.* Acta Pædiatrica, 1991. **80**: p. 63-65.
65. Martinsson, T., et al., *Linkage of a locus for carbohydrate-deficient glycoprotein syndrome type I (CDG1) to chromosome 16p, and linkage disequilibrium to microsatellite marker D16S406.* Hum Mol Genet, 1994. **3**(11): p. 2037-42.
66. Matthijs, G., et al., *Evidence for Genetic Heterogeneity in the Carbohydrate-Deficient Glycoprotein Syndrome Type I (CDG1).* Genomics, 1996. **35**(3): p. 597-599.
67. Matthijs, G., et al., *Mutations in PMM2, a phosphomannomutase gene on chromosome 16p13, in carbohydrate-deficient glycoprotein type I syndrome (Jaeken syndrome).* Nat Genet, 1997. **16**(1): p. 88-92.
68. Schollen, E., et al., *Lack of Hardy-Weinberg equilibrium for the most prevalent PMM2 mutation in CDG-Ia (congenital disorders of glycosylation type Ia).* Eur J Hum Genet, 2000. **8**(5): p. 367-71.
69. Matthijs, G., et al., *Lack of homozygotes for the most frequent disease allele in carbohydrate-deficient glycoprotein syndrome type 1A.* Am J Hum Genet, 1998. **62**(3): p. 542-50.

70. Thiel, C., et al., *Targeted disruption of the mouse phosphomannomutase 2 gene causes early embryonic lethality.* Mol Cell Biol, 2006. **26**(15): p. 5615-20.
71. Panneerselvam, K., et al., *Abnormal Metabolism of Mannose in Families with Carbohydrate-Deficient Glycoprotein Syndrome Type 1.* Biochemical and Molecular Medicine, 1997. **61**(2): p. 161-167.
72. Giurgea, I., et al., *Underdiagnosis of mild congenital disorders of glycosylation type Ia.* Pediatric Neurology, 2005. **32**(2): p. 121-123.
73. Grunewald, S., et al., *High residual activity of PMM2 in patients' fibroblasts: possible pitfall in the diagnosis of CDG-Ia (phosphomannomutase deficiency).* Am J Hum Genet, 2001. **68**(2): p. 347-54.
74. Westphal, V., et al., *A frequent mild mutation in ALG6 may exacerbate the clinical severity of patients with congenital disorder of glycosylation Ia (CDG-Ia) caused by phosphomannomutase deficiency.* Hum Mol Genet, 2002. **11**(5): p. 599-604.
75. Damen, G., et al., *Gastrointestinal and other clinical manifestations in 17 children with congenital disorders of glycosylation type Ia, Ib, and Ic.* J Pediatr Gastroenterol Nutr, 2004. **38**(3): p. 282-7.
76. Clayton, P.T., B.G. Winchester, and G. Keir, *Hypertrophic obstructive cardiomyopathy in a neonate with the carbohydrate-deficient glycoprotein syndrome.* J Inherit Metab Dis, 1992. **15**(6): p. 857-61.
77. de Lonlay, P., et al., *A broad spectrum of clinical presentations in congenital disorders of glycosylation I: a series of 26 cases.* Journal of Medical Genetics, 2001. **38**(1): p. 14-19.
78. Coman, D., et al., *The skeletal manifestations of the congenital disorders of glycosylation.* Clin Genet, 2008. **73**(6): p. 507-15.
79. Schade van Westrum, S.M., et al., *Skeletal dysplasia and myelopathy in congenital disorder of glycosylation type IA.* J Pediatr, 2006. **148**(1): p. 115-7.
80. Petersen, M.B., et al., *Early manifestations of the carbohydrate-deficient glycoprotein syndrome.* The Journal of Pediatrics, 1993. **122**(1): p. 66-70.
81. Jaeken, J. and H. Carchon, *The carbohydrate-deficient glycoprotein syndromes: an overview.* J Inherit Metab Dis, 1993. **16**(5): p. 813-20.
82. Fiumara, A., et al., *Carbohydrate deficient glycoprotein syndrome type I: ophthalmic aspects in four Sicilian patients.* British Journal of Ophthalmology, 1994. **78**(11): p. 845-846.
83. Casteels, I., et al., *Evolution of ophthalmic and electrophysiological findings in identical twin sisters with the carbohydrate deficient glycoprotein syndrome type 1 over a period of 14 years.* British Journal of Ophthalmology, 1996. **80**(10): p. 900-902.
84. Miller, B.S. and H.H. Freeze, *New disorders in carbohydrate metabolism: congenital disorders of glycosylation and their impact on the endocrine system.* Rev Endocr Metab Disord, 2003. **4**(1): p. 103-13.
85. Shanti, B., et al., *Congenital disorder of glycosylation type Ia: Heterogeneity in the clinical presentation from multivisceral failure to hyperinsulinaemic hypoglycaemia as leading symptoms in three infants with phosphomannomutase deficiency.* J Inherit Metab Dis, 2009.
86. Barone, R., et al., *Clinical phenotype correlates to glycoprotein phenotype in a sib pair with CDG-Ia.* American Journal of Medical Genetics Part A, 2008. **146A**(16): p. 2103-2108.

87. Coman, D., et al., *Congenital disorder of glycosylation type 1a: Three siblings with a mild neurological phenotype.* Journal of Clinical Neuroscience, 2007. **14**(7): p. 668-672.
88. Drouin-Garraud, V., et al., *Neurological presentation of a congenital disorder of glycosylation CDG-Ia: Implications for diagnosis and genetic counseling.* American Journal of Medical Genetics, 2001. **101**(1): p. 46-49.
89. Matthijs, G., et al., *PMM (PMM1), the human homologue of SEC53 or yeast phosphomannomutase, is localized on chromosome 22q13.* Genomics, 1997. **40**(1): p. 41-7.
90. Pirard, M., et al., *Kinetic properties and tissular distribution of mammalian phosphomannomutase isozymes.* Biochem J, 1999. **339 (Pt 1)**: p. 201-7.
91. Pirard, M., et al., *Comparison of PMM1 with the phosphomannomutases expressed in rat liver and in human cells.* FEBS Lett, 1997. **411**(2–3): p. 251-254.
92. Cromphout, K., et al., *The normal phenotype of Pmm1-deficient mice suggests that Pmm1 is not essential for normal mouse development.* Mol Cell Biol, 2006. **26**(15): p. 5621-35.
93. Veiga-da-Cunha, M., et al., *Mammalian phosphomannomutase PMM1 is the brain IMP-sensitive glucose-1,6-bisphosphatase.* J Biol Chem, 2008. **283**(49): p. 33988-93.
94. Niehues, R., et al., *Carbohydrate-deficient glycoprotein syndrome type Ib. Phosphomannose isomerase deficiency and mannose therapy.* J Clin Invest, 1998. **101**(7): p. 1414-20.
95. Jaeken, J., et al., *Phosphomannose isomerase deficiency: a carbohydrate-deficient glycoprotein syndrome with hepatic-intestinal presentation.* Am J Hum Genet, 1998. **62**(6): p. 1535-9.
96. Babovic-Vuksanovic, D., et al., *Severe hypoglycemia as a presenting symptom of carbohydrate-deficient glycoprotein syndrome.* J Pediatr, 1999. **135**(6): p. 775-81.
97. de Lonlay, P., et al., *Hyperinsulinemic hypoglycemia as a presenting sign in phosphomannose isomerase deficiency: A new manifestation of carbohydrate-deficient glycoprotein syndrome treatable with mannose.* J Pediatr, 1999. **135**(3): p. 379-83.
98. Schollen, E., et al., *Genomic organization of the human phosphomannose isomerase (MPI) gene and mutation analysis in patients with congenital disorders of glycosylation type Ib (CDG-Ib).* Human Mutation, 2000. **16**(3): p. 247-252.
99. Eklund, E.A. and H.H. Freeze, *The congenital disorders of glycosylation: a multifaceted group of syndromes.* NeuroRx, 2006. **3**(2): p. 254-63.
100. Freeze, H.H., *Genetic defects in the human glycome.* Nat Rev Genet, 2006. **7**(7): p. 537-551.
101. Freeze, H.H., *Towards a therapy for phosphomannomutase 2 deficiency, the defect in CDG-Ia patients.* Biochim Biophys Acta, 2009. **1792**(9): p. 835-40.
102. Harms, H.K., et al., *Oral mannose therapy persistently corrects the severe clinical symptoms and biochemical abnormalities of phosphomannose isomerase deficiency.* Acta Paediatr, 2002. **91**(10): p. 1065-72.
103. Kjaergaard, S., et al., *Failure of short-term mannose therapy of patients with carbohydrate-deficient glycoprotein syndrome type 1A.* Acta Paediatr, 1998. **87**(8): p. 884-8.
104. Mayatepek, E. and D. Kohlmüller, *Mannose supplementation in carbohydrate-deficient glycoprotein syndrome type I and phosphomannomutase deficiency.* European Journal of Pediatrics, 1998. **157**(7): p. 605-606.

105. Gao, N., J. Shang, and M.A. Lehrman, *Analysis of glycosylation in CDG-Ia fibroblasts by fluorophore-assisted carbohydrate electrophoresis: implications for extracellular glucose and intracellular mannose 6-phosphate.* J Biol Chem, 2005. **280**(18): p. 17901-9.
106. Gao, N., et al., *Mannose-6-phosphate regulates destruction of lipid-linked oligosaccharides.* Mol Biol Cell, 2011. **22**(17): p. 2994-3009.
107. Mavilio, F. and G. Ferrari, *Genetic modification of somatic stem cells. The progress, problems and prospects of a new therapeutic technology.* EMBO Rep, 2008. **9 Suppl 1**: p. S64-9.
108. Menniti, M., et al., *Serum and glucocorticoid-regulated kinase Sgk1 inhibits insulin-dependent activation of phosphomannomutase 2 in transfected COS-7 cells.* Am J Physiol Cell Physiol, 2005. **288**(1): p. C148-55.
109. Eklund, E.A., et al., *Hydrophobic Man-1-P derivatives correct abnormal glycosylation in Type I congenital disorder of glycosylation fibroblasts.* Glycobiology, 2005. **15**(11): p. 1084-93.
110. Rutschow, S., et al., *Membrane-permeant derivatives of mannose-1-phosphate.* Bioorg Med Chem, 2002. **10**(12): p. 4043-9.
111. Hardré, R., et al., *Mono, di and tri-mannopyranosyl phosphates as mannose-1-phosphate prodrugs for potential CDG-Ia therapy.* Bioorganic & Medicinal Chemistry Letters, 2007. **17**(1): p. 152-155.
112. Imbach, T., et al., *Deficiency of dolichol-phosphate-mannose synthase-1 causes congenital disorder of glycosylation type Ie.* J Clin Invest, 2000. **105**(2): p. 233-9.
113. Maeda, Y., et al., *Human dolichol-phosphate-mannose synthase consists of three subunits, DPM1, DPM2 and DPM3.* EMBO J, 2000. **19**(11): p. 2475-82.
114. Lefeber, D.J., et al., *Deficiency of Dol-P-Man Synthase Subunit DPM3 Bridges the Congenital Disorders of Glycosylation with the Dystroglycanopathies.* Am J Hum Genet, 2009. **85**(1): p. 76-86.
115. Almeida, A.M., et al., *Hypomorphic promoter mutation in PIGM causes inherited glycosylphosphatidylinositol deficiency.* Nat Med, 2006. **12**(7): p. 846-51.
116. Tiscornia, G., O. Singer, and I.M. Verma, *Production and purification of lentiviral vectors.* Nat. Protocols, 2006. **1**(1): p. 241-245.
117. Schneider, A., et al., *Successful prenatal mannose treatment for congenital disorder of glycosylation-Ia in mice.* Nat Med, 2012. **18**(1): p. 71-73.
118. Silvaggi, N.R., et al., *The X-ray crystal structures of human alpha-phosphomannomutase 1 reveal the structural basis of congenital disorder of glycosylation type 1a.* J Biol Chem, 2006. **281**(21): p. 14918-26.
119. DeRossi, C., et al., *Ablation of mouse phosphomannose isomerase (Mpi) causes mannose 6-phosphate accumulation, toxicity, and embryonic lethality.* J Biol Chem, 2006. **281**(9): p. 5916-27.
120. de la Fuente, M., P.F. Penas, and A. Sols, *Mechanism of mannose toxicity.* Biochem Biophys Res Commun, 1986. **140**(1): p. 51-5.
121. de la Fuente, M. and A. Hernanz, *Enzymes of mannose metabolism in murine and human lymphocytic leukaemia.* Br J Cancer, 1988. **58**(5): p. 567-9.
122. Davis, J.A. and H.H. Freeze, *Studies of mannose metabolism and effects of long-term mannose ingestion in the mouse.* Biochim Biophys Acta, 2001. **1528**(2-3): p. 116-26.
123. Guérardel, Y., et al., *Glycomic survey mapping of zebrafish identifies unique sialylation pattern.* Glycobiology, 2006. **16**(3): p. 244-257.

124. Lieschke, G.J. and P.D. Currie, *Animal models of human disease: zebrafish swim into view.* Nat Rev Genet, 2007. **8**(5): p. 353-367.
125. Chu, J. and K.C. Sadler, *New school in liver development: lessons from zebrafish.* Hepatology, 2009. **50**(5): p. 1656-63.
126. Summerton, J. and D. Weller, *Morpholino antisense oligomers: design, preparation, and properties.* Antisense Nucleic Acid Drug Dev, 1997. **7**(3): p. 187-95.
127. Hogan, B.M., et al., *Manipulation of gene expression during zebrafish embryonic development using transient approaches.* Methods Mol Biol, 2008. **469**: p. 273-300.
128. LeClair, E.E., et al., *Craniofacial skeletal defects of adult zebrafish Glypican 4 (knypek) mutants.* Dev Dyn, 2009. **238**(10): p. 2550-63.
129. Lin, Y.Y., et al., *Zebrafish Fukutin family proteins link the unfolded protein response with dystroglycanopathies.* Hum Mol Genet, 2011. **20**(9): p. 1763-75.
130. Flanagan-Steet, H., C. Sias, and R. Steet, *Altered chondrocyte differentiation and extracellular matrix homeostasis in a zebrafish model for mucolipidosis II.* Am J Pathol, 2009. **175**(5): p. 2063-75.
131. Song, Y., et al., *Neural and Synaptic Defects in <italic>slytherin</italic>, a Zebrafish Model for Human Congenital Disorders of Glycosylation.* PLoS ONE, 2010. **5**(10): p. e13743.
132. Stanley, P. and T. Okajima, *Roles of glycosylation in Notch signaling.* Curr Top Dev Biol, 2010. **92**: p. 131-64.
133. Haltiwanger, R.S. and J.B. Lowe, *Role of glycosylation in development.* Annu Rev Biochem, 2004. **73**: p. 491-537.
134. Senderek, J., et al., *Hexosamine biosynthetic pathway mutations cause neuromuscular transmission defect.* Am J Hum Genet, 2011. **88**(2): p. 162-72.
135. Sharma, V., et al., *Phosphomannose isomerase inhibitors improve N-glycosylation in selected phosphomannomutase-deficient fibroblasts.* J Biol Chem, 2011. **286**(45): p. 39431-8.
136. Chu, J., et al., *A zebrafish model of congenital disorders of glycosylation with phosphomannose isomerase deficiency reveals an early opportunity for corrective mannose supplementation.* Dis Model Mech, 2012.

FIGURES

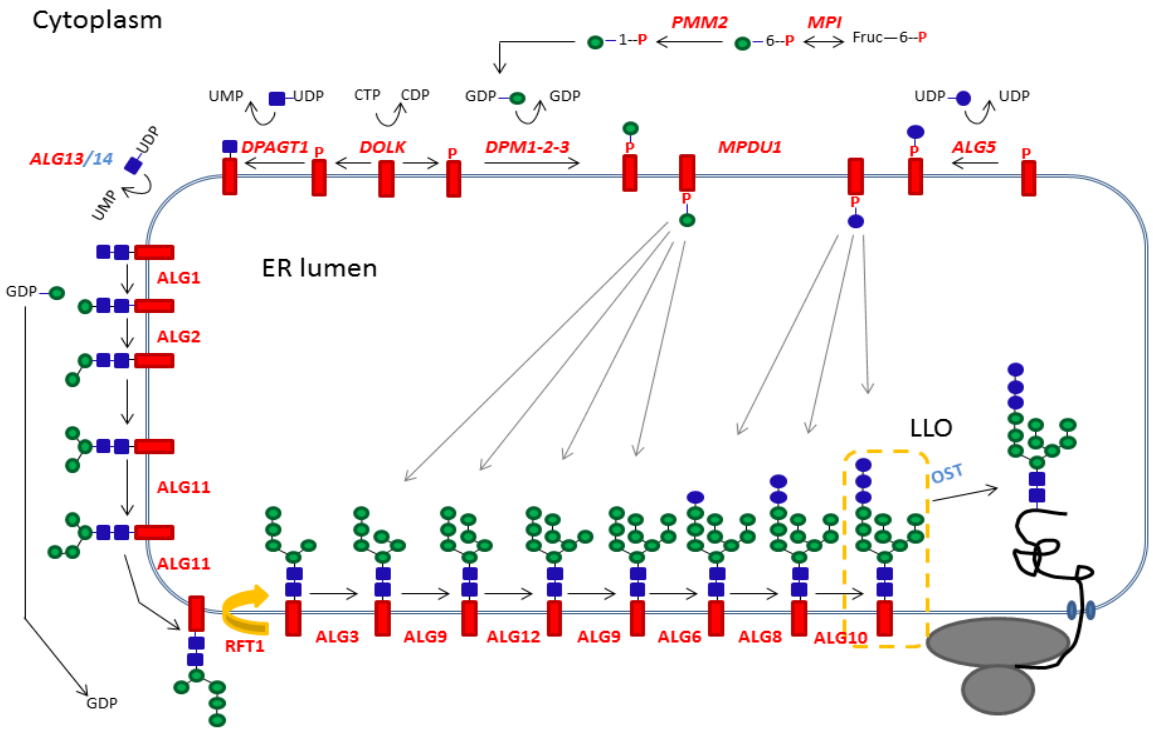

Figure 1.1 Pathway of LLO biosynthesis. Following phosphorylation of the lipid carrier dolichol, two GlcNAc, nine Man, and three Glc are added by various glycosyltransferases. The gene symbols are designated next to the catalyzed reactions. The 15 genes associated with CDG type I are marked in red. Adapted from Haeuptle, M.A. et al.(2009).

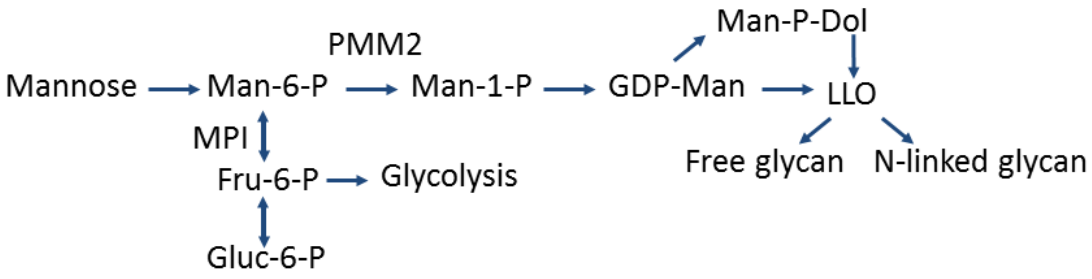

Figure 1.2. Metabolic pathway in glycan synthesis. PMM2-CDG is caused by PMM2 deficiency, which affects the first committed step required for the synthesis of activated mannose donors.

CHAPTER 2: A ZEBRAFISH MODEL OF PMM2-CDG REVEALS CRANIOFACIAL DEFECTS AND ALTERED NEUROGENESIS[1]

[1] Cline, A., et al., *A Zebrafish Model Of PMM2-CDG Reveals Altered Neurogenesis And A Substrate-Accumulation Mechanism For N-Linked Glycosylation Deficiency.* Mol Biol Cell, 2012. Reprinted here with permission of the publisher

ABSTRACT

Congenital Disorder of Glycosylation PMM2-CDG results from mutations in *PMM2*, which encodes the phosphomannomutase that converts mannose-6-P to mannose-1-P. Patients have wide-spectrum clinical abnormalities associated with impaired protein N-glycosylation. In order to explore the developmental consequences of Pmm2 deficiency, we generated a morpholino-based PMM2-CDG model in zebrafish. Morpholinos were successful in decreasing PMM2 activity and morphant embryos had developmental abnormalities consistent with PMM2-CDG patients, including craniofacial defects and impaired motility. Our results show that malformation of the lower jaw is associated with altered chondrocyte morphology. The motility defect, seen most prominently at 3dpf, was found to be associated with altered motor neurogenesis within the spinal cord. Due to the role Notch-Delta plays in neurogenesis, the expressions of several Notch effector genes were examined. The craniofacial and motility defects can be rescued in the majority of the embryos by expression of wild type *pmm2* within the morphant background, indicating that the craniofacial and motility defects are due to a specific reduction in Pmm2 activity.

BACKGROUND

The Congenital Disorders of Glycosylation (CDGs) are a group of heterogenous, hypomorphic, inherited diseases characterized by deficient N-glycosylation, typically detected by underglycosylation of serum glycoproteins.[1, 2] Traditionally divided into two groups, the type I CDGs are classified by genetic defects at loci known to participate in the biosynthesis of the lipid-linked oligosaccharide (LLO) $Glc_3Man_9GlcNAc_2$-P-P-dolichol ($G_3M_9Gn_2$-P-P-Dol), the

glycan donor for N-glycosylation. This includes loci encoding proteins and enzymes involved in sugar and lipid metabolism, endoplasmic reticulum (ER)-localized glycosyltransferases, and proteins that facilitate utilization of substrates [3]. First recognized in the clinic by Jaeken in the 1980s, the most common subtype of CDG is caused by deficiency of the metabolic enzyme, phosphomannomutase 2 (PMM2) [4]. This enzyme converts mannose 6-phosphate (Man-6-P) to mannose 1-phosphate (Man-1-P), the substrate needed for the synthesis of GDP-mannose and the eventual production of LLO. Designated PMM2-CDG (this subtype was formerly referred to as CDG-Ia), patients with this disease exhibit a constellation of symptoms including psychomotor and mental retardation, cerebellar atrophy, peripheral neuropathy, hypotonia, and ataxia [5-7]. There are no current therapies for PMM2-CDG, and little is known about the relationship between the underglycosylation of proteins and the clinical features of the disease [8, 9].

Much of our lack of insight into the pathophysiology of type I CDG can be attributed to the paucity of suitable animal models. While many of the predicted CDG biochemical phenotypes have been confirmed by analyses of LLO and glycoprotein synthesis in cultured fibroblasts and leukocytes from patients, such culture systems fail to recapitulate the more complex physiological relationships that exist within the entire organism, yielding inconsistent results [10]. Attempts to generate viable mouse models for PMM2-CDG, the most common form of CDG, have also been particularly challenging. Complete knockout of PMM2, or knock-in of the most common human PMM2-CDG allele, R137H, into this null background resulted in early embryonic lethality [11]. In contrast, knock-in of another common allele, F118L, resulted in only mild loss of enzymatic activity and no detectable phenotypes [12]. Compound heterozygotes with both the R137H and F118L alleles, however, survived to embryonic day 9.5 [12]. These embryos had reduced staining with wheat germ agglutinin, a plant lectin able to bind

to sialic acid and N-acetylglucosamine residues and therefore capable of detecting several classes of glycoconjugates including N-linked glycans. Strikingly, when the water given to the pregnant dams was supplemented with mannose, many of these embryos were born live, survived past weaning, and regained normal wheat germ agglutinin staining patterns. These data suggest that the R137H/F118L embryos had glycosylation deficiencies that were reversible by maternal mannose supplementation. Despite these findings, a tractable animal model that closely replicates the genetic, developmental, and glycosylation deficiencies documented for PMM2-CDG patients is still needed for a thorough biochemical and behavioral evaluation of the disease mechanisms and experimental treatments.

To overcome the present limitations of PMM2-CDG mouse models, we took advantage of the genetic and experimental attributes of zebrafish (*Danio rerio*), an excellent vertebrate system for both the study of embryonic development and the modeling of genetic diseases. Suppression of *pmm2* expression using a morpholino-based approach resulted in morphant embryos that exhibit several cellular and molecular phenotypes consistent with the human disease, including altered craniofacial cartilage development and impaired motility. These defects can be rescued in the majority of the embryos by expression of wild type *pmm2* within the morphant background, indicating that the craniofacial and motility defects are due to a specific reduction in Pmm2 activity. Together, these results yield new insights into the cellular and molecular basis of type I CDGs and further highlight the utility of the zebrafish system in the investigation of inherited metabolic disorders.

MATERIALS AND METHODS

Fish strains, maintenance, and husbandry

Wild type zebrafish were obtained from the commercial source Fish2U (Gibsonton, FL) and maintained using standard protocols. Embryos were staged according to the criteria established by Kimmel [13]. When necessary pigment formation was inhibited by addition of 0.003% 1-phenyl-2-thiourea (PTU) to embryonic growth medium. Although the data presented are derived primarily from experiments in F2U, all MO-generated phenotypes (e.g. craniofacial and motility defects) were confirmed in multiple genetic backgrounds (AB, TAB14, *fli1a*:EGFP). For analysis of neuronal phenotypes, morphants were generated in the *hb9*:GFP, or the *hb9*:GFP/*sox10*:mRFP transgenic background. Handling and euthanasia of fish for all experiments were carried out in compliance with the University of Georgia's Institutional Animal Care and Use Committee (permit number: A2011 8-144).

Anti-sense morpholino injection and mRNA rescue

Expression of *pmm2* was inhibited by injection of anti-sense morpholinos (MO) into the yolks of 1-2 cell embryos. Translation blocking (5'- GAATCCACGGTAGAGCCAGACATTG-3') and splice blocking (5'-TTCCGCATTAATTCACTCACTTGAC-3') MOs were designed to target either the *pmm2* 5' UTR or the *pmm2* exon 1- intron 1 splice junction, respectively (Gene Tools, Eugene, OR). Optimal MO dosages were determined by Pmm2 activity assays and RT-PCR analyses. Maximal inhibition (33% of control) of Pmm2 activity was achieved following injection of 0.5 nL of a 1μM solution (0.52 μM final concentration) of the splice blocking MO.

The maximal inhibition achievable with the translation blocking MO (60%) was found following injection of 0.5 nl of a 1µM solution (0.52 µM final). In order to facilitate various recovery analyses, the full length coding region of *pmm2* was cloned by RT-PCR from mRNA isolated from 3 dpf embryos using the following primers: (ttccaaatatcacaatgtctggc and tcagctgaaaaagagctccctgcag). The resulting product was cloned into TA site of pCR2.1 (Life Technologies Inc, Grand Island, NY) and subsequently excised by from vector derived EcoRI and XbaI sites. This product was subcloned into pCSII. pCSII-*pmm2* plasmid DNA was linearized with KpnI and full length mRNA generated with Message Machine SP6 kit (Roche Applied Science, Indianapolis, IN.) Rescue experiments were performed by sequential injection of 0.52 µM splice blocking MO and 200 pg of purified *pmm2* mRNA into the yolks of 1-2 cell embryos.

RT-PCR analysis of pmm2 expression and Pmm2/Mpi activity assay

Total RNA was extracted from approximately 30 3 dpf embryos using TRIzol reagent (Invitrogen Corp). RNA was reverse transcribed to cDNA using iScript cDNA Synthesis Kit (Bio-Rad). RT-PCR analysis of *pmm2* expression performed with primers flanking the first intron (tcacaatgtctggctctaccg and gagacattcagcattccattcc). Pmm2 transcript abundance was normalized to RPL4 transcripts. Using this method, we did not detect an accumulation of the larger PCR product expected if the intron were retained in an mRNA exported from the nucleus. This was assessed with two different primer pairs, including one yielding a smaller product to ensure ample amplification. We therefore, conclude that mRNA was reduced by the mechanism of non-sense mediated degradation. For analysis of Pmm2 enzyme activity 50-100 embryos were collected at the indicated time points and the yolks manually removed. Embryos were

lysed in 50 mM Na-HEPES, pH 7.4, sonicated, and total protein quantitated using a microBCA protein assay kit (Pierce). Pmm2/Mpi enzyme activity assays were performed as previously described [14]. Briefly, Pmm2 activity is assayed by a coupled enzyme assay system that relies on the spectrophotometric detection of the reduction of NADP+ to NADPH using Man-1-P as a substrate. Samples were measured 60 minutes after adding the substrate. Units were calculated as mU of enzyme activity/mg of protein based on the change in OD during the reaction time.

Histochemistry, immunohistochemistry, and whole-mount in situ analysis

To visualize craniofacial cartilage embryos were stained with Alcian blue as described previously [15]. Stained animals were photographed on an Olympus SZ16 stereoscope outfitted with a Retiga CCD camera. Morphometric measurements of Alcian blue stained animals were performed using Adobe Photoshop. In order to account for differences in animal size, all measurements were normalized to inter-lens distance. Secondary motoneuron identities were assessed by whole mount immunohistochemistry using the zn-5 antibody (ZIRC, Eugene, OR). Immuno-whole mounts were performed as previously described [15]. Confocal images were acquired on an Olympus FV100 laser-scanning microscope using a 40x (N.A.1.2) water immersion objective. Whole mount *in situ* hybridization for *pmm2, her15.1,* and *her4.3* was performed as previously described by Thisse and Thisse [16].

Motility assays

For assessment of early spontaneous and elicited motility, embryos were dechorionated at 22 hours post-fertilization (hpf) and allowed to age to 24 hpf. The number of spontaneous tail curls was then measured in a 60 second interval. 50 fish were measured at a time from 4

separate injections. Elicited responses were measured at 24 hpf by touching embryos on the head near the otilith and the number and quality of subsequent tail responses recorded. For assessment of later stage elicited motility, 3 dpf embryos were placed in the center of a petri dish marked by three concentric rings. Embryos were touched beside the otilith and their response recorded. Swimming distance of individual embryos was assigned as 1, 2, or 3, according to the number of rings crossed. Zones 1, 2, and 3 had diameters of 3, 6, and 8cm, respectively. 50 fish were measured at a time from 3 separate injections.

RESULTS

Pmm2 activity is significantly reduced in zebrafish embryos using a morpholino-based strategy

In order to inhibit Pmm2 expression, two different anti-sense morpholinos (MO) directed against zebrafish *pmm2* – one that inhibits mRNA translation (translation blocker, TB MO) and one that inhibits mRNA splicing (splice blocker, SB MO) - were tested (**Figure 2.1A**). Over a 0 - 1.77μM concentration range, the degree of knockdown with each morpholino was assessed by either RT-PCR (SB MO) or Pmm2 activity assays (SB and TB MOs). Although morpholinos do not always act by causing loss of their target mRNAs, as shown in **Figure 2.1B**, we observed suppression of *pmm2* transcripts that was maximal with 0.52μM of the SB MO. Surprisingly, in both the F2U strain (used for most of the experiments presented in this study) and the TAB14 strain, *pmm2* transcript abundance increased with higher MO concentrations for reasons that are unclear (**Figure 2.1B** and data not shown). To determine the effect of MO inhibition on enzyme expression, Pmm2 activity was measured in lysates using a coupled assay. Pmm2 activity was

reduced to 33.4% of control with the SB MO, which paralleled the RT-PCR results, and to 58% of control with the TB MO. However, like the corresponding transcript, the enzymatic activity of PMM2 could not be completely suppressed, and rebounded at the highest SB MO concentration, suggesting the presence of compensatory mechanisms (**Figure 2.1C**).

Based upon these considerations, 0.52µM SB MO was used for the remainder of the study. At this concentration, Pmm2 activity was stably reduced for the first 4 days of development (data not shown). Co-injection of the SB MO and full-length *pmm2* mRNA (whose sequence is non-homologous to the SB MO) rescued PMM2 activity to near normal levels, demonstrating the efficacy of the injected mRNA (**Figure 2.1D**). *In situ* hybridization analyses of *pmm2* revealed global expression throughout the heads of control embryos with transcript concentration notably increased in ventral regions (**Figure 2.1E**, arrows highlight ventral concentration). Low levels of *pmm2* expression were also noted in embryonic spinal cords (data not shown). Consistent with decreased enzyme activity, both transcript patterns were clearly reduced in *pmm2* morphant embryos (**Figure 2.1E**).

pmm2 morphants exhibit alterations in craniofacial cartilage development

Motivated by the fact that PMM2-CDG patients exhibit craniofacial and skeletal malformations, we were prompted to analyze developing cartilage in *pmm2* morphants in detail by staining with Alcian blue, a dye that binds acidic components of the extracellular matrix. *pmm2* morphant embryos displayed several defects in cartilage morphogenesis, including protracted Meckel's (M) cartilages, misshapen palatoquadrate (PQ) and ceratohyal (CH) structures, and kinked pectoral fins (**Figure 2. 2A**). Each of these phenotypes was rescued by co-injection of *pmm2* mRNA, suggesting that they were specific to Pmm2 reduction and not

potential off-target MO effects. Furthermore, simultaneous suppression of *pmm2* and *p53* did not ameliorate the craniofacial phenotypes (data not shown), indicating that the *pmm2* MO does not induce these abnormalities by promoting non-specific apoptosis. This is an important consideration, as several studies have shown that one common off-target effect of morpholinos is the induction of p53-directed apoptosis [17, 18].

Morphometric measurements of the cartilage structures showed that they were not only misshapen, but also shorter than control cartilages (**Figure 2.2B**). In addition, the distance between the Meckel's (M) and ceratohyal (CH) cartilages was reduced by 35% in the *pmm2* morphants. With the exception of the length of the CH cartilage, co-injection of *pmm2* mRNA significantly improved the size and shape of the craniofacial cartilages (**Figure 2.1B**). The lack of CH recovery may be accounted for by the fact that this structure finishes developing after the M and PQ structures and may therefore be outside the window of mRNA rescue.

While analyses of control and morphant flat-mounted cartilages showed no significant differences in the total number of cells (data not shown), they did reveal alterations in the morphology of morphant chondrocytes (**Figure 2. 2C**). Unlike control chondrocytes, which were oblong in shape and had converged to form a single line of cells, morphant cells remained round and were arranged in multi-cellular layers, yielding a "cobblestone"-like appearance. To quantitatively measure these differences in cellular shape, the ratio between the short and long axes of individual chondrocytes was calculated. The ratio between these axes was significantly larger in the morphants (**Figure 2.2D**), reflecting increased cellular roundness. Again, co-injection of *pmm2* mRNA restored the typical oblong cellular morphology of the morphant chondrocytes.

To ask whether the alterations in cell shape reflected an early defect in chondrocyte maturation, control and morphant embryos were stained with peanut agglutinin (PNA, a lectin that does not require interaction with mannosyl residues to bind target glycans, and thus is unlikely to be affected directly by Pmm2 deficiency), which labels pre-chondrocytic mesenchymal cells, and type II collagen, one of the earliest markers of chondrocyte differentiation. No differences in the intensity, distribution, or timing of the expression of either marker was detected between control and morphant chondrocytes, suggesting that initial aspects of differentiation are unaffected by *pmm2* knockdown (data not shown). Collectively, these findings indicate that reduced Pmm2 activity is associated with changes in craniofacial cartilage formation, resulting from altered chondrocyte morphogenesis.

pmm2 morphants exhibit multiple motility defects

Because PMM2-CDG patients exhibit hypotonia, ataxia, and delayed motor development, we investigated whether *pmm2* morphants demonstrated motor system defects. These analyses revealed multiple deficits at two developmental stages in morphant embryos when compared to controls. By 1 day post-fertilization (dpf), normal zebrafish embryos exhibit two different motility behaviors: spontaneous movements, consisting of slow alternating tail flexures, and elicited movements, where embryos respond to external stimuli with several rapid tail flexures. Analyses of 1 dpf embryos revealed a slight but significant decrease in the number of spontaneous tail curls generated by *pmm2* morphants (11.0 vs 8.2) (**Figure 2.3A**). In addition, *pmm2* morphants exhibited reduced response to touch at 1 dpf. Although both produced a similar number of tail curls following stimulation, 88% of control embryos responded with a complete curl that made contact with the body. In contrast, the majority of morphant embryos

(75%) only flexed the tip of their tail, never touching the body. By 3 dpf, deficits in touch responsiveness within the *pmm2* morphants were further illustrated by both aberrant escape and swimming behaviors.

To quantify these behaviors, embryos were placed in the center of a plate marked with a series of concentric rings, which were used to assign swimming distances (**Figure 2.3B**). Following stimulation, control embryos robustly swam away from the stimulus ultimately crossing multiple rings. In contrast, morphant embryos typically swam in a circle toward the stimulus, remaining within the first ring. Both the early (1 dpf) and late (3 dpf) stage defects in elicited motility were significantly (in >50% of the embryos assayed) rescued by co-injection of *pmm2* mRNA (**Figure 2.3C**). Together these data suggest that reduction of *pmm2* activity alters embryonic motility behaviors, possibly by affecting aspects of neural or muscular development.

Reduced motility of *pmm2* morphants is associated with abnormal motoneuron development

Previous studies on zebrafish mutants with impaired glycosylation have demonstrated altered migration, organization, and proliferation of multiple classes of motoneurons [19, 20]. In particular, the *slytherin* (*srn*) and *towhead* (*twd*) mutants, which carry distinct mutations in GDP-mannose-4,6-dehydratase (GMDS) - the rate limiting enzyme in fucose metabolism - display increased motor neurogenesis and aberrant migration of motoneuron progenitors, respectively. To determine whether similar defects in neuronal development underlie the *pmm2* motility phenotypes, morphants were generated within the *hb9*:GFP transgenic background, in which both primary and secondary motoneurons express green-fluorescent protein under the control of the *hb9* promoter [21]. Confocal analysis of control and morphant embryos at 1 dpf and 3 dpf

revealed an increase in the number of motoneurons within morphant spinal cords, which was apparent both in the number of cell bodies and in the overall width of motoneuron occupancy within the spinal cord (**Figures 2.4A-B**). Inhibition of Pmm2 activity did not obviously affect the developing skeletal muscle (as assessed with phalloidin staining) or motor axon trajectories and synaptic development. The increase in motoneuron number was rescued in >60% of the animals co-injected with *pmm2* mRNA. Further, morphologic analysis of GFP-labeled cell bodies suggested that the increased motoneuron population was likely restricted to the secondary lineage. Although primary motoneurons, which are typically larger than secondary motoneurons, can be identified by both position and size, embryos were additionally stained with the secondary motoneuron marker zn-5. Analysis of zn-5 confirmed that increase in cell number primarily affected the population of secondary motoneurons (**Figures 2.4C-D**).

Defects in neurogenesis of *pmm2* morphants is not due to Notch-Delta signaling reduction

A role for Notch signaling is well established in early neural development, and is known to regulate neural progenitor maintenance and differentiation in animals.[22-24] In vertebrates, Notch signaling has been shown to inhibit neuronal differentiation, and deficiencies in Notch result in increased numbers of primary motor neurons.[25] The extracellular domain of Notch receptors is glycosylated with O-fucose and O-glucose glycans, as well as N-glycans. Though loss of N-glycans on Notch was not found to cause defective signaling during embryonic development, we investigated if the increased population of secondary motoneurons found in *pmm2*morphants could be due to deficient Notch signaling. [26, 27] Confocal analysis revealed no obvious differences in the number of neuron-associated glia were detected between control and morphant embryos, also shown in **Figure 2.5A**. If Notch signaling was altered in the

*pmm2*morphants and resulting in increased motoneurons, this would be predicted to correlate with a decreased glia.[28] Since no differences in glia were observed between control and *pmm2*morphants, this data suggests that Notch signaling is not affected in the *pmm2*morphants. As an indication of Notch transcriptional activity, we used *in situ* hybridization to examine the expression of several Notch affected genes, including *her15.1*and *her4.3*. No obvious differences were detected in transcript abundance in either the brains or spinal cords of control and morphant embryos (**Figure 2.5B**). The pattern and intensity of staining was indistinguishable between the controls and morphants at 3dpf, the time point at which motility was most severely affected. While this supports the idea that the abnormal neurogenesis noted in the *pmm2* morphants is not due to a reduction in Notch signaling, we cannot at this time rule out this possibility. The differences in transcript amount may not be detectable through *in situ* hybridization, and further analysis with qPCR may be required.

DISCUSSION

PMM2-CDG, the most common and first identified subtype of CDG, provides clear evidence for the importance of proper glycosylation in human physiology. Multisystem abnormalities affecting the development and function of multiple organ systems are manifested by heritable deficiencies in the PMM2 enzyme. This enzyme converts Man-6-P to Man-1-P, the immediate precursor of GDP-mannose. GDP-mannose is required for the biosynthesis of at least four highly distinct classes of mannosyl conjugates (O-linked mannosyl glycans, C-linked mannose, glycosylphosphatidylinositol anchors, and N-linked glycans). Although many studies have demonstrated a clear association between *PMM2* gene defects and aberrant N-glycosylation

of the serum glycoprotein transferrin, the disease has proved to be confounding for both basic scientists and clinicians with regard to its pathophysiology and treatment. The availability of valid, tractable animal models of PMM2-CDG would greatly aid the thorough evaluation of pharmacological approaches, and thus accelerate the search for useful clinical treatments.

Null mutation or knockout of glycosylation genes are embryonic lethal in mice, hindering the development of traditional mammalian CDG models. Knock-in of two different PMM2 mutations frequently found in PMM2-CDG patients yielded different phenotypes. A knock-in of the most common mutation in PMM2-CDG patients resulted in no differences compared to control mice. A knock in of the second most common mutation was then found to be embryonic lethal. The inability of the mouse model for PMM2-CDG to recapitulate patient phenotypes highlights the need for new animal systems to model CDGs.

The zebrafish system is a useful animal model amenable to multiple forms of experimentation, both to explore potential treatments and to provide mechanistic understandings of the systemic abnormalities of the disease. The zebrafish model of *pmm2* deficiency reported here is reminiscent of human PMM2-CDG disease in several important ways: (i) *pmm2* activity is suppressed; (ii) craniofacial defects resonant of PMM2-CDG patients were detected; and (iii) pmm2 morphants displayed pronounced motility defects at both early and late time points. Along with the validation of this system as a CDG model, our observation that increased numbers of spinal motoneurons are associated with *pmm2* deficiency provides novel and unprecedented insight into the cellular basis for the neurological defects associated with PMM2-CDG. This insight will inform the future studies geared at identifying the specific glycoproteins that are responsible for these neurological phenotypes. In light of the fact that over 2,200 N-linked sites

were recently documented in zebrafish [29], the identification of these glycoproteins is beyond the scope of this study.

With a useful animal model now in hand, these insights should enable specific, hypothesis-driven studies aimed at understanding the identified alterations in neurogenesis, as well as the roles of developmental time, tissue specificity, and enzyme concentration in the etiology of PMM2-CDG.

REFERENCES

1. Jaeken, J. and G. Matthijs, *Congenital disorders of glycosylation.* Annu Rev Genomics Hum Genet, 2001. 2: p. 129-51.
2. Marquardt, T. and H. Freeze, *Congenital disorders of glycosylation: glycosylation defects in man and biological models for their study.* Biol Chem, 2001. 382(2): p. 161-77.
3. Haeuptle, M.A. and T. Hennet, *Congenital disorders of glycosylation: an update on defects affecting the biosynthesis of dolichol-linked oligosaccharides.* Hum Mutat, 2009. 30(12): p. 1628-41.
4. Matthijs, G., et al., *Mutations in PMM2, a phosphomannomutase gene on chromosome 16p13, in carbohydrate-deficient glycoprotein type I syndrome (Jaeken syndrome).* Nat Genet, 1997. 16(1): p. 88-92.
5. Freeze, H.H., et al., *Neurology of inherited glycosylation disorders.* Lancet Neurol, 2012. 11(5): p. 453-66.
6. Coman, D., et al., *The skeletal manifestations of the congenital disorders of glycosylation.* Clin Genet, 2008. 73(6): p. 507-15.
7. de Lonlay, P., et al., *A broad spectrum of clinical presentations in congenital disorders of glycosylation I: a series of 26 cases.* J Med Genet, 2001. 38(1): p. 14-9.
8. Freeze, H.H., *Update and perspectives on congenital disorders of glycosylation.* Glycobiology, 2001. 11(12): p. 129R-143R.
9. Freeze, H.H., *Towards a therapy for phosphomannomutase 2 deficiency, the defect in CDG-Ia patients.* Biochim Biophys Acta, 2009. 1792(9): p. 835-40.
10. Gao, N., J. Shang, and M.A. Lehrman, *Analysis of glycosylation in CDG-Ia fibroblasts by fluorophore-assisted carbohydrate electrophoresis: implications for extracellular glucose and intracellular mannose 6-phosphate.* J Biol Chem, 2005. 280(18): p. 17901-9.
11. Thiel, C., et al., *Targeted disruption of the mouse phosphomannomutase 2 gene causes early embryonic lethality.* Mol Cell Biol, 2006. 26(15): p. 5615-20.
12. Schneider, A., et al., *Successful prenatal mannose treatment for congenital disorder of glycosylation-Ia in mice.* Nat Med, 2012. 18(1): p. 71-3.
13. Kimmel, C.B., et al., *Stages of embryonic development of the zebrafish.* Dev Dyn, 1995. 203(3): p. 253-310.
14. Van Schaftingen, E. and J. Jaeken, *Phosphomannomutase deficiency is a cause of carbohydrate-deficient glycoprotein syndrome type I.* FEBS Lett, 1995. 377(3): p. 318-20.
15. Flanagan-Steet, H., C. Sias, and R. Steet, *Altered chondrocyte differentiation and extracellular matrix homeostasis in a zebrafish model for mucolipidosis II.* Am J Pathol, 2009. 175(5): p. 2063-75.
16. Thisse, C. and B. Thisse, *High-resolution in situ hybridization to whole-mount zebrafish embryos.* Nat Protoc, 2008. 3(1): p. 59-69.
17. Ekker, S.C., *Morphants: a new systematic vertebrate functional genomics approach.* Yeast, 2000. 17(4): p. 302-306.
18. Bill, B.R., et al., *A primer for morpholino use in zebrafish.* Zebrafish, 2009. 6(1): p. 69-77.
19. Song, Y., et al., *Neural and synaptic defects in slytherin, a zebrafish model for human congenital disorders of glycosylation.* PLoS One, 2010. 5(10): p. e13743.

20. Ohata, S., et al., *Neuroepithelial cells require fucosylated glycans to guide the migration of vagus motor neuron progenitors in the developing zebrafish hindbrain.* Development, 2009. 136(10): p. 1653-63.
21. Flanagan-Steet, H., et al., *Neuromuscular synapses can form in vivo by incorporation of initially aneural postsynaptic specializations.* Development, 2005. 132(20): p. 4471-81.
22. Louvi, A. and S. Artavanis-Tsakonas, *Notch signalling in vertebrate neural development.* Nat Rev Neurosci, 2006. 7(2): p. 93-102.
23. Pierfelice, T., L. Alberi, and N. Gaiano, *Notch in the vertebrate nervous system: an old dog with new tricks.* Neuron, 2011. 69(5): p. 840-55.
24. Stanley, P. and T. Okajima, *Roles of glycosylation in Notch signaling.* Curr Top Dev Biol, 2010. 92: p. 131-64.
25. Gray, M., et al., *Zebrafish deadly seven functions in neurogenesis.* Dev Biol, 2001. 237(2): p. 306-23.
26. Johansen, K.M., R.G. Fehon, and S. Artavanis-Tsakonas, *The notch gene product is a glycoprotein expressed on the cell surface of both epidermal and neuronal precursor cells during Drosophila development.* J Cell Biol, 1989. 109(5): p. 2427-2440.
27. Haltiwanger, R.S. and J.B. Lowe, *Role of glycosylation in development.* Annu Rev Biochem, 2004. 73: p. 491-537.
28. Park, H.C. and B. Appel, *Delta-Notch signaling regulates oligodendrocyte specification.* Development, 2003. 130(16): p. 3747-55.
29. Zielinska, D.F., et al., *Mapping N-Glycosylation Sites across Seven Evolutionarily Distant Species Reveals a Divergent Substrate Proteome Despite a Common Core Machinery.* Mol Cell, 2012. 46(4): p. 542-8.

FIGURES

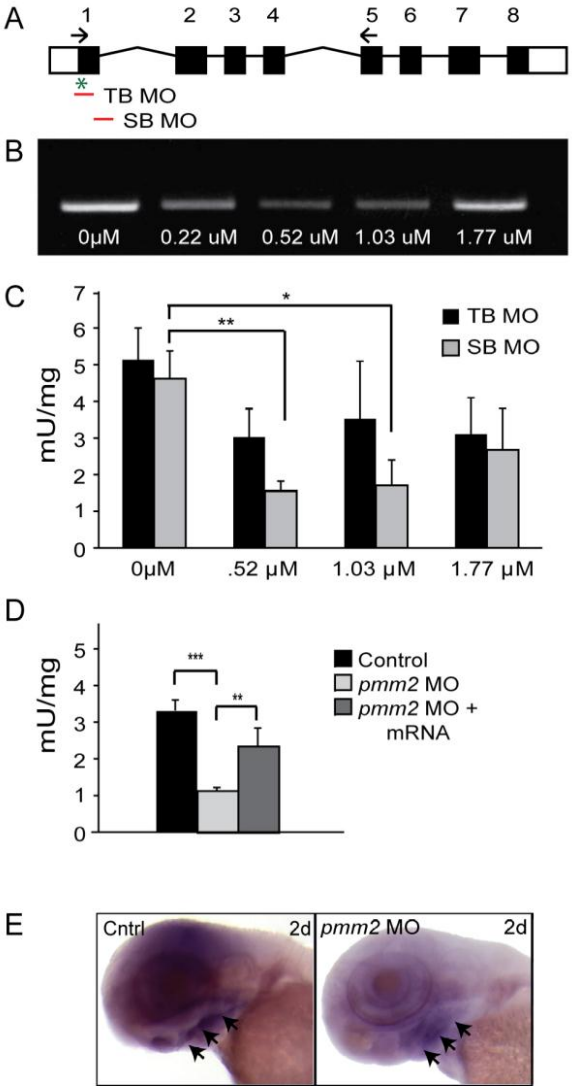

Figure 2.1. Injection of *pmm2* directed anti-sense morpholinos into zebrafish embryos reduces *pmm2* transcript abundance and activity. (A) Schematic representation of *pmm2* gene. The positions of translation blocking (TB) and splice blocking (SB) MOs are indicated, as is the transcriptional start site (*). Arrows indicate position of one set of primers used to assess transcript abundance (see Materials and Methods). **(B)** RT-PCR of 3 dpf embryos following injection of indicated concentrations of SB MO. **(C)** Pmm2 activity measurements of 3 dpf embryos following injection of either the TB or SB MO. *n=4 experiments.* In all places throughout the paper, * (single asterisk) refers to a pvalue<0.05 and ** (double asterisk) refers to a p-value < 0.01 (Student's t-test). **(D)** Measurement of Pmm2 and Mpi activity in 3 dpf control embryos, embryos injected with 0.52 uM SB and mRNA rescued morphants. *n=25 experiments* **(E)** *In situ* analysis of *pmm2* expression in control and *pmm2* morphant (MO) embryos. Arrowheads indicate ventral concentration of staining.

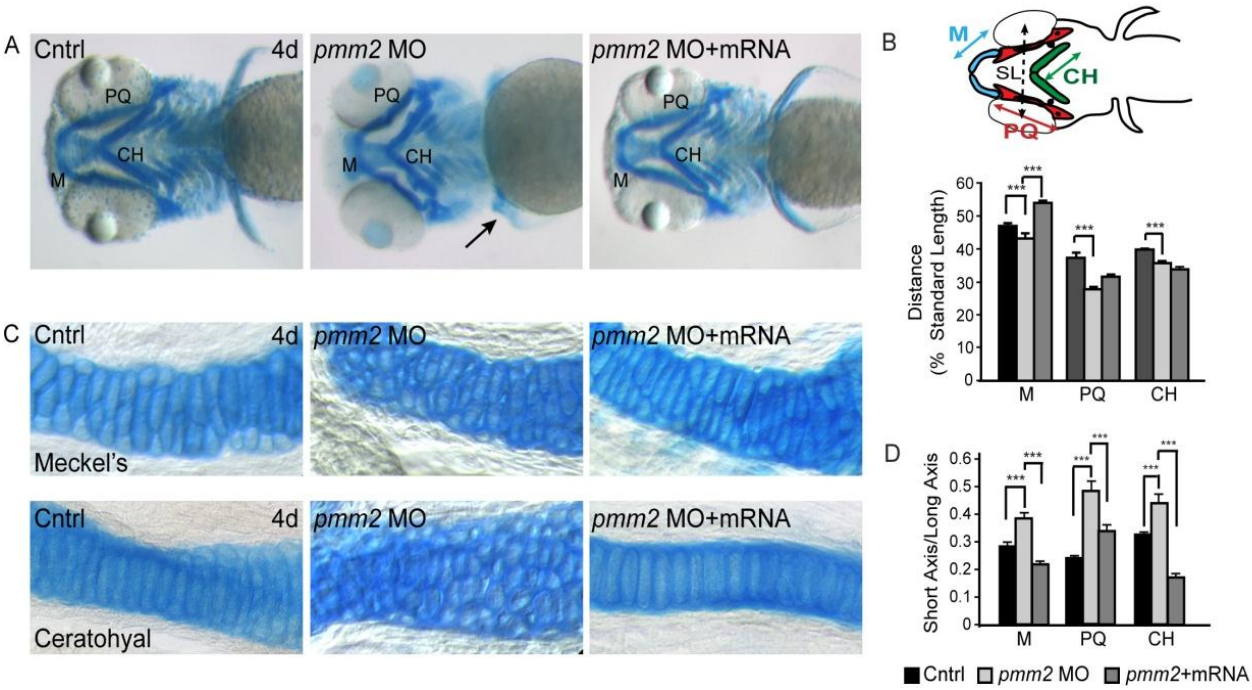

Figure 2. ***pmm2* morphants have dysmorphic craniofacial cartilage. (A)** Alcian blue stains of 4 dpf control and *pmm2* morphant (MO) embryos revealed altered size and shape of Meckel's cartilage (M), as well as the palatoquadrate (PQ) and certohyal (CH) cartilages. These defects were rescued by co-injection of *pmm2* mRNA. n=30-50 embryos per condition over 3 experiments. Arrow shows kinked pectoral fins in the *pmm2* morphants. **(B)** The length of individual structures was measured and normalized to a standard length (SL), which was set as the distance between the eyes. Individual cartilage measurements are outlined in the fish schematic. n=30-50 embryos per condition over 3 experiments. Here and throughout, *** (triple asterisk) refers to a pvalue < 0.001. **(C)** 4 dpf WT, *pmm2* morphant (MO), and *pmm2* mRNA rescued embryos were dissected and the cartilages mounted flat. Analysis of these preparations showed morphant chondrocytes were more round and under intercalated compared to WT chondrocytes. This was rescued by co-injection of *pmm2* mRNA. n=12-15 embryos per condition in 3 experiments. **(D)** Chondrocyte shape was measured in each of the affected structures by determining the ratio of the cells' short axes to their long axes. The closer this number is to 1, the more round the cells. n=12-15 embryos per condition in 3 experiments.

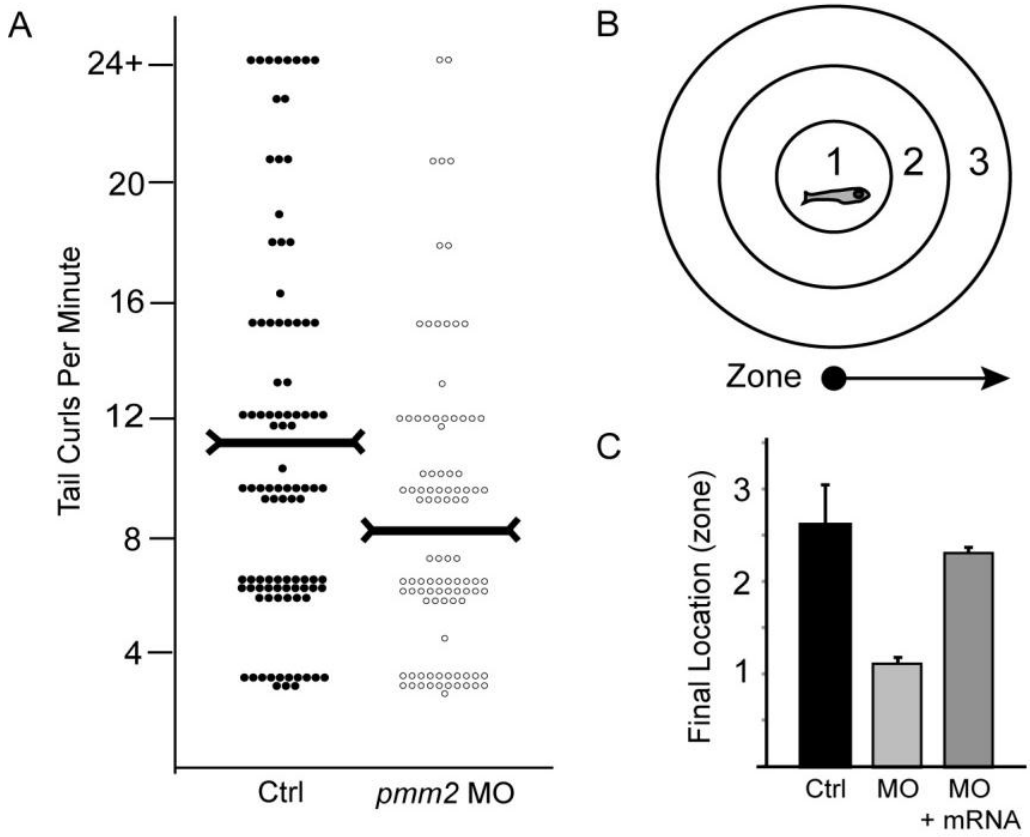

Figure 2.3. *pmm2* morphants exhibit pronounced motility defects. (A) At 1 dpf the number of times control and *pmm2* morphant (MO) embryos spontaneously curled their tails in 1 minute was counted and plotted. Each dot on the scatter plot represents one animal. 225 embryos per condition were scored over five separate experiments. Horizontal markers indicate the median values. **(B)** At 3 dpf the swimming behaviors and "escape" responses of control, morphant and *pmm2* mRNA rescued embryos were assessed by placing individual animals in the center of a petri dish marked with 3 concentric rings. Embryos were lightly touched on the head and their behavior and final destination (zone 1, 2 or 3) recorded. For each condition the average "final location" of 100 embryos from 3 experiments is graphed in **(C)**.

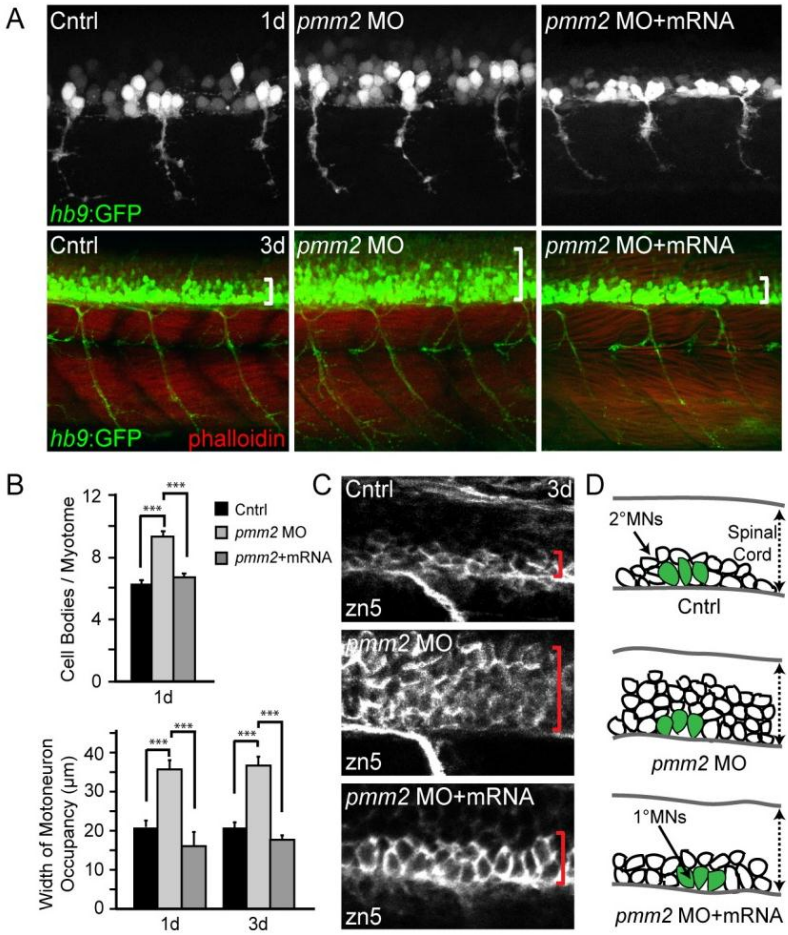

Figure 2.4. ***pmm2*** **morphant spinal cords contain increased numbers of secondary motoneurons. (A)** Confocal images of control and *pmm2* morphant (MO) embryos generated in the *hb9:*GFP background reveal increased numbers of motoneurons at 1 dpf (upper row) and 3 dpf (bottom row) of development. Phalloidin staining of muscle fibers showed no differences in myotomal architecture between control and morphant embryos. White brackets indicate representative distances between the ventral spinal cord and upper end of motoneuron occupancy. n=~30 embryos per condition. **(B)** Quantitation of the number of GFP-positive cell bodies per myotome at 1 dpf and width of motoneuron occupancy within both 1 dpf and 3 dpf embryonic spinal cords demonstrated significant differences between control and *pmm2* morphant (MO) embryos that were rescued by co-injection of *pmm2* mRNA. n= ~30 embryos per condition. **(C)** Whole mount immunohistochemical stains of 3 dpf embryos using the secondary motoneuron marker zn5 show that the majority of neuronal increase occurs in the secondary motoneuron lineage of *pmm2* morphant (MO) embryos. This increase is rescued by co-injection with *pmm2* mRNA. Red brackets delineate the ventral edge of the spinal cord on upper limit of motoneuron occupancy. n= 22 embryos. **(D)** Schematic representation of increased numbers of motoneurons, which appears to primarily affect the secondary motoneuron (MN) population, represented as white cells, while the number of primary motoneurons (MN) is unaltered, represented as large green cells. The dotted arrow shows that the width of the spinal cord (SC) is similar between control (Cntrl), MO, and mRNA rescued embryos.

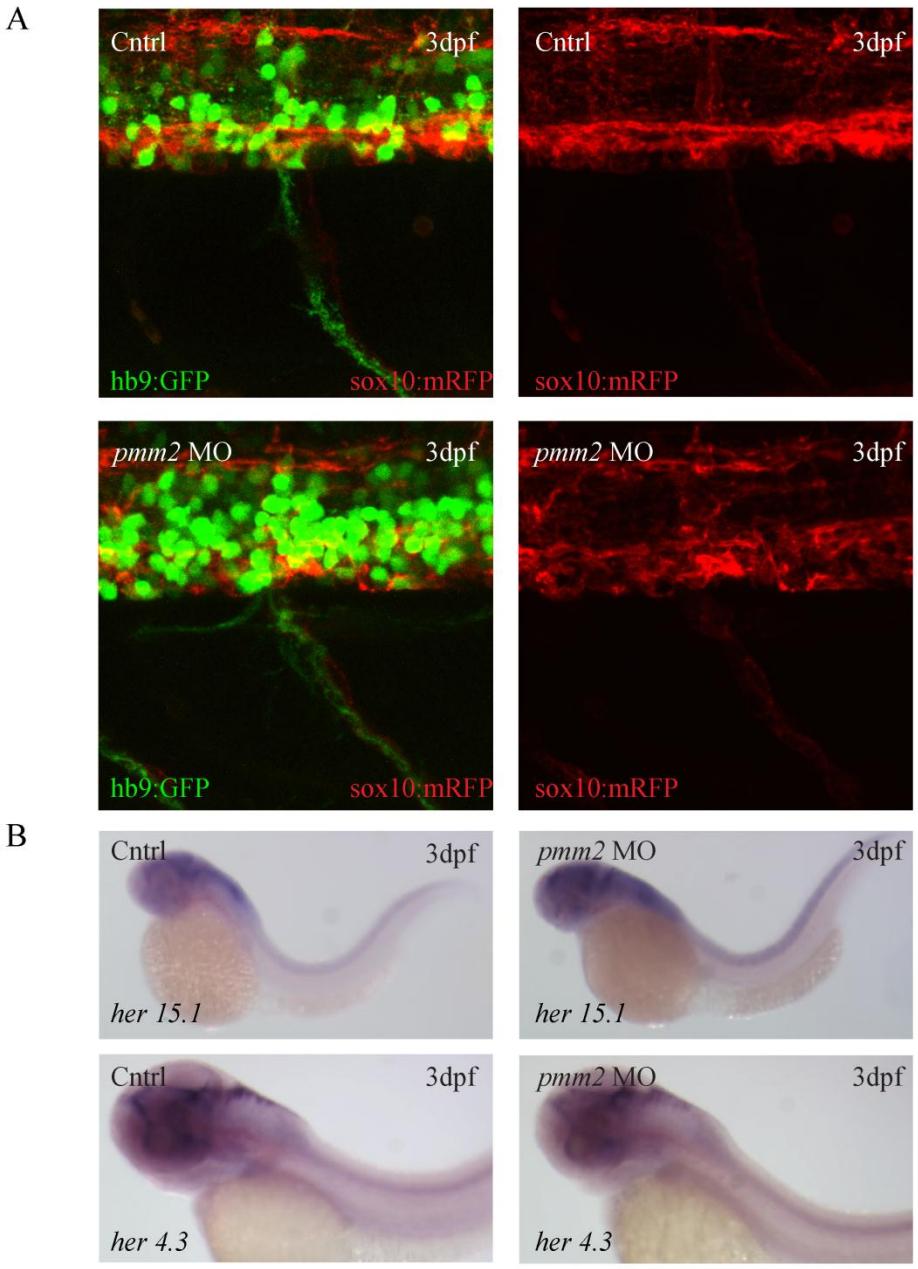

Figure 2.5 *pmm2* morphants do not display altered Notch signaling. (A) Confocal images of control and *pmm2* morphant (MO) embryos generated in the *hb9:*GFP/*sox10*:mRFP background does not reveal increased motorneurons at the expense of decreased glia (Right Panels). **(B)** *In situ* analysis of *her15.1* (Top) and *her4.3* (Bottom) expression in control and *pmm2* morphant (MO) embryos.

CHAPTER 3: A ZEBRAFISH MODEL OF PMM2-CDG UNCOVERS A SUBSTRATE-ACCUMULATION MECHANISM FOR N-LINKED GLYCOSYLATION DEFICIENCY[1]

[1] Cline, A., et al., *A Zebrafish Model Of PMM2-CDG Reveals Altered Neurogenesis And A Substrate-Accumulation Mechanism For N-Linked Glycosylation Deficiency.* Mol Biol Cell, 2012. Reprinted here with permission of the publisher.

ABSTRACT

Mutations in *PMM2* give rise to PMM2-CDG due to deficiency of phosphomannomutase 2 (PMM2), which converts mannose-6-P to mannose-1-P. Though widely proposed that PMM2 deficiency depletes mannose-1-P, a precursor of GDP-mannose, and consequently suppresses lipid-linked oligosaccharide (LLO) levels needed for N-glycosylation, these deficiencies have not been demonstrated in patients or any animal model. We generated a zebrafish model for PMM2-CDG using a morpholino-based strategy to decrease Pmm2 activity. Significantly, global N-linked glycosylation and LLO levels were reduced in *pmm2* morphants. Although insufficient to reduce mannose-1-P and GDP-mannose levels, Pmm2 depletion unexpectedly caused accumulation of mannose-6-P, shown earlier to promote LLO cleavage *in vitro*. In *pmm2* morphants, the free glycan by-products of LLO cleavage increased nearly two-fold. Suppression of the mannose-6-P synthesizing enzyme, mannose phosphate isomerase, within the *pmm2* background normalized mannose-6-P levels and certain aspects of the craniofacial phenotype, and abrogated *pmm2*-dependent LLO cleavage. In summary, we report the first zebrafish model of PMM2-CDG and uncover novel cellular insights not possible with other systems, including a mannose-6-P accumulation mechanism for under-glycosylation.

BACKGROUND

In humans, inherited deficiencies in the N-glycosylation pathway are referred to as the Congenital Disorders of Glycosylation (CDG). CDGs represent multiorgan diseases, with patients displaying psychomotor and intellectual disability, dysmorphic features, hypotonia, and

neurological symptoms.[1] To date, some 45 identified CDG subtypes impair either the synthesis of the lipid linked oligosaccharide (LLO) precursor or the processing of the N-linked oligosaccharide.[2] By far, the most common disorder is PMM2-CDG, which is caused by mutations in *PMM2* encoding phosphomannomutase 2.[3] This enzyme converts Man-6-P to Man-1-P, the immediate precursor for GDP-Man. GDP-Man serves as the mannose donor to the LLO on the cytoplasmic side of the ER, so defects in GDP-Man synthesis are believed to inhibit maturation of the LLO.

Studies using [^{3}H] mannose-labeled LLOs in PMM2-CDG dermal fibroblasts have reported reduced quantities of mature LLO and accumulation of immature LLO intermediates.[4-6] Thus, the PMM2-CDG phenotypes have been explained by an inadequate supply of mature LLO coupled with an overabundance of immature LLO that are poor oligosaccharyltransferse (OST) substrates. Analysis of total [^{3}H]mannose-labeled glycoprotein pools from PMM2-CDG fibroblasts have indicated hypoglycosylation[4-7]; however, studies examining specific N-linked glycoproteins from culture PMM2-CDG fibroblasts found no glycosylation defects.[8-10] This inconsistency has been associated with the low glucose media used in the [^{3}H] mannose pulse-labeling of LLOs. Such media is frequently used to increase labeling of cellular glycoconjugates with sugar precursors. When using media with physiological glucose, PMM2-CDG fibroblasts showed normal glycosylation of glycoproteins. This discrepancy might be explained if LLO synthesis in PMM2-CDG fibroblasts was not seriously defective in physiological glucose. Thus, the basis for the glycosylation deficiency seen in patients required reevaluation.

To address these points, a non-radioactive method was used to quantitatively analyze steady-state LLO pools in PMM2-CDG fibroblasts.[11] In fluorophore-assisted carbohydrate electrophoresis (FACE) analysis, sugar, lipid, and protein fractions of lysates are separated by

ion-exchange columns. The reducing ends of mono and oligosaccharides are then exposed to mild acid hydrolysis and coupled to fluorophores. Products are separated by electrophoretic minigels for detection with UV light. This technique detects sugar phosphates, dolichol-linked glycans such as full length LLO, and free glycans, which are generated from hydrolysis of LLO or by removal of N-glycans from proteins. The remaining protein fraction can also be measure to detect N-linked glycan pools.[12]

FACE analysis of PMM2-CDG fibroblasts revealed that low glucose conditions accounted for previous observations of accumulated [^{3}H]LLO intermediates. When PMM2-CDG fibroblasts were grown in physiological glucose, FACE experiments detected full length LLO without hypoglycosylation. However, FACE analyses demonstrated that PMM2-CDG fibroblasts accumulate Man-6-P, which stimulates LLO hydrolysis and release of free glycan from the dolichol link through interacts with the oligosaccharyltransferase (OST).[11, 13] This cleavage can account for both hypoglycosylation and the clinical failure of dietary mannose therapy in PMM2-CDG patients. Though dietary mannose corrected LLO defects in cultured PMM2-CDG fibroblasts, it failed to improve protein glycosylation or symptoms in PMM2-CDG patients.[6, 14] If hypoglycosylation in PMM2-CDG patients involves an inhibitory effect of Man-6-P, then increases Man-6-P would not rescue LLO levels.

This study also indicated that PMM2-CDG dermal fibroblasts are not adequate models for clinical hypoglycosylation. The lack of a suitable animal model hinders the investigation of CDG pathogenesis and limits the development of therapies for patients. Though mouse models were created, they failed to replicate phenotypes and deficient glycosylation of PMM2-CDG patients.[15] Knock-in of the most common mutation in PMM2-CDG patients resulted was embryonic lethal, while another knock-in of the second most common mutation resulted in

mutant mice indistinguishable from controls. Compound heterozygotes for both mutations survived to embryonic day 9.5 and were noted to have defective glycosylation. Mannose supplementation to pregnant dams overcame the embryonic lethality observed in the compound heterozygous mice, but mannose supplementation did not improve glycosylation profiles seen in PMM2-CDG patients.[14, 15] The inconsistencies seen *in vitro* and in mice emphasize the need for a functional animal model that closely imitates the developmental and glycosylation defects seen in PMM2-CDG patients.

Due to the inadequacies present in PMM2-CDG cell lines and mouse models, we took advantage of the genetic and experimental attributes of zebrafish (*Danio rerio*). This vertebrate system is ideal for both the study of embryogenesis and the modeling of genetic diseases. Using a morpholino-based approach to suppress *pmm2* expression levels, *pmm2* morphant embryos exhibited several cellular and molecular phenotypes consistent with the human disease. Phenotypic analysis revealed altered craniofacial cartilage development, impaired motility, and abnormal neurogenesis. Biochemical investigations uncovered reduced protein N-glycosylation, decreased LLO levels, and accumulation of sugar precursors. Surprisingly, while our analytical methods failed to detect diminished steady-state Man-1-P and GDP-mannose concentrations, an increase in the level of Man-6-P, a Pmm2 substrate, was consistently observed. Additional genetic and biochemical experiments revealed that loss of N-glycosylation in the *pmm2* morphants was best explained by accelerated hydrolysis of LLO triggered by the accumulated Man-6-P, not a deficiency of Man-1-P or GDP-mannose. These results give new understandings into the cellular and molecular basis of type I CDGs, lend support to the concept of flux-based therapy, and emphasize the utility of the zebrafish system in the investigation of inherited metabolic disorders.

MATERIALS AND METHODS

Fish strains, maintenance, and husbandry

Wild type zebrafish were obtained from the commercial source Fish2U (Gibsonton, FL) and maintained using standard protocols. Embryos were staged according to the criteria established by Kimmel [16]. When necessary pigment formation was inhibited by addition of 0.003% 1-phenyl-2-thiourea (PTU) to embryonic growth medium. Although the data presented are derived primarily from experiments in F2U, all MO-generated phenotypes (e.g. craniofacial and motility defects) were confirmed in multiple genetic backgrounds (AB, TAB14, *fli1a*:EGFP). For analysis of neuronal phenotypes, morphants were generated in the *hb9*:GFP transgenic background. Handling and euthanasia of fish for all experiments were carried out in compliance with the University of Georgia's Institutional Animal Care and Use Committee (permit number: A2011 8-144).

Anti-sense morpholino injection and mRNA rescue

Expression of *pmm2* was inhibited by injection of anti-sense morpholinos (MO) into the yolks of 1-2 cell embryos. Translation blocking (5'- GAATCCACGGTAGAGCCAGACATTG-3') and splice blocking (5'-TTCCGCATTAATTCACTCACTTGAC-3') MOs were designed to target either the *pmm2* 5' UTR or the *pmm2* exon 1- intron 1 splice junction, respectively (Gene Tools, Eugene, OR). Optimal MO dosages were determined by Pmm2 activity assays and RT-PCR analyses. Maximal inhibition (33% of control) of Pmm2 activity was achieved following injection of 0.5 nL of a 1μM solution (0.52 μM final concentration) of the splice blocking MO. The maximal inhibition achievable with the translation blocking MO (60%) was found following injection of 0.5 nl of a 1μM solution (0.52 μM final). In order to facilitate various recovery

analyses, the full length coding region of *pmm2* was cloned by RT-PCR from mRNA isolated from 3 dpf embryos using the following primers: (ttccaaatatcacaatgtctggc and tcagctgaaaaagagctccctgcag). The resulting product was cloned into TA site of pCR2.1 (Life Technologies Inc, Grand Island, NY) and subsequently excised by from vector derived EcoRI and XbaI sites. This product was subcloned into pCSII. pCSII-*pmm2* plasmid DNA was linearized with KpnI and full length mRNA generated with Message Machine SP6 kit (Roche Applied Science, Indianapolis, IN.) Rescue experiments were performed by sequential injection of 0.52 μM splice blocking MO and 200 pg of purified *pmm2* mRNA into the yolks of 1-2 cell embryos. For mpi knockdown a translation blocking MO was designed to the 5' portion of the gene. This MO was validated using the described Mpi activity assay (see below) over a range of MO concentrations (see **Table 1**). Because no phenotypic defects resulted in this concentration range, we did not examine the presence of off-target effects by mRNA rescue. However, our recent work has demonstrated that all phenotypic effects caused by injection of higher *mpi* morpholino concentrations are rescued by co-injection of *mpi* mRNA (Chu et al., submitted).

Pmm2/Mpi activity assay

For analysis of Pmm2 enzyme activity 50-100 embryos were collected at the indicated time points and the yolks manually removed. Embryos were lysed in 50 mM Na-HEPES, pH 7.4, sonicated, and total protein quantitated using a microBCA protein assay kit (Pierce). Pmm2/Mpi enzyme activity assays were performed as previously described [3]. Briefly, Pmm2 activity is assayed by a coupled enzyme assay system that relies on the spectrophotometric detection of the reduction of NADP+ to NADPH using Man-1-P as a substrate. Samples were measured 60 minutes after adding the substrate. Units were calculated as mU of enzyme activity/mg of protein

based on the change in OD during the reaction time.

Fluorophore-assisted carbohydrate electrophoresis (FACE) analysis of zebrafish saccharides and glycoconjugates

In the Steet lab, embryos were collected by centrifugation, excess water was removed, 1 mL of methanol (room temperature) was added to the tube, and the contents disrupted by brief probe sonication (Branson Sonifier 150; low setting, 3 x 5 sec pulses). The suspension was transferred to a 15-mL conical tube, and an additional 10-12 mL of methanol was added. Following thorough vortexing, the tubes were capped and sealed with parafilm, and sent by express shipping at room temperature to the Lehrman lab. At that point, samples were dried and processed for FACE analyses as described [13, 17]. In brief, after removal of most lipids by extraction with chloroform:methanol (2:1), aqueous saccharides were recovered by extraction with water, and LLOs were then obtained by extraction with chloroform:methanol:water (10:10:3) with N-linked glycoproteins remaining in the residual material. Ion exchange fractionation of the aqueous saccharides yielded free sugars and free glycans in an uncharged fraction, sugar monophosphates in a weakly anionic fraction, and both nucleotide-sugars and sugar 1,6-bisphosphates in a more strongly anionic fraction. Phosphate esters of the 1-postion of mono- and oligosaccharides were released with weak acid (a condition that retained 6-phosphate esters), and N-glycans were released with peptide N-glycosidase F. All monosaccharide species were then conjugated with 2-aminoacridone (AMAC) and separated on a monosaccharide profiling gel, while all oligosaccharide species were conjugated with 7-amino-1,3-naphthalenedisulfonic acid (ANDS) and detected with an oligosaccharide profiling gel. Where appropriate, standards were included consisting of monosaccharide mixtures, glucose oligomers,

or LLO-derived glycans. Fluorescent saccharide conjugates were detected with a Biorad Fluor-S scanner and quantified with Quantity-One software. Loading of various quantities of standards established that detection was linear, with a sensitivity of ~2 pmol saccharide. For quantitation of free glycan experiments, only the portions in the size range delimited by the G_4 and G_7 standards were used.

RESULTS

Pmm2 deficiency in zebrafish results in global suppression of N-linked glycosylation

Hypoglycosylation of the serum glycoprotein, transferrin, is typically used in the clinical diagnosis of type I CDGs. In the absence of such a validated marker for zebrafish, we quantified the pool of N-glycans in protein fractions from entire animals by release with PNGase F, FACE analysis, and normalization to protein content. Although no qualitative differences were detected in the profile of N-glycans, the size of the pool was reduced on average to 86% of control after *pmm2* knockdown (**Figure 3.1 A and Appendix Figure 1A**). These reductions of N-glycan levels were mitigated by rescue with *pmm2* mRNA, arguing against an off-target effect of the *pmm2* morpholino (**Figure 3.1A)**. Accordingly, it appeared that N-glycan processing was not strongly affected by *pmm2* knockdown, only the amount of glycan transferred to endogenous protein acceptors, which is highly reminiscent of PMM2-CDG patients.

Zebrafish yolk contains a large amount of N-glycosylated proteins (e.g. vitellogenin) that originate from the egg, and therefore are not subject to hypoglycosylation due to injection of *pmm2* morpholinos into embryos. This prompted us to determine whether the presence of yolk was masking a more pronounced change in morphant N-glycan content. As shown in **Appendix Figure 1B**, N-linked glycans were readily observed in zebrafish eggs, and the quantities in

embryos were greatly reduced by removal of yolk. Importantly, removal of yolk from the 4 dpf embryos showed that the N-glycan pool in *pmm2* morphants was actually reduced on average to 54% of control, compared to a value of 78% of control measured when yolks were present (**Figure 3.1B**). This demonstrated a robust masking effect of yolk-derived N-glycans. The qualitative profile of the N-glycans was unchanged in the morphants following yolk removal, again indicating that processing of embryonic N-link glycoproteins was not substantially affected (**Appendix Figure 1B**). The loss of Pmm2 activity and the deficiency of N-glycosylation indicate that the *pmm2* morphants developed here represent a valid zebrafish model of PMM2-CDG disease.

LLO levels are suppressed in *pmm2* morphants

It has been widely hypothesized that hypoglycosylation in PMM2-CDG patients is a result of reduced LLO concentrations, but no direct LLO analyses of patient biopsy material have been reported. Recent mass spectrometry data from PMM2-CDG patient fibroblasts grown in culture with physiological glucose indicate that the PMM2 deficiency creates a significant bottleneck for flux of mannosyl precursors [18]. However, in physiological glucose, PMM2-CDG fibroblasts also have normal steady-state levels of LLO, and have normal glycoform distributions for alpha$_1$-antitrypsin and other N-linked glycoproteins [8-10]. These results leave open the question as to whether LLO levels in patients are truly reduced by PMM2 deficiency.

To begin to address this question, we used FACE to measure steady-state LLO levels in *pmm2* morphants. **Figures 3.1C-D** show that *pmm2* morphants have 58% of control levels of $G_3M_9Gn_2$-P-P-Dol. This amount is returned to normal after rescue by co-injecting *pmm2* mRNA. Moreover, no relative accumulations of LLO intermediates were detected within the

range M_3Gn_2-P-P-Dol - $G_2M_9Gn_2$-P-P-Dol, which is the functional resolution established previously for the FACE system [11]. These results show that LLOs levels are suppressed in this animal model of *pmm2* deficiency, with the most obvious explanation being inhibition of a step prior to the synthesis of M_3Gn_2-P-P-Dol.

Metabolic analysis of *pmm2* morphants demonstrates an accumulation of Man-6-P

In order to elucidate the cause of the LLO deficiency, we subjected 4 dpf (i.e., larval stage) whole embryos to sugar analysis using FACE with reductive amination and fluorescence detection. An obvious caveat to this approach is that it measures sugars in total embryos, averaged over all the individual cell types, and is weighted toward those cells with higher sugar contents. Similarly, the embryos might contain unknown compounds able to interfere with the analysis. In preliminary experiments, we found that whole-embryo sugar phosphate contents were highly variable through 3 dpf, but stabilized somewhat by 4 dpf. Consequently, we opted to analyze sugars in 4 dpf embryos.

An obvious explanation for LLO deficiency in *pmm2* morphants is a reduction in the synthesis of Man-1-P (which requires Pmm2 activity), and consequently lower concentrations of GDP-mannose that limit early mannose-dependent steps of LLO synthesis. FACE offers an advantage over other analytical methods in that sugar phosphates (Man-1-P and Man-6-P) and nucleotide sugars (like GDP-mannose) can be recovered from the same samples used for the earlier measurements of LLOs and N-glycans. Although they were only weakly detected by FACE due to the limited amounts of embryonic material, surprisingly we did not observe obvious deficiencies of either Man-1-P or GDP-mannose in *pmm2* morphants (data not shown). Moreover, mannosyl-1,6-bisphosphate (the cofactor for Pmm2) was also unaffected as measured

by FACE. Taken together, our preliminary analyses did not detect any loss of mannosyl precursors in LLO-deficient *pmm2* morphants, although such possibilities cannot be ruled out at this time.

Curiously, our FACE experiments with *pmm2* morphants suggested an increase in Man-6-P, which is readily identified on the same gels used to evaluate Man-1-P (**Figure 3.1C**). FACE analyses of sugars isolated from the same three morphant and rescue samples used for the LLO analysis of **Figure 3.1C** were particularly useful. As shown in **Figure 3.1C**, *pmm2* morphants exhibited an average increase of 1.9-fold in Man-6-P levels, which was reduced by co-injection of *pmm2* mRNA (**Figures 3.1C-D**). This increase in Man-6-P was independently confirmed by an HPLC-based method able to directly assess levels of this sugar phosphate in an aqueous extract (**Appendix Table 1**). Our HPLC method, which could resolve a Man-1-P standard, also failed to reveal any clear decreases in Man-1-P in the *pmm2* morphants. The increase of Man-6-P can be explained by the fact that Man-6-P is normally consumed by Pmm2 for Man-1-P synthesis, and therefore might accumulate in *pmm2* morphants. Interestingly, a recent study provided evidence that under certain conditions Man-6-P could promote the hydrolysis of LLO both in permeabilized and intact cells, causing release of the $G_3M_9Gn_2$ glycan and Dol-P-P [13]. The outcome was loss of LLO with no accumulation of truncated LLO biosynthetic intermediates. Since this result was similar to that observed in *pmm2* morphants (**Figure 3.5**), we designed experiments to test the hypothesis that LLO depletion in the *pmm2* morphants was caused by accumulated Man-6-P (resulting in LLO hydrolysis) rather than loss of Man-1-P and GDP-mannose.

LLO levels in *pmm2* morphants are stabilized by manipulating *mpi*, the gene encoding the Man-6-P-synthesizing enzyme mannose-6-phosphate isomerase

Man-6-P can be formed from fructose-6-P in a reversible reaction catalyzed by mannose phosphate isomerase (*mpi*) (see **Figure 3.1E**). In the disease MPI-CDG, patients have reduced MPI activity and an N-glycosylation deficiency similar to that in PMM2-CDG. There is good evidence that the etiology of MPI-CDG is due to impaired conversion of fructose-6-P to Man-6-P leading to suppressed Man-1-P concentrations [6, 19]. Moreover, morpholino suppression of *mpi* resulted in properties expected for a zebrafish model of MPI-CDG including reduced steady-state levels of LLOs.[20]

In light of these data, we hypothesized that the relative contributions of reduced Man-1-P and excess Man-6-P on the biochemical phenotypes associated with *pmm2* deficiency could be tested by simultaneous knockdown of both *pmm2* and *mpi* (**Figure 3.1E**). If the LLO deficiencies in the *pmm2* and *mpi* morphants were both due solely to lower concentrations of Man-1-P and GDP-mannose, then we would expect a synergistic suppression of LLO levels in double morphants (**Figure 3.1E**, *model A*). Conversely, if higher concentrations of Man-6-P caused the LLO deficiency in *pmm2* morphants, we would predict offsetting effects in double morphants. As indicated in **Figure 3.1E** (*model B*), while *mpi* knockdown might cause LLO deficiency on its own due to Man-1-P depletion, it might also counteract the effect of the *pmm2* knockdown by inhibiting synthesis of Man-6-P. According to model B, the net result of a simultaneous knockdown of *pmm2* and *mpi* could be a loss of LLO no more severe than the loss due to either knockdown alone.

In order to address whether reducing *mpi* levels in the *pmm2* morphant would in fact mitigate the increase of Man-6-P, we generated an *mpi*-targeted translation blocking MO.[20]

Using the described enzyme activity assay, *mpi* knockdown was validated over a range of MO concentrations in control and *pmm2* morphant embryos (**Supplemental Figure 3**). In an effort to lower but not eliminate *mpi* levels, we ultimately chose to work with 0.02 μM, which reduced Mpi activity to 47% and 36% of WT in the control and *pmm2* morphant backgrounds, respectively (**Figure 3.2A**). This degree of suppression, though less robust than that studied in Chu et al. (< 20% *mpi* expression)[20], was nonetheless desirable as it resulted in a re-balance of the normal 1:1.5 ratio of Pmm2:Mpi activity in the *pmm2* morphants **(Supplemental Figure 3**). Although this concentration of the *mpi* MO on its own caused no developmental defects, they were clearly observed with higher degrees of knockdown.[20] Interestingly while morpholino-based suppression of *pmm2* and *mpi*, either separately or combined, resulted in decreased enzymatic activities (**Figure 3.2A**), individual inhibition of *pmm2* expression also consistently resulted in a slight decrease in Mpi activity. However, the same reciprocal decrease in Pmm2 activity was not observed when *mpi* was individually inhibited.

Knockdown of either *pmm2* or *mpi* alone caused the expected losses of LLO **(Figure 3.2B)**. Strikingly, double morphants had LLO concentrations no lower than either individual morphant. In some individual experiments, LLO levels in the double morphants appeared to increase. In four sets of samples, sugar phosphate data obtained by FACE suggested that Man-6-P increased ~175% in the *pmm2* morphant, was not significantly increased in the *mpi* morphant, and returned to control levels in the double morphant (**Figure 3.2B**). Consequently, this genetic approach supports the hypothesis that elevated Man-6-P concentrations make a significant contribution to the LLO deficiency in *pmm2* morphants, a phenotype that cannot be readily explained solely by a loss of Man-1-P.

Free glycans, the products of Man-6-P-dependent LLO cleavage, are increased in *pmm2* morphants

Whether triggered *in vitro* with pure Man-6-P [11], or in cultured cells by activating Man-6-P signaling [13], the cleavage of LLO results in release of free glycans into the ER lumen. These free glycans then appear to undergo remodeling reactions within the secretory pathway, resulting in a heterogeneous mixture. We assessed free glycans in the same sample of *pmm2* morphants utilized for LLO and sugar phosphate analysis (see **Figure 3.2**). As shown in **Figure 3.3A**, total free glycans were increased ~2-fold in *pmm2* morphants, and returned to control levels following co-injection of *pmm2* mRNA. However, there were no obvious qualitative differences in oligoform noted the free glycan pools, suggesting that remodeling reactions in the secretory pathway were unaffected in *pmm2* morphants (**Figure 3.3B**). Consistent with a Man-6-P-driven phenomenon (**Figures 3.3B-C**), the increase in free glycan pool size was suppressed by simultaneous knockdown of *pmm2* and *mpi*.

In previous studies regarding the Man-6-P-dependent production of free glycans in mammalian cells, it was possible to demonstrate by selective permeabilization of plasma membranes that the released glycans were present in lumenal, not cytosolic compartments [13]. This was not feasible in our zebrafish system and, in principle, the results could be due to greater production of cytosolic free glycans generated by ER-associated degradation (ERAD) of glycoproteins that failed to fold due to impaired acquisition of N-glycans. However, this is unlikely for two reasons. First, knockdown of *pmm2* did not induce mRNAs encoding GRP78/BiP or CHOP, both markers for ER stress, although *pmm2* message itself was diminished to about 20% of controls (data not shown). Secondly, in deliberate attempts to increase ERAD by exposing mammalian cells to agents that impair folding, there were no changes in cytosolic

free glycans [13]. Consequently, the results of **Figure 3.3** are best explained by increased production of lumenal free glycans from LLO. Taken together, our data with zebrafish *pmm2* morphants strongly support a substrate-accumulation mechanism where elevation of Man-6-P increases LLO hydrolysis, expanding the lumenal free glycan pool, and impairing protein N-glycosylation.

Reducing Mpi levels in the *pmm2* morphant background improves chondrocyte morphology

Although Man-6-P and free glycan levels were normalized in *mpi/pmm2* double morphants, these animals still had their respective enzyme levels reduced to one-third of normal (**Figure3.2A**), and still had appreciable LLO deficiencies (**Figure 3.2B**). For these reasons we did not expect suppression of *mpi* to mitigate all of the phenotypic defects associated with *pmm2* deficiency, and indeed, many *pmm2* morphant phenotypes including the motility deficits were not significantly corrected by *mpi* knockdown. However, analysis of *mpi/pmm2* double morphant embryos demonstrated that there was substantial recovery of the chondrocyte morphology phenotype (**Figure 3.4**). Flat mount preparations of Alcian blue stained embryos revealed that while the size of individual cartilage structures was not significantly changed by *mpi* suppression, the round chondrocyte morphology characteristic of *pmm2* deficiency was corrected (**Figure 3.4A**). In each of the three structures analyzed, *mpi/pmm2* double morphant chondrocytes regained the elongated architecture typical of control chondrocytes (**Figure 3.4B**). Further, the organization of these cells was significantly improved following *mpi* suppression. Unlike *pmm2* morphant cells, which are present in multi-layered stacks of cells, the chondrocytes of *mpi/pmm2* double morphant cartilages have intercalated to form a single cellular layer. It is

noteworthy that, while additional aspects of the *pmm2* morphant phenotypes (in particular motility) were not significantly improved, they were also not exacerbated by additional *mpi* knockdown. These results suggest that while many of the *pmm2* morphant phenotypes associate with reduced Pmm2 enzyme and LLO levels, chondrocyte morphology defects appear to correlate with accumulation of Man-6-P and free glycans.

DISCUSSION

PMM2-CDG demonstrates the importance of proper glycosylation in human physiology. Heritable deficiencies in the PMM2 enzyme result in multisystem abnormalities affecting the development and function of multiple organ systems. PMM2 converts Man-6-P to Man-1-P, the precursor of GDP-mannose, which is required for the biosynthesis of at least four highly distinct classes of mannosyl conjugates (O-linked mannosyl glycans, C-linked mannose, glycosylphosphatidylinositol anchors, and N-linked glycans). Although many studies have demonstrated a clear association between PMM2 gene defects and aberrant N-glycosylation of glycoproteins, this disease perplexes both basic scientists and clinicians with regard to its pathophysiology and treatment.

Recent work by several groups has shown that bypassing defective metabolic steps or enhancing metabolic flux through depleted glycosylation pathways represents a promising mode of therapy for some type I CDGs. [18, 21-23] This concept is perhaps best supported by the clinical improvement of MPI-CDG patients who receive oral mannose supplementation. Recent studies have demonstrated the same phenomenon in zebrafish; *mpi* morphants are rescued with

mannose addition to their water.[20] Uptake of mannose into cells and rapid conversion to Man-6-P circumvents the need for MPI to produce Man-6-P from fructose-6-P.

In contrast, there is no clear clinical benefit for PMM2-CDG patients given mannose supplements. [23] Although mannose-derived Man-6-P in CDG-MPI cells has a direct metabolic path into N-glycans, in CDG-PMM2, the Man-6-P is still dependent upon impaired PMM2 activity for downstream use. While this may help explain the lack of efficacy with mannose supplementation, it also highlights the metabolic complexity that underlies PMM2-CDG. For example, prenatal mannose supplementation was successful in overcoming embryonic lethality in compound heterozygous PMM2 mice bearing a combination of disease alleles, suggesting that the timing of mannose supplementation may be critical.[15] In addition, other studies have provided support for therapeutic strategies for PMM2-CDG that either enhance mannose supplementation, or are entirely independent of it. For example, with cultured CDG-PMM2 fibroblasts, the drug metformin significantly improved the efficiency of mannose correction, by increasing mannose uptake [24]. Treatment of DPM1-CDG fibroblasts with zaragoic acid, which is thought to divert lipid precursors towards dolichol synthesis, was shown to rescue impaired N-glycosylation [25]. By a similar mechanism, high concentrations of ketoconazole were reported to counteract the effects of the glycosylation blocker tunicamycin [26]. By lessening the demand on the LLO biosynthetic pathway, the translation attenuators diamide and disulfiram improved the quality of LLOs and the glycans transferred to protein [27]. And recently, a compound that inhibited MPI diverted mannose-derived Man-6-P away from glycolytic catabolism and toward glycoconjugate production, providing a proof-of-principal for the strategy of enhancing glycosylation in PMM2-CDG cells by altering flux through key metabolic pathways [18, 22]. The availability of valid, tractable animal models of PMM2-CDG

would greatly aid the thorough evaluation of such pharmacological approaches, and thus accelerate the search for useful clinical treatments.

While there is no doubt that PMM2-CDG etiology involves loss of PMM2 expression and can result in hypoglycosylation of N-linked glycoproteins, the biochemical cause like the search for a treatment has remained enigmatic. In physiological (5 mM) glucose, cultured PMM2-CDG fibroblasts have normal LLO levels [11] and do not exhibit abnormal protein glycoforms detectable with immunoblots [8-10]. However, the Pmm2 deficiency in these cells clearly causes a metabolic constriction that can be demonstrated in sub-physiological (2.5 mM) glucose [11], or with physiological concentrations of stable isotopic glucose monitored by mass spectrometry [18]. Moreover, the recently validated marker for glycosylation deficiency, cell-surface ICAM-1, is diminished in PMM2-CDG fibroblasts cultured with physiological glucose and restored upon introduction of a functional Pmm2 gene [28]. The picture is confounded further by chronic ER stress in these cells, which can alter LLO synthesis in several ways [27, 29]. The apparent contradictions in some of these results may originate from differences in the actual disease allele, donor age, and cell passage number. This emphasizes the need for a useful animal model amenable to multiple forms of experimentation, both to explore potential treatments and to provide mechanistic understandings of the systemic abnormalities of the disease.

As previously described, we generated and characterized PMM2-CDG models in zebrafish to further understand the pathogenesis of this disease, to investigate the defective glycosylation pathway, and to develop therapeutic approaches. Although LLO levels were reduced in *pmm2* morphants, the underlying mechanism revealed by our experiments was unexpected. In part due to the limits of sensitivity of our analytical methods, we obtained no

evidence that our suppression of Pmm2 was robust enough to deplete its product, Man-1-P, or its immediate downstream metabolites. Nonetheless, accumulation of the Pmm2 substrate Man-6-P in a manner specific for the genetic lesion was detected. The loss of LLO is most easily explained by Man-6-P promoting LLO hydrolysis, as reported previously in mammalian cells [13]. This conclusion was supported by demonstrating both epistasis with *mpi*, the gene encoding the Man-6-P synthesizing enzyme mannose phosphate isomerase, and the Pmm2-dependent appearance of free glycans that are markers for LLO hydrolysis. While our data shows clear changes in the levels of key metabolic precursors within the *pmm2* morphants, it is unclear at this time whether these changes occur in a tissue-specific manner. In other words, it is possible that certain tissues or cell types such as neurons or chondrocytes are more susceptible to Man-6-P accumulation and LLO hydrolysis than others. Furthermore, we cannot rule out that still other tissues in the embryo are subject to undergycosylation due to loss of Man-1-P and GDP-mannose.

Our studies therefore suggest that two separate and potentially synergistic mechanisms of LLO loss and glycosylation deficiency, that may differ in significance depending upon the cell and tissue type, and the point in development, should be considered in PMM2-CDG: absence of Man-1-P, limiting the synthesis of mannosyl conjugates; and excess Man-6-P causing hydrolysis of LLO. The latter mechanism also raises the possibility of processed, lumenal free glycans acting as competitive inhibitors of vesicular lectin-dependent processes. Our results help explain the ineffectiveness of mannose supplementation for PMM2-CDG patients, that we suggest may ameliorate the loss Man-1-P but at the same time exacerbate the Man-6-P accumulation. The offsetting nature of these two mechanisms may explain why further decreases in N-glycosylation of serum glycoproteins have not been detected in PMM2-CDG patients infused with mannose.

In addition, substantial LLO loss attributed to Man-6-P accumulation may not always be sufficient to impair N-glycosylation: in one study with mouse fibroblasts carrying a null allele for Mpi, high concentrations of Man-6-P were measured and LLO levels were substantially reduced, but no change in overall protein N-glycosylation was detected.[22] Manipulating metabolic flux is therefore likely to be a useful therapeutic approach, but it will require careful attention to conditions that offer beneficial effects while minimizing potential damage.

REFERENCES

1. Eklund, E.A. and H.H. Freeze, *The congenital disorders of glycosylation: a multifaceted group of syndromes.* NeuroRx, 2006. **3**(2): p. 254-63.
2. Jaeken, J., *Congenital disorders of glycosylation.* Ann N Y Acad Sci, 2010. **1214**: p. 190-8.
3. Van Schaftingen, E. and J. Jaeken, *Phosphomannomutase deficiency is a cause of carbohydrate-deficient glycoprotein syndrome type I.* FEBS Lett, 1995. **377**(3): p. 318-20.
4. Körner, C., L. Lehle, and K. von Figura, *Abnormal synthesis of mannose 1-phosphate derived carbohydrates in carbohydrate-deficient glycoprotein syndrome type I fibroblasts with phosphomannomutase deficiency.* Glycobiology, 1998. **8**(2): p. 165-171.
5. Powell, L.D., et al., *Carbohydrate-deficient glycoprotein syndrome: not an N-linked oligosaccharide processing defect, but an abnormality in lipid-linked oligosaccharide biosynthesis?* J Clin Invest, 1994. **94**(5): p. 1901-1909.
6. Panneerselvam, K. and H.H. Freeze, *Mannose corrects altered N-glycosylation in carbohydrate-deficient glycoprotein syndrome fibroblasts.* J Clin Invest, 1996. **97**(6): p. 1478-87.
7. Krasnewich, D.M., et al., *Abnormal synthesis of dolichol-linked oligosaccharides in carbohydrate-deficient glycoprotein syndrome.* Glycobiology, 1995. **5**(5): p. 503-10.
8. Marquardt, T., et al., *Carbohydrate-deficient glycoprotein syndrome (CDGS)--glycosylation, folding and intracellular transport of newly synthesized glycoproteins.* Eur J Cell Biol, 1995. **66**(3): p. 268-73.
9. Marquardt, T., et al., *Carbohydrate-deficient glycoprotein syndrome type I: determination of the oligosaccharide structure of newly synthesized glycoproteins by analysis of calnexin binding.* J Inherit Metab Dis, 1996. **19**(2): p. 246-50.
10. Dupre, T., et al., *Defect in N-glycosylation of proteins is tissue-dependent in congenital disorders of glycosylation Ia.* Glycobiology, 2000. **10**(12): p. 1277-81.
11. Gao, N., J. Shang, and M.A. Lehrman, *Analysis of glycosylation in CDG-Ia fibroblasts by fluorophore-assisted carbohydrate electrophoresis: implications for extracellular glucose and intracellular mannose 6-phosphate.* J Biol Chem, 2005. **280**(18): p. 17901-9.
12. Hu, G.F., *Fluorophore-assisted carbohydrate electrophoresis technology and applications.* J Chromatogr A, 1995. **705**(1): p. 89-103.
13. Gao, N., et al., *Mannose-6-phosphate regulates destruction of lipid-linked oligosaccharides.* Mol Biol Cell, 2011. **22**(17): p. 2994-3009.
14. Marquardt, T. and H. Freeze, *Congenital Disorders of Glycosylation: Glycosylation Defects in Man and Biological Models for Their Study*, in *Biological Chemistry*2001. p. 161.
15. Schneider, A., et al., *Successful prenatal mannose treatment for congenital disorder of glycosylation-Ia in mice.* Nat Med, 2012. **18**(1): p. 71-73.
16. Kimmel, C.B., et al., *Stages of embryonic development of the zebrafish.* Dev Dyn, 1995. **203**(3): p. 253-310.
17. Gao, N. and M.A. Lehrman, *Non-radioactive analysis of lipid-linked oligosaccharide compositions by fluorophore-assisted carbohydrate electrophoresis.* Methods Enzymol, 2006. **415**: p. 3-20.

18. Sharma, V., et al., *Phosphomannose isomerase inhibitors improve N-glycosylation in selected phosphomannomutase-deficient fibroblasts.* J Biol Chem, 2011. **286**(45): p. 39431-8.
19. Niehues, R., et al., *Carbohydrate-deficient glycoprotein syndrome type Ib. Phosphomannose isomerase deficiency and mannose therapy.* J Clin Invest, 1998. **101**(7): p. 1414-20.
20. Chu, J., et al., *A zebrafish model of congenital disorders of glycosylation with phosphomannose isomerase deficiency reveals an early opportunity for corrective mannose supplementation.* Dis Model Mech, 2012.
21. Freeze, H.H., *Towards a therapy for phosphomannomutase 2 deficiency, the defect in CDG-Ia patients.* Biochim Biophys Acta, 2009. **1792**(9): p. 835-40.
22. Higashidani, A., et al., *Exogenous mannose does not raise steady state mannose-6-phosphate pools of normal or N-glycosylation-deficient human fibroblasts.* Mol Genet Metab, 2009. **96**(4): p. 268-72.
23. Mayatepek, E. and D. Kohlmüller, *Mannose supplementation in carbohydrate-deficient glycoprotein syndrome type I and phosphomannomutase deficiency.* European Journal of Pediatrics, 1998. **157**(7): p. 605-606.
24. Shang, J. and M.A. Lehrman, *Metformin-stimulated mannose transport in dermal fibroblasts.* J Biol Chem, 2004. **279**(11): p. 9703-12.
25. Haeuptle, M.A., et al., *Improvement of dolichol-linked oligosaccharide biosynthesis by the squalene synthase inhibitor zaragozic acid.* J Biol Chem, 2011. **286**(8): p. 6085-91.
26. Harding, H.P., et al., *Bioactive small molecules reveal antagonism between the integrated stress response and sterol-regulated gene expression.* Cell Metab, 2005. **2**(6): p. 361-71.
27. Shang, J., et al., *Translation attenuation by PERK balances ER glycoprotein synthesis with lipid-linked oligosaccharide flux.* J Cell Biol, 2007. **176**(5): p. 605-16.
28. He, P., et al., *Identification of intercellular cell adhesion molecule 1 (ICAM-1) as a hypo-glycosylation marker in congenital disorders of glycosylation cells.* J Biol Chem, 2012.
29. Shang, J., et al., *Extension of lipid-linked oligosaccharides is a high-priority aspect of the unfolded protein response: endoplasmic reticulum stress in Type I congenital disorder of glycosylation fibroblasts.* Glycobiology, 2002. **12**(5): p. 307-17.

FIGURES

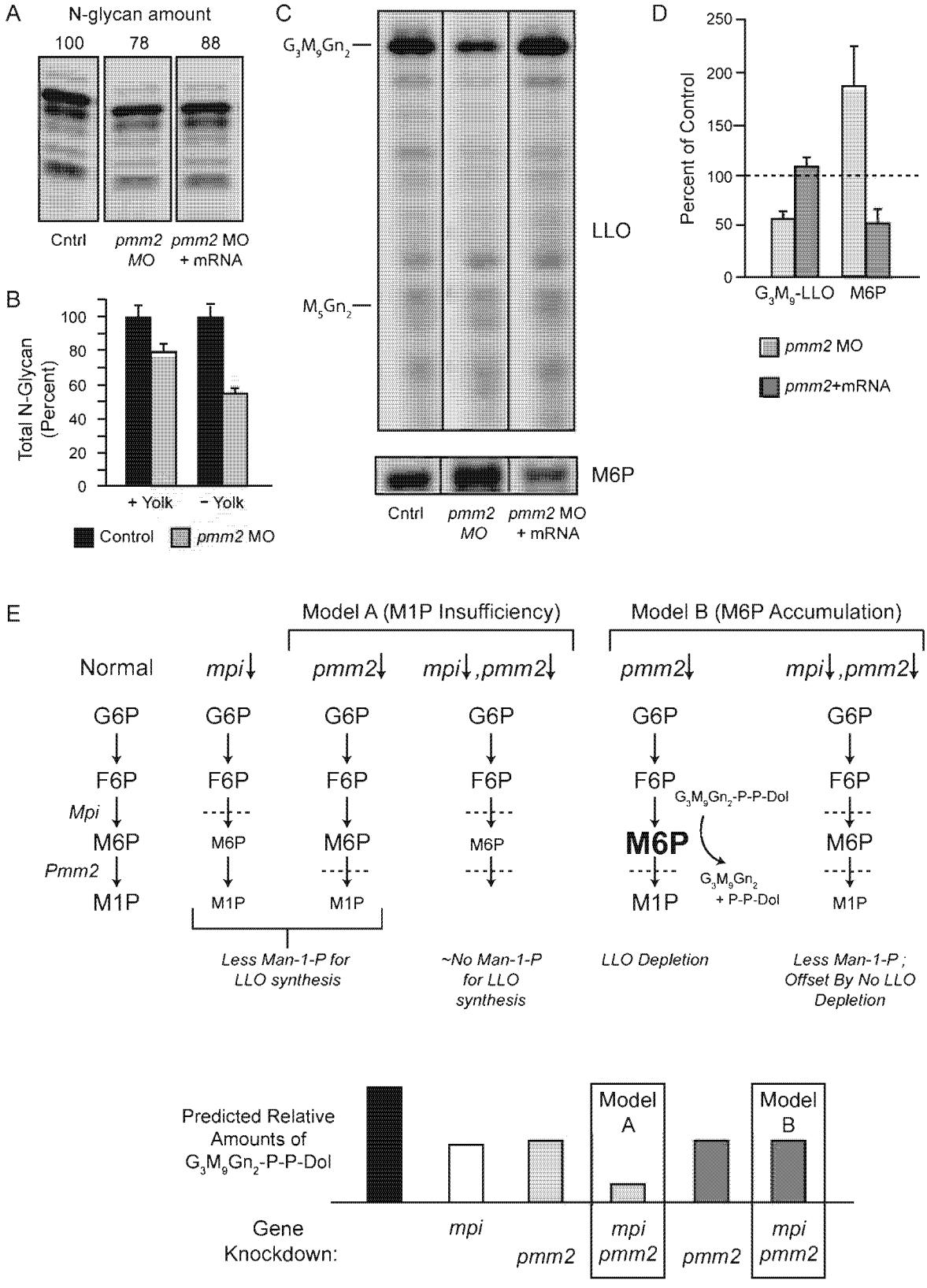
A
N-glycan amount
100
78
88
Cntrl
pmm2 MO
pmm2 MO + mRNA
B
Total N-Glycan (Percent)
100
80
60
40
20
0
+ Yolk
- Yolk
Control
pmm2 MO
C
G3M9Gn2
M5Gn2
LLO
M6P
Cntrl
pmm2 MO
pmm2 MO + mRNA
D
Percent of Control
250
200
150
100
50
0
G3M9-LLO
M6P
pmm2 MO
pmm2+mRNA
E
Model A (M1P Insufficiency)
Model B (M6P Accumulation)
Normal
mpi↓
pmm2↓
mpi↓,pmm2↓
pmm2↓
mpi↓,pmm2↓
G6P
F6P
Mpi
M6P
Pmm2
M1P
G3M9Gn2-P-P-Dol
G3M9Gn2 + P-P-Dol
Less Man-1-P for LLO synthesis
~No Man-1-P for LLO synthesis
LLO Depletion
Less Man-1-P ; Offset By No LLO Depletion
Predicted Relative Amounts of G3M9Gn2-P-P-Dol
Model A
Model B
Gene Knockdown:
mpi
pmm2
mpi pmm2
pmm2
mpi pmm2

Figure 3.1. **G3M9Gn2-P-P-Dol suppression and restoration in *pmm2* morphants.** G3M9Gn2-P-P-Dol and M6P were measured with FACE techniques from the same samples of zebrafish. Similar numbers of 4 dpf embryos (50-200 depending upon need) were used for each comparison. All measurements were normalized to total protein, which did not vary significantly among the different genetically modified groups of fish. **(A)** Representative FACE gel for total N-glycans released from the proteins of yolkcontaining zebrafish embryos. Total N-glycan amounts (normalized to control) are indicated above each lane. **(B)** Bar graph depicting the average percentage loss of total N-glycans in *pmm2* morphants (with and without yolks) in two separate experiments (mean ± S.E.M.), normalized to control embryos. Direct comparison of the control samples showed that yolk-free embryos had 49% of the N-glycan content of whole embryos. Related information is provided in Supplemental Figure 1. **(C)** Representative FACE images showing LLO glycans (M5Gn2 and G3M9Gn2 standards are indicated) and M6P from a single set of control fish, *pmm2* morphants, and morphants rescued by coinjection of *pmm2* mRNA. Vertical lines denote electronic removal of irrelevant lanes from the image. The portion below the M5Gn2-LLO standard on FACE gels generally contains mostly non-LLO species, but it is included here because this is where any accumulation of M3Gn2 - M4Gn2-LLO is likely to appear. Related information is provided in Supplemental Figure 2. **(D)** G3M9Gn2-LLO and M6P measured in 3 independent experiments, mean ± S.E.M. Control levels were arbitrarily set as 100% (dashed line). **(E)** (*upper*) Schematic comparisons of hypotheses for M1P insufficiency (Model A) and M6P accumulation (Model B). (*lower*) Models A and B are indicated by light and dark gray bars, respectively, and contrasting double-morphant outcomes are highlighted with boxes.

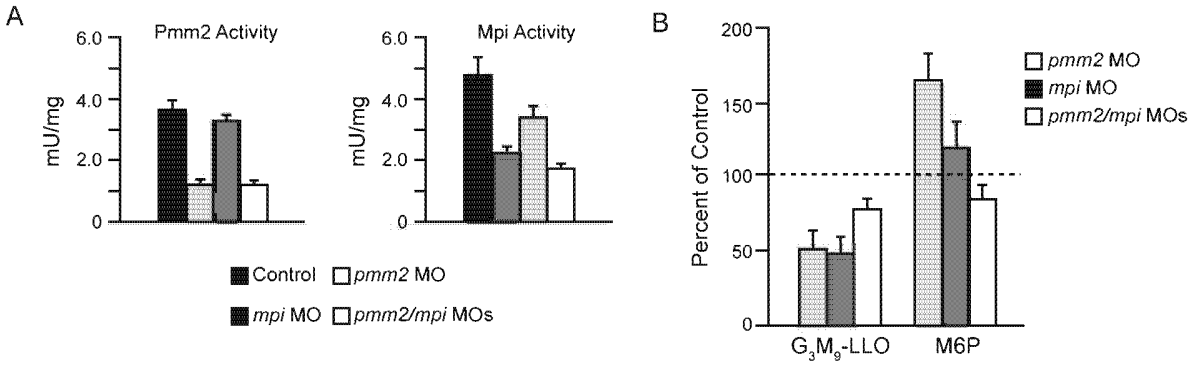

Figure 3.2. **Knockdown of *mpi* in the *pmm2* background normalizes M6P levels, with no further loss of G3M9Gn2-LLO. (A)** Pmm2 and Mpi enzyme activity for control embryos, *pmm2* morphants, *mpi* morphants, and *pmm2/mpi* double morphants **(B)** G3M9Gn2-P-P-Dol and M6P were measured in control embryos, *pmm2* morphants, *mpi* morphants, and *pmm2/mpi* double morphants. Results for 4 independent experiments, mean ± S.E.M, with control values set as 100% are shown.

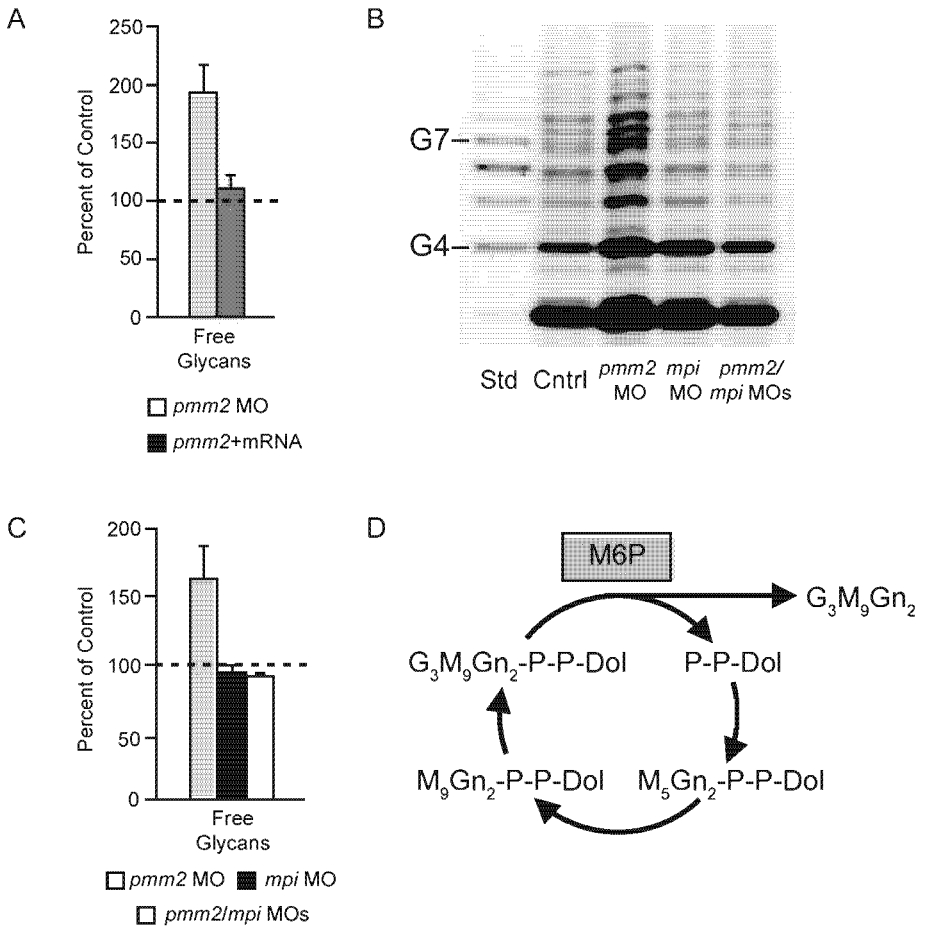

Figure 3.3. **Free glycans in *pmm2* morphants.** Total free glycans were measured with FACE techniques from the same samples of zebrafish presented in **Figures 3.1-2**. **(A)** Free glycans were measured in control embryos, *pmm2* morphants, and morphants rescued by co-injection of *pmm2* mRNA. Results of 3 independent experiments, mean ± S.E.M. Control levels were arbitrarily set as 100%. **(B)** Representative FACE image showing total free glycans from control embryos, *pmm2* morphants, *mpi* morphants, and *pmm2/mpi* double morphants. Glucose oligomer standards (G4 – G7) are shown. As shown previously (Gao et al., 2011), G3M9Gn2 released from the LLO pool by M6P action is glycosidically degraded, resulting in the heterogeneous mixture of free glycans detected. The most abundant glycan detected near the bottom of the gel is likely to be M2Gn2, based upon migration. **(C)** Results for 4 independent experiments as in B., mean ± S.E.M, with control set as 100%. **(D)** Schematic showing that dolichol pyrophosphate can be recycled for multiple rounds of LLO synthesis while free glycans are released by the action of M6P. This explains why the molar increase of free glycans in *pmm2* morphants vastly exceeds the measured loss of LLO (see Discussion).

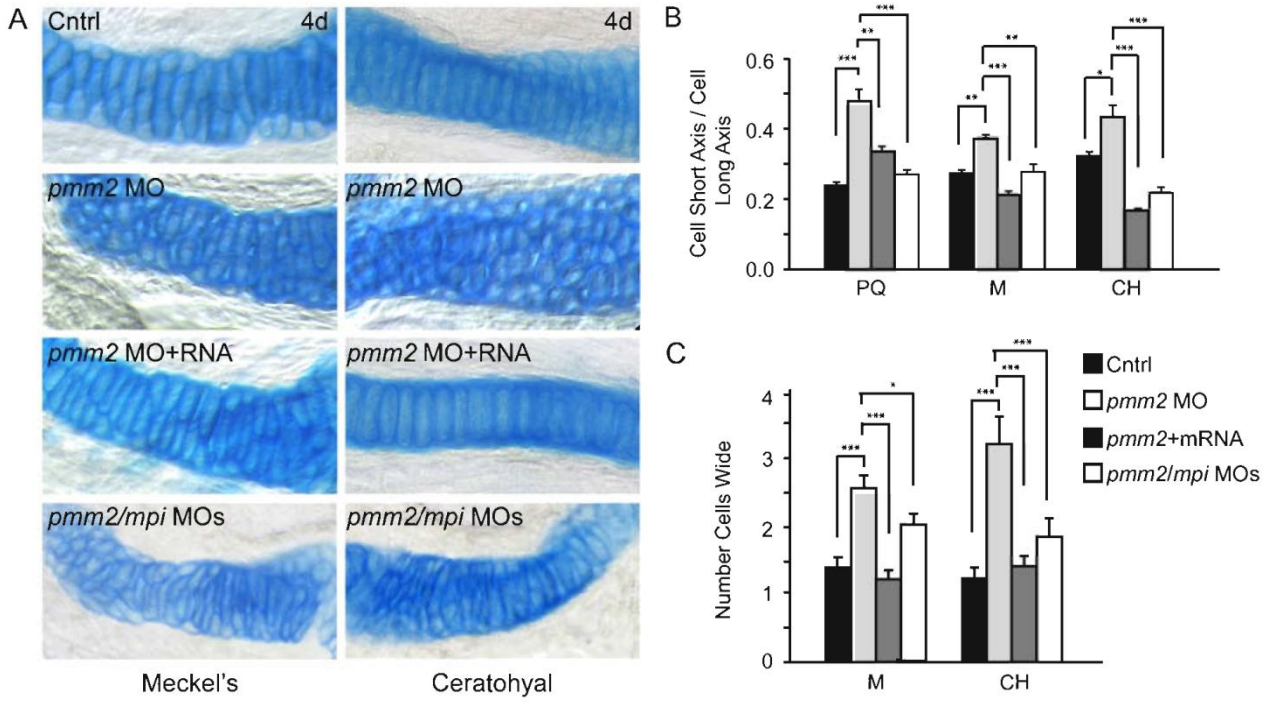

Figure 3.4. Inhibition of *mpi* in the *pmm2* background improves craniofacial chondrocyte morphology. (A) Alcian blue stains of 4 dpf control, *pmm2* morphant, mRNA rescued, and *pmm2/mpi* double morphant embryonic cartilage revealed significant improvement following *mpi* manipulation. Unlike *pmm2* morphant chondrocytes, which were round and unorganized, reducing *mpi* in *pmm2* morphants restored the elongated shape of chondrocytes within the Meckel's, ceratohyal, and palatoquadrate (not shown) cartilages. **(B)** Quantitative measurement of cell shape demonstrated significant recovery of cell elongation in *pmm2* morphants following either introduction of *pmm2* mRNA or reduction of *mpi* expression. Briefly, the long and short axes of individual chondrocytes were measured, and their ratio calculated. A ratio of 1 indicates equivalence of these axes and a perfectly round cell. **(C)** Cellular organization was also partially improved in *pmm2* morphants following by *mpi* manipulation. This is quantitavely demonstrated in the number of cells spanning the width of the Meckel's and Ceratohyal elements.

CHAPTER 4: ZEBRAFISH PMM1 IS A FUNCTIONAL PHOSPHOMANNOMUTASE[1]

[1] To be submitted to Journal of Biological Chemistry

ABSTRACT

Phosphomannomutases (PMMs), enzymes that are responsible for the isomerization of Man-6-P to Man-1-P, are essential for the N-glycosylation of glycoproteins. Man-1-P serves as the precursor for the biosynthesis of GDP-mannose and ultimately the lipid-linked oligosaccharide (LLO).Two highly conserved PMMs exist: PMM1 and PMM2. Although both PMM1 and PMM2 possess PMM activity, only mutations causing a deficiency in PMM2 result in Congenital Disorder of Glycosylation Type PMM2 (PMM2-CDG). This rare genetic defect is the most common type of CDG and is characterized by hypoglycosylation of serum glycoproteins. PMM1 has not yet been implicated in any disease, and its contribution to protein glycosylation remains elusive. Recently, a zebrafish model for PMM2-CDG was generated and characterized to investigate the pathophysiology seen in patients. These Pmm2 knockdown fish are an ideal platform to study the potential role of Pmm1 in the N-glycosylation pathway. In zebrafish, RT-PCR revealed similar expression patterns of *pmm1* and *pmm2* in embryos and adult tissues. *pmm1*transcript levels increased relative to control following morpholino-knockdown of *pmm2*, suggesting a possible compensating role for *pmm1* . Furthermore, overexpression of *pmm1*mRNA in the *pmm2* morphant background not only resulted in increased PMM activity, but also corrected abnormal phenotypes and deficient glycosylation profiles. Together, these data suggest that zebrafish Pmm1 can function as a PMM in the protein glycosylation pathway, providing a target for potential therapeutic strategies in treating PMM2-CDG.

BACKGROUND

Phosphomannomutase (PMM) catalyzes the interconversion of Mannose-6-P (Man-6-P) and Mannose-1-P (Man-1-P). Man-1-P is required for the synthesis of GDP-mannose, an essential intermediate for the synthesis of the lipid-linked oligosaccharide (LLO) in the N-glycosylation pathway[1]. In humans, two genes encode active phosphomannomutases: *PMM1* and *PMM2*. Human PMM1 and PMM2 are quite similar (65% identical), and a comparison of the sequence and gene structure of *PMM1* and *PMM2* indicated that these genes have probably arisen by duplication.[2, 3] In humans, PMM1 is predominately expressed in brain and lungs, whereas PMM2 is ubiquitously expressed. [4] The expression pattern and presence of these two highly conserved PMM suggests that each may have a distinct function. Though PMM1 has not been implicated in any known disease, mutations in PMM2 are associated with a rare genetic defect known as the Congenital Disorder of Glycosylation (CDG)-Type PMM2.[5-7]

Mutations in *PMM2* that decrease its activity result in PMM2-CDG, which is characterized by LLO pools depletion, glycoprotein hypoglycosylation, and severe physical and developmental abnormalities. PMM2-CDG is autosomal recessive and its locus has been mapped to chromosome 16p13, while *PMM1* is localized to chromosome 22q13. [7, 8] Although both PMM2 and PMM1 show PMM activity *in vitro*, several studies suggest that PMM1 is not able to compensate for PMM2 deficiency.[5] Considering the residual activity observed in most patients is less than 10% normal activity, PMM1 is expected to contribute only a minor part of the PMM activity present in tissues. [4] A recent study by Cromphout et al. demonstrates that although

PMM1 is primarily expressed in brain in adults, its embryonic expression profile is more widespread.

Analysis of tissues from E17 mice revealed high *Pmm1* expression in most organ systems: nervous system, gastrointestinal tract, endocrine glands, urinary system, and respiratory system.[9]Previously, PMM1 expression profiles were limited to adult stage of human, rat and mouse tissues.[6, 10] Examining the expression level of PMM1 in E17 embryonic mouse tissues revealed high expression in most tissues, with brain having the highest expression level. As expected from previous studies, this widespread expression pattern was down regulated post-natally to the more restricted pattern found in adult tissues. Though expression levels were still high in the brain, expression levels in the liver, pancreas, and lung were low. This suggests PMM1 may have functions that are not required post-natally.[9]

Given the expression pattern data, embryonic loss of PMM1 in mice was expected to impact the developing brain and peripheral organs; however, PMM1-deficient mice did not present a detectable phenotype and were indistinguishable from their wild-type littermates. A detailed histological and glycohistochemical analysis did not reveal any abnormalities, suggesting that although *Pmm1*may have a role in protein glycosylation, its function is not essential to maintain sufficient levels of glycosylation. Probing with a PMM2 specific antibody showed similar levels in both PMM1-knockout mice and wild-type mice, indicating that PMM2 is not responding to loss of PMM1 activity.[9] This data suggests that loss of PMM1 does not decrease phosphomannomutase activity below a necessary threshold that would affect N-glycosylation. Alternatively, PMM1 may have a developmental function independent of PMM activity, which would explain why PMM1 does not compensate for loss of PMM2 activity in PMM2-CDG patients.

In contrast to PMM2, PMM1 has been found to have equivalent PMM and phosphoglucomutase activities. Where PMM2 and PMM1 convert Man-1-P to Man-6-P at the same rate, PMM1 is 20 times more active in the conversion of glucose-1-phosphate into glucose-6-P than PMM2. Furthermore, PMM1, but not PMM2, has significant phosphatase activity on hexose-1,6-bisphosphates, and the ability to form mannose-1,6-bisphosphate using fructose-1,6-bisphosphate as a phosphoryl-group donor.[5] This phosphatase activity lead researchers to confirm that PMM1 is the glucose-1,6-bisphosphatase stimulated by inosine monophosphate (IMP) previously described by Guha and Rosa.[11-13] IMP was found to stimulate glucose-1,6-bisphosphatase activity of PMM1 while inhibiting its phosphoglucomutase activity. In the presence of PMM1, IMP binds to the same site as hexose monophosphates, preventing the re-formation of the bisphosphate cofactor and thereby inhibiting the phosphomutase activity. Despite its close structural similarity to PMM1, PMM2 showed no such sensitivity to IMP.[11] Thus despite their close structural similarity, PMM1 and PMM2 have distinctly different properties.

It is well established that PMM2 serves an essential role in the N-glycosylation pathway; however, the role of PMM1 has not fully been determined. Though the PMM1-deficient mice showed no difference in phenotype or glycohistochemical analysis compared to wild-type litter mates, to fully exclude the role of PMM1 in protein glycosylation, PMM1 overexpression or deficiency in a PMM2 null background would have to be analyzed. Due to early embryonic lethality of PMM2-deficient mice, this question would be difficult to answer in the mouse model.[14] Fortunately, we previously generated and characterized a zebrafish model of PMM2-CDG that may provide the ideal platform to address the role of PMM1 in the N-glycosylation pathway.[15] Suppression of *pmm2* expression using a morpholino-based approach reduced

Pmm2 activity to 33% of control with higher concentrations of morpholino resulting in increased PMM activity. The inability for PMM activity to be completely suppressed with the *pmm2* morpholino may be explained by the presence of a compensatory enzyme, such as Pmm1.

To elucidate the physiological function of Pmm1, we characterized expression of Pmm1 in PMM2-CDG zebrafish. To determine if *pmm1* expression is altered when Pmm2 activity is reduced, we documented its expression within embryos and adult tissues isolated from control and PMM2-CDG fish. To determine if Pmm1 can rescue phenotypic and biochemical defects within the *pmm2*morphant background, we overexpressed *pmm1*mRNA in PMM2-CDG zebrafish and analyzed them by the same parameters previously established in the generation of the PMM2-CDG zebrafish model. Overexpression of Pmm1 within a Pmm2-deficient background increased PMM activity to 45% of control levels. This increased activity was sufficient to rescue phenotypes and biochemical profiles of the PMM2-CDG zebrafish, suggesting that Pmm1 can function as a phosphomannomutase.

MATERIALS AND METHODS

Fish strains, maintenance, and husbandry

Wild type zebrafish were obtained from the commercial source Fish2U (Gibsonton, FL) and maintained using standard protocols. Embryos were staged according to the criteria established by Kimmel [16]. When necessary pigment formation was inhibited by addition of 0.003% 1-phenyl-2-thiourea (PTU) to embryonic growth medium. Although the data presented are derived primarily from experiments in F2U, all MO-generated phenotypes (e.g. craniofacial and motility defects) were confirmed in multiple genetic backgrounds (AB, TAB14, *fli1a*:EGFP). For

analysis of neuronal phenotypes, morphants were generated in the *hb9*:GFP transgenic background. Handling and euthanasia of fish for all experiments were carried out in compliance with the University of Georgia's Institutional Animal Care and Use Committee (permit number: A2011 8-144).

Anti-sense morpholino injection and mRNA rescue

Expression of *pmm2* was inhibited by injection of anti-sense morpholinos (MO) into the yolks of 1-2 cell embryos. Splice blocking (5'-TTCCGCATTAATTCACTCACTTGAC-3') MO was designed to target the *pmm2* exon 1- intron 1 splice junction, respectively (Gene Tools, Eugene, OR). Optimal MO dosages were determined by PMM activity assays and RT-PCR analyses. Maximal inhibition (33% of control) of Pmm2 activity was achieved following injection of 0.5 nL of a 1μM solution (0.52 μM final concentration) of the splice blocking MO. In order to facilitate various recovery analyses, the full length coding region of *pmm1* was synthesized by Life Technologies™ and cloned into vector pMA-T via EcoRI and XbaI restriction sites flanking the coding region. After restriction digest at these sites, the resulting product was subcloned into pCSII. pCSII-*pmm1* plasmid DNA was linearized with NotI and full length sense mRNA generated with Message Machine SP6 kit (Roche Applied Science, Indianapolis, IN.) The full length coding region of *pmm2* was cloned by RT-PCR from mRNA isolated from 3 dpf embryos using the following primers: (ttccaaatatcacaatgtctggc and tcagctgaaaaagagctccctgcag). The resulting product was cloned into TA site of pCR2.1 (Life Technologies Inc, Grand Island, NY) and subsequently excised by vector derived EcoRI and XbaI sites. This product was subcloned into pCSII, which was linearized with KpnI and full length mRNA generated with Message

Machine SP6 kit (Roche Applied Science, Indianapolis, IN.) Rescue experiments were performed by sequential injection of 0.52 µM splice blocking MO and 200-300 pg of purified *pmm2*or *pmm1* mRNA into the yolks of 1-2 cell embryos.

RT-PCR analysis of pmm1 expression and PMM activity assay

Total RNA was extracted from approximately 30 3 dpf embryos using TRIzol reagent (Invitrogen Corp). RNA was reverse transcribed to cDNA using iScript cDNA Synthesis Kit (Bio-Rad). RT-PCR analysis of *pmm1* expression performed with primers flanking the first gene (cccagagagaagatcgaccca and tctggtaaagcgcaggcctt). Pmm1 transcript abundance was normalized to RPL4 transcripts. For analysis of PMM enzyme activity 50-100 embryos were collected at the indicated time points and the yolks manually removed. Embryos were lysed in 50 mM Na-HEPES, pH 7.4, sonicated, and total protein quantitated using a microBCA protein assay kit (Pierce). Pmm enzyme activity assays were performed as previously described [17]. Briefly, Pmm activity is assayed by a coupled enzyme assay system that relies on the spectrophotometric detection of the reduction of NADP+ to NADPH using M1P as a substrate. Samples were measured 60 minutes after adding the substrate. Units were calculated as mU of enzyme activity/mg of protein based on the change in OD during the reaction time.

Histochemistry, immunohistochemistry, and whole-mount in situ analysis

To visualize craniofacial cartilage embryos were stained with Alcian blue as described previously [18]. Stained animals were photographed on an Olympus SZ16 stereoscope outfitted

with a Retiga CCD camera. Morphometric measurements of Alcian blue stained animals were performed using Adobe Photoshop. In order to account for differences in animal size, all measurements were normalized to inter-lens distance. Whole mount *in situ* hybridization for *pmm1* was performed as previously described by Thisse and Thisse [19].

Motility assays

For assessment of elicited motility, 3 dpf embryos were placed in the center of a petri dish marked by three concentric rings. Embryos were touched beside the otilith and their response recorded. Swimming distance of individual embryos was assigned as 1, 2, or 3, according to the number of rings crossed. Zones 1, 2, and 3 had diameters of 3, 6, and 8cm, respectively. 50 fish were measured at a time from 3 separate injections.

Fluorophore-assisted carbohydrate electrophoresis (FACE) analysis of zebrafish saccharides and glycoconjugates

Embryos were collected by centrifugation, excess water was removed, 1 mL of methanol (room temperature) was added to the tube, and the contents disrupted by brief probe sonication (Branson Sonifier 150; low setting, 3 x 5 sec pulses). The suspension was transferred to a 15-mL conical tube, and an additional 10-12 mL of methanol was added. Following thorough vortexing, the tubes were capped and sealed with parafilm, and sent by express shipping at room temperature to the Lehrman lab. At that point, samples were dried and processed for FACE analyses as described [20, 21]. In brief, after removal of most lipids by extraction with chloroform:methanol (2:1), aqueous saccharides were recovered by extraction with water, and

LLOs were then obtained by extraction with chloroform:methanol:water (10:10:3) with N-linked glycoproteins remaining in the residual material. Ion exchange fractionation of the aqueous saccharides yielded free sugars and free glycans in an uncharged fraction, sugar monophosphates in a weakly anionic fraction, and both nucleotide-sugars and sugar 1,6-bisphosphates in a more strongly anionic fraction. Phosphate esters of the 1-postion of mono- and oligosaccharides were released with weak acid (a condition that retained 6-phosphate esters), and N-glycans were released with peptide N-glycosidase F. All monosaccharide species were then conjugated with 2-aminoacridone (AMAC) and separated on a monosaccharide profiling gel, while all oligosaccharide species were conjugated with 7-amino-1,3-naphthalenedisulfonic acid (ANDS) and detected with an oligosaccharide profiling gel. Where appropriate, standards were included consisting of monosaccharide mixtures, glucose oligomers, or LLO-derived glycans. Fluorescent saccharide conjugates were detected with a Biorad Fluor-S scanner and quantified with Quantity-One software. Loading of various quantities of standards established that detection was linear, with a sensitivity of ~2 pmol saccharide. For quantitation of free glycan experiments, only the portions in the size range delimited by the G_4 and G_7 standards were used.

RESULTS

Alignment of PMM1 and PMM2 in Zebrafish

Alignment of previously identified Pmm1and Pmm2 zebrafish sequences reveal that the two proteins are quite similar, sharing 64% overall identity (**Figure 4.1 A**). Though there are dissimilar residues scattered throughout the sequences, the key active-site residues required for PMM activity are conserved in Pmm1. Among these, motif 1 contributes the catalytic

nucleophile, Asp^{28} and the putative acid/base residue Asp^{30}. Motif 2 contributes Ser^{63}, which helps position the phosphoryl group. The positions for the salt bridge residue, Lys, contributed by motif 3 and the metal-binding residue, Asp, contributed by motif 4, do not appear to be align with the Pmm2 sequence. Instead, Lys^{194} and Asp^{212} may function in these roles though they are not found in sequences similar to Pmm2.

Due to the degree of similarity between these genes, we investigated whether the *pmm2* morphlino could bind to the *pmm1* transcript. To determine the likelihood of the *pmm2*splice blocking morpholino binding to *pmm1* transcript, genomic fish DNA was sequenced using primers directed against *pmm1*or *pmm2*. Sequence data revealed that while the splice blocking morpholino is identical to the *pmm2* exon 1-intron 1 splice junction, it was not identical to the *pmm1* exon 1-intron 1 splice junction (**Figure 4.1B**). These two junctions are only 38% similar, therefore it is unlikely that the *pmm2* splice blocking morpholino would bind to this *pmm1* junction.

pmm1 and *pmm2*Transcript Levels are Detected in Zebrafish Embryos and Adult Tissues

Previously published data show that in adult mammals PMM2 is ubiquitously expressed, while PMM1 is restricted to the brain and lungs.[7] To determine whether this is also the case in zebrafish, we used RT-PCR to examine normal transcript levels of *pmm1*and *pmm2* in adult and embryonic tissues (**Figure 4.2**). RT-PCR of 30 4dpf embryos revealed that *pmm1*and *pmm2*transcripts are both present in embryonic tissues, possibly suggesting that Pmm1 may have a role in developing embryos. Surprisingly, analysis of RNA from various adult control fish organs revealed similar expression patterns of *pmm1*and *pmm2*. Both transcripts were detected

in heart, brain, muscle, testes, and ovaries of adult fish (**Figure 4.2**). Similar to PMM1 mammalian expression profiles, zebrafish *pmm1* transcript was highest in the brain. As a control we confirmed that *pmm1* primers were not cross reacting with *pmm2* transcripts (and vice versa) by sequencing the RT-PCR products. Sequencing confirmed the amplicons represented the expected *pmm1*or *pmm2* transcripts.

*pmm1*Transcript Levels Increase in *pmm2* Morphants

After confirmation that primers successfully distinguished between *pmm1*and *pmm2*transcripts, we investigated whether suppression of *pmm2* influenced *pmm1*transcription levels. We performed RT-PCR using RNA isolated from control and PMM2-CDG morphants over a time course spanning 1-3dpf. As shown in **Figure 4.3A**, although *pmm1* transcripts were not detected in controls embryos until 2dpf, *pmm1* transcripts were present at 1dpf in *pmm2*morphants. Throughout the time course, higher levels of *pmm1* transcript were noted in *pmm2* morphants compared to controls, with maximal *pmm1* expression at 3dpf. To confirm these results, we performed *in situ* hybridization analyses of *pmm1* in control and *pmm2* morphants. Consistent with RT-PCR, *pmm1*showed increased expression in the heads of *pmm2*morphants when compared control embryos at both 1 and 3dpf (**Figure 4.3 B**).

Overexpression of PMM1 in *pmm2* Morphant Background Increases PMM Activity

Motivated by the fact that mouse PMM1 shows PMM activity *in vitro* [4], we analyzed whether overexpression of zebrafish Pmm1 would increase PMM activity in the *pmm2* morphant

background. Co-injection of full length *pmm1* mRNA with the *pmm2* SB morpholino increased PMM activity from 34% to 51% of control activity (**Figure 4.4A**), suggesting that Pmm1 is a functional phosphomannomutae enzyme. To address whether Pmm1 was equivalent to Pmm2 in its ability to convert Man-6-P to Man-1-P, we performed a similar experiment where we injected 200pg of either *pmm1*or *pmm2* RNA into the *pmm2*morphant background. We based the RNA amount, 200pg, on the previously established concentration used for the *pmm2* mRNA rescue experiments of the *pmm2* morphants. Over a timecourse of 1-4dpf, PMM activity was measured in controls, *pmm2*morphants, *pmm2* mRNA injected *pmm2* morphants, and *pmm1* mRNA injected *pmm2* morphants (**Figure 4.4B**). In this assay, Pmm2 consistently rescued PMM levels throughout the timecourse, and even showed greater PMM activity than control levels. At the same RNA concentration, Pmm1 was not successful in restoring PMM activity in *pmm2*morphants. From the previous experiment, we concluded that Pmm1requires an RNA concentration of greater than 300pg to raise PMM activity within *pmm2* morphants. This is the concentration of *pmm1*mRNA used for the remainder of this study.

Overexpression of PMM1 Successfully Rescues *pmm2* Morphant Phenotypes

In light of its detectable PMM activity, we investigated if phenotypes noted in the *pmm2* morphants could be rescued by *pmm1* overexpression. We previously described two developmental abnormalities in *pmm2* morphants: alterations in craniofacial cartilage development characterized by altered chondrocyte morphology and a pronounced motility defect at 3dpf[15]. Since these phenotypes were rescued by the expression of wild type *pmm2* within

the morphant background, we analyzed if *pmm1*would also ameliorate these developmental defects.

Alcian blue stains of developing cartilage, revealed that injection of 300pg of *pmm1* mRNA successfully rescued defects seen in *pmm2*morphants (>50%), including protracted Meckel's (M) cartilages, misshapened palatoquadrate (PQ) and ceratohyal (CH) structures, and kinked pectoral fins (**Figure 4.5A)**. Morphometric measurements of the cartilage structures revealed that coinjection of *pmm1*mRNA also improved the shape and size of *pmm2* morphant cartilage structures (**Figure 4.5B**). The malformation of the lower jaw seen in *pmm2* morphant embryos is associated with altered chondrocyte morphology. Unlike control chondrocytes, which are oblong in shape and converge to form a single line of cells, morphant cells remain round and disorganized (**Figure 4.5C**). The chondrocytes of *pmm1* mRNA injected *pmm2* morphants displayed normal chondrocyte morphogenesis, suggesting that overexpression of *pmm1*is sufficient to compensate for loss of *pmm2*.

In addition to altered craniofacial chondrogenesis, *pmm2* morphants displayed deficits in touch responsiveness and swimming behaviors at 3dpf. To ask whether Pmm1 could functionally rescue these defects, we utilized a previously described elicited motility assay that evaluates swimming behavior. Embryos were placed in the center of a plate marked with a series of concentric rings, which were used to assign swimming distances (**Figure 4.5D**). Control embryos normally swam to the outermost ring (Zone 3) in response to the stimulus. Following elicitation, *pmm2* morphant embryos typically swam in a circle towards the stimulus, remaining the first ring (Zone 1). In contrast, *pmm1* mRNA injected *pmm2* morphants swam away from the stimulus and ultimately crossed multiple rings (Zone2-3). Co-injection of *pmm1* mRNA into the

*pmm2*morphant background significantly rescued the elicited motility defect seen in the morphant fish (**Figure 4.5 E**).

Together these data suggest that *pmm1* overexpression rescues activity to above the necessary threshold of PMM activity. Since PMM activity is sufficient in *pmm1* rescued embryos, no phenotypes are seen; however, as enzyme levels fall below the necessary level, as seen with the *pmm2*morphants, phenotypic presentation becomes increasingly severe. Therefore, to confirm this theory and see if *pmm1*rescue also improved the deficient N-glycosylation pathway of *pmm2*morphants, we investigated metabolites of N-glycosylation.

Coinjection of *pmm1* mRNA into *pmm2* Morphants Corrects Deficient Glycosylation Profiles

Fluorophore Assisted Carbohydrate Electrophoresis (FACE) analysis has been successfully used to examine substrates in the N-glycosylation pathway.[15, 20-24] This technique is a simple, accurate, and quantitative method for direct measurement of metabolites in the N-glycosylation pathway such as sugar phosphates, lipid-linked oligosaccharides (LLO), N-glycans, and free glycans.[20] Utilizing FACE, steady state LLO levels were found to be suppressed in *pmm2* morphants to 45% of control levels (**Figure 4.6A**). [15] Since this amount was returned to normal after co-injection of *pmm2* mRNA, we asked whether *pmm1* mRNA would also restore LLO levels in the *pmm2* morphant background. Overexpression of *pmm1*mRNA in the *pmm2*morphant background successfully restored LLO levels to 99% of control levels (**Figure 4.6A-C**).

Previously, we demonstrated that *pmm2* knockdown reduced LLO levels. Our analysis indicated this was due to a Man-6-P accumulation that promoted cleavage of LLO and increase in free glycan pools.[15] To determine what effect Pmm1 may have on Man-6-P pools, sugar phosphate levels were analyzed in *pmm1*mRNA injected *pmm2* morphants (**Figure 4.6B-C**). Man-6-P levels were found to be reduced in *pmm1*mRNA injected *pmm2* morphants when compared to *pmm2* morphants. Although *pmm2* morphants displayed ~200% increase in Man-6-P pools, *pmm1* mRNA injected *pmm2*morphants reduced Man-6-P pools to only a slightly increased 128% of control. This data suggests that Pmm1 is a functional phosphomannomutase in the zebrafish N-glycosylation pathway as it effectively reduced the Man-6-P accumulation observed in *pmm2*morphants.

To test whether coinjection with *pmm1* mRNA would also alleviate such LLO hydrolysis found in *pmm2* morphants, we assessed total free glycan levels. Whether *in vivo* with pure Man-6-P or *in vitro* with accumulation of Man-6-P due to deficient Pmm2 activity, hydrolysis of LLO causes release of free glycans into the ER lumen. As shown in **Figure 4.6D**, total free glycans were increased in *pmm2* morphants, and were almost returned to control levels following co-injection of *pmm1*mRNA. As previously noted, the oligoform noted in the free glycan pools had no qualitative differences, suggesting incomplete forms of LLO were not accumulated. [15]

Finally, N-glycan from the protein fraction were released with PNGase F, and analyzed by FACE to determine if N-glycan levels were ultimately rescued with *pmm1*overpression in the *pmm2*morphant background (**Figure 4.6D**). Total N-glycan pools in the *pmm2* morphants were found to be 54% of control. Co-injection of *pmm1*mRNA into the Pmm2 deficient background restored N-glycan levels back to control levels. No qualitative differences were noted between samples, indicating only the amount of glycan transferred to proteins was affected.

Taken together, this data supports a role for zebrafish Pmm1 as a phosphomannomutase that can contribute in the N-glycosylation pathway. Not only did overexpression of *pmm1*within the morphant background increase PMM activity, it also successfully corrected the deficient glycosylation profile observed in *pmm2*morphants. This data suggests that increased levels of Pmm1 were able to decrease the Man-6-P accumulation, restoring LLO levels, and increase proper protein glycosylation. Although *pmm1*mRNA injection in *pmm2* morphants still showed a slight increase of Man-6-P and free glycan levels when compared to controls, if LLO cleavage did occur, LLO pools were normalized to facilitate proper N-glycosylation.

DISCUSSION

Several previous studies phosphomannomutases, PMM1 and PMM2, have suggested that PMM1 and PMM2 have both similar and distinct roles in vertebrate development. The early expression suggest that while both PMM1 and PMM2 function in embryogenesis, postnatally PMM1 may be most important for brain and lung function.[7, 9] Unlike mammals, zebrafish Pmm1 transcripts were found throughout both embryonic and adult tissues, revealing a similar expression pattern to Pmm2. Additionally, morpholino-based reduction of *pmm2* expression resulted in earlier and increased transcription of *pmm1*when compared to controls. This data suggests that zebrafish Pmm1 may be compensating for loss of Pmm2 expression, possibly explaining the inability for PMM activity to be completely suppressed with the *pmm2* morpholino.

To ask whether Pmm1 has phosphomannomutase activity, we overexpressed *pmm1*mRNA in the PMM2-CDG zebrafish. Not only did PMM activity increase with

introduction of *pmm1*mRNA, but the phenotypes and altered biochemical profiles charactertistic of *pmm2*morphants were also rescued. Even though this indicates that Pmm1 may function in zebrafish protein glycosylation, Pmm1deficiency within a *pmm2*morphant background would have to be analyzed to fully understand Pmm1's role. The ideal model for this investigation is the zebrafish system, where utilization of morpholinos could be used to target *pmm1*and *pmm2*. This *pmm1*/*pmm2* double morphant might also elucidate why PMM activity levels could only be decreased to 34% of control activity in the *pmm2*morphants. If Pmm1 is compensating for loss of Pmm2 activity in the *pmm2*morphants, one would expect co-injection of *pmm1*and *pmm2*morpholinos would decrease PMM activity levels even further. This would allow us to further investigate PMM2-CDG by creating a more severe model. If PMM activity levels are further decreased in these double morphants, phenotypes and biochemical profiles might become more severe, providing a deeper understanding of phosphomannomutase's essential function in protein glycosylation.

In addition to PMM activity, PMM1 also has been characterized as an IMP sensitive glucose-1,6-bisphosphatase in the brain. [11] Although zebrafish Pmm1 was found to have phosphomannomutase activity, its function as a glucose-1,6-bisphosphatase in zebrafish remains to be investigated. To determine whether Pmm1 can function as a glucose-1,6-bisphosphatase, future investigations will involve analysis of potential glucose-1,6,-bisphosphatase activity and IMP sensitivity. Treatment of fish lysates with IMP would be predicted to inhibit Pmm1's phosphomannomutase activity and increase in its glucose-1,6-bisphosphatase activity.[11] If Pmm1 is found to have glucose-1,6-bisphosphatase activity, this could expand potential therapeutic approaches for PMM2-CDG patients that could be tested in the *pmm2*morphants.

This unique function of PMM1 could be utilized in deficient N-glycosylation pathways by providing an alternate route for the nucleotide sugar precursor Man-1-P. Although PMM1 has been shown to have glucose-1,6-bisphosphatase activity, it has also been reported to act on other hexose-1,6-bisphosphates as well.[5] With use of IMP to stimulate PMM1's hexose-1,6-bisphosphatase activity, mannose-1,6-bisphosphate could be degraded to Man-1-P. Furthermore, use of IMP would not affect residual PMM2 activity, as PMM2 was not found to react to IMP.[11] This reaction could bypass the defective isomerization step present in PMM2-CDG patients due to reduced PMM2 activity. If PMM2 activity was found to be severely decreased and thereby resulting in decreased Man-1-P levels for GDP-Man, this potential strategy could help store Man-1-P levels. On the other hand, the hexose-1,6-bisphosphatase activity of PMM1 could lead to more accumulation of Man-6-P and further exacerbate LLO hydrolysis. PMM1's phosphatase activity may lead to the generation of Man-6-P, not Man-1-P. This would contribute to the already increased Man-6-P pools, causes increased cleavage of the LLO and release of free glycans. Therefore, treatment with IMP in PMM2-CDG zebrafish could exacerbate *pmm2*morphant phenotypes and biochemical profiles. Nevertheless, whether zebrafish Pmm1 even functions as a phosphatase remains to be seen, and these prospects are potential future avenues of study.

The ability of Pmm1 to successfully correct *pmm2* morphant phenotypes and biochemical profiles offers hope in possibly treating PMM2-CDG patients. Although no activator of PMM1 has yet been reported, PMM1 may provide an additional candidate to screen for small molecule activators. The coupled enzyme assay for phosphomannomutase and phosphatase activity could be adapted for high through-put screening of compounds. If PMM1 can be found to compensate for loss of PMM2, then a potential activator could help correct deficient protein glycosylation,

regardless of the mutant form of PMM2. One disadvantage to this approach would be the restricted pattern of PMM1 found in humans. Since it is only found in the brain and lungs, activation of PMM1 would not ubiquitously correct the loss of PMM2. However, future investigations of transcriptional factors may provide insight into promoting expression of *PMM1* in tissues. The intricate relationship between PMM1 and PMM2 remains to explored, and further analysis of these homologous enzymes may provide a therapeutic approach for PMM2-CDG patients. Nonetheless, this model for PMM2-CDG is available and amenable to manipulating of metabolic flux to enable further investigations into this complex glycosylation pathway.

REFERENCES

1. Freeze, H.H., *Genetic defects in the human glycome.* Nat Rev Genet, 2006. **7**(7): p. 537-551.
2. Silvaggi, N.R., et al., *The X-ray crystal structures of human alpha-phosphomannomutase 1 reveal the structural basis of congenital disorder of glycosylation type 1a.* J Biol Chem, 2006. **281**(21): p. 14918-26.
3. Schollen, E., et al., *Comparative analysis of the phosphomannomutase genes PMM1, PMM2 and PMM2psi: the sequence variation in the processed pseudogene is a reflection of the mutations found in the functional gene.* Hum Mol Genet, 1998. **7**(2): p. 157-64.
4. Matthijs, G., et al., *Mutations in PMM2, a phosphomannomutase gene on chromosome 16p13, in carbohydrate-deficient glycoprotein type I syndrome (Jaeken syndrome).* Nat Genet, 1997. **16**(1): p. 88-92.
5. Pirard, M., et al., *Kinetic properties and tissular distribution of mammalian phosphomannomutase isozymes.* Biochem J, 1999. **339 (Pt 1)**: p. 201-7.
6. Pirard, M., et al., *Comparison of PMM1 with the phosphomannomutases expressed in rat liver and in human cells.* FEBS Lett, 1997. **411**(2–3): p. 251-254.
7. Matthijs, G., et al., *PMM (PMM1), the human homologue of SEC53 or yeast phosphomannomutase, is localized on chromosome 22q13.* Genomics, 1997. **40**(1): p. 41-7.
8. Martinsson, T., et al., *Linkage of a locus for carbohydrate-deficient glycoprotein syndrome type I (CDG1) to chromosome 16p, and linkage disequilibrium to microsatellite marker D16S406.* Hum Mol Genet, 1994. **3**(11): p. 2037-42.
9. Cromphout, K., et al., *The normal phenotype of Pmm1-deficient mice suggests that Pmm1 is not essential for normal mouse development.* Mol Cell Biol, 2006. **26**(15): p. 5621-35.
10. Heykants, L., et al., *Identification and localization of two mouse phosphomannomutase genes, Pmm1 and Pmm2.* Gene, 2001. **270**(1-2): p. 53-9.
11. Veiga-da-Cunha, M., et al., *Mammalian phosphomannomutase PMM1 is the brain IMP-sensitive glucose-1,6-bisphosphatase.* J Biol Chem, 2008. **283**(49): p. 33988-93.
12. Guha, S.K. and Z.B. Rose, *Brain glucose bisphosphatase requires inosine monophosphate.* J Biol Chem, 1982. **257**(12): p. 6634-7.
13. Guha, S.K. and Z.B. Rose, *Role of inosine 5'-phosphate in activating glucose-bisphosphatase.* Biochemistry, 1983. **22**(6): p. 1356-61.
14. Thiel, C., et al., *Targeted disruption of the mouse phosphomannomutase 2 gene causes early embryonic lethality.* Mol Cell Biol, 2006. **26**(15): p. 5615-20.
15. Cline, A., et al., *A Zebrafish Model Of PMM2-CDG Reveals Altered Neurogenesis And A Substrate-Accumulation Mechanism For N-Linked Glycosylation Deficiency.* Mol Biol Cell, 2012.
16. Kimmel, C.B., et al., *Stages of embryonic development of the zebrafish.* Dev Dyn, 1995. **203**(3): p. 253-310.
17. Van Schaftingen, E. and J. Jaeken, *Phosphomannomutase deficiency is a cause of carbohydrate-deficient glycoprotein syndrome type I.* FEBS Lett, 1995. **377**(3): p. 318-20.
18. Flanagan-Steet, H., C. Sias, and R. Steet, *Altered chondrocyte differentiation and extracellular matrix homeostasis in a zebrafish model for mucolipidosis II.* Am J Pathol, 2009. **175**(5): p. 2063-75.

19. Thisse, C. and B. Thisse, *High-resolution in situ hybridization to whole-mount zebrafish embryos.* Nat Protoc, 2008. **3**(1): p. 59-69.
20. Gao, N. and M.A. Lehrman, *Non-radioactive analysis of lipid-linked oligosaccharide compositions by fluorophore-assisted carbohydrate electrophoresis.* Methods Enzymol, 2006. **415**: p. 3-20.
21. Gao, N., et al., *Mannose-6-phosphate regulates destruction of lipid-linked oligosaccharides.* Mol Biol Cell, 2011. **22**(17): p. 2994-3009.
22. Chu, J., et al., *A zebrafish model of congenital disorders of glycosylation with phosphomannose isomerase deficiency reveals an early opportunity for corrective mannose supplementation.* Dis Model Mech, 2012.
23. Gao, N., J. Shang, and M.A. Lehrman, *Analysis of glycosylation in CDG-Ia fibroblasts by fluorophore-assisted carbohydrate electrophoresis: implications for extracellular glucose and intracellular mannose 6-phosphate.* J Biol Chem, 2005. **280**(18): p. 17901-9.
24. Lehrman, M.A., *Stimulation of N-linked glycosylation and lipid-linked oligosaccharide synthesis by stress responses in metazoan cells.* Crit Rev Biochem Mol Biol, 2006. **41**(2): p. 51-75.

FIGURES

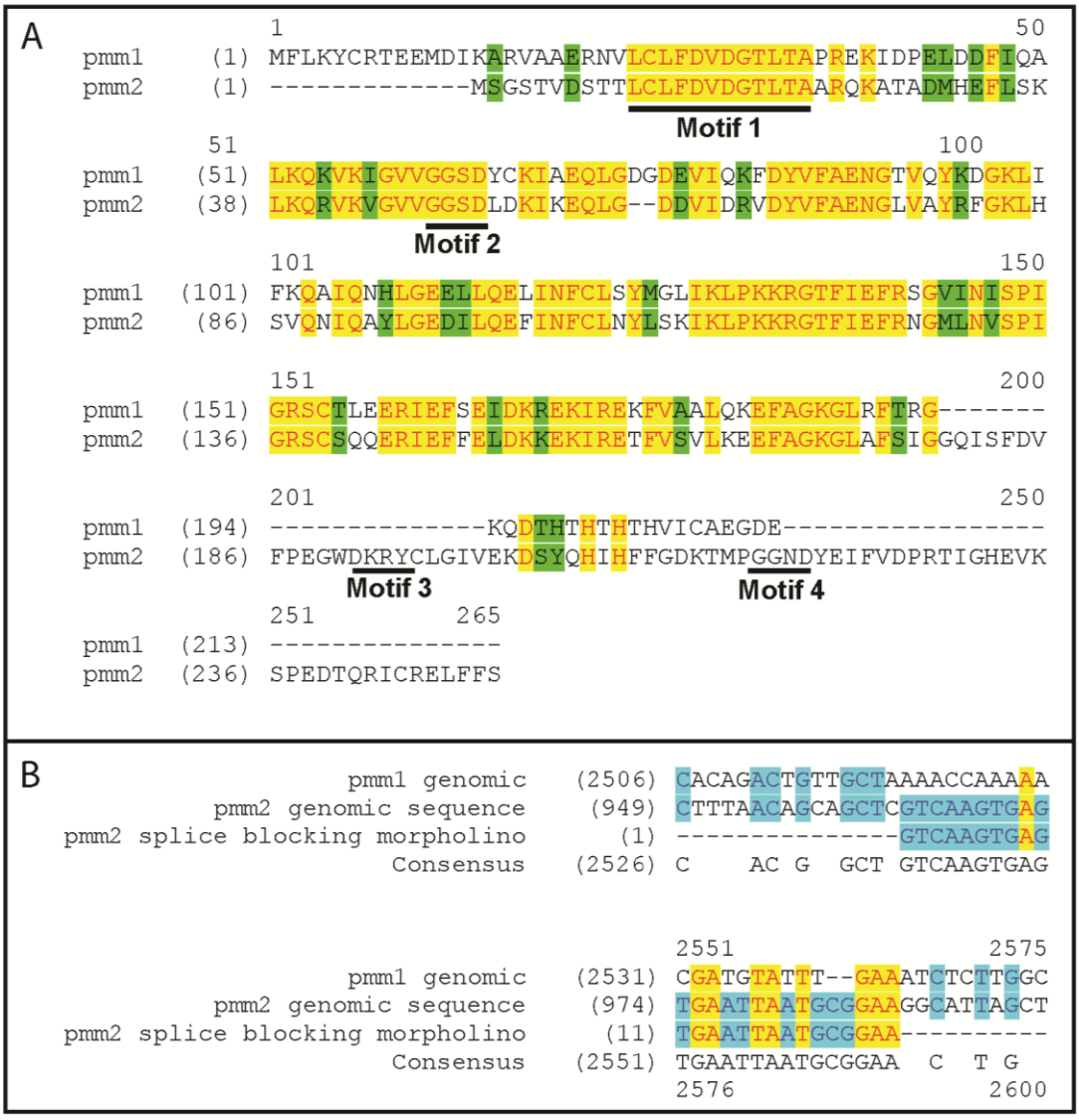
A
pmm1 (1) MFLKYCRTEEMDIKARVAAERNVLCLFDVDGTLTAPREKIDPELDDFIQA
pmm2 (1) ----------MSGSTVDSTTLCLFDVDGTLTAARQKATADMHEFLSK
Motif 1
pmm1 (51) LKQKVKIGVVGGSDYCKIAEQLGDGDEVIQKFDYVFAENGTVQYKDGKLI
pmm2 (38) LKQRVKVGVVGGSDLDKIKEQLG--DDVIDRVDYVFAENGLVAYRFGKLH
Motif 2
pmm1 (101) FKQAIQNHLGEELLQELINFCLSYMGLIKLPKKRGTFIEFRSGVINISPI
pmm2 (86) SVQNIQAYLGEDILQEFINFCLNYLSKIKLPKKRGTFIEFRNGMLNVSPI
pmm1 (151) GRSCTLEERIEFSEIDKREKIREKFVAALQKEFAGKGLRFTRG-------
pmm2 (136) GRSCSQQERIEFFELDKKEKIRETFVSVLKEEFAGKGLAFSIGGQISFDV
pmm1 (194) --------------KQDTHTHTHTHVICAEGDE-----------------
pmm2 (186) FPEGWDKRYCLGIVEKDSYQHIHFFGDKTMPGGNDYEIFVDPRTIGHEVK
Motif 3
Motif 4
pmm1 (213) ----------------
pmm2 (236) SPEDTQRICRELFFS
B
pmm1 genomic (2506) CACAGACTGTTGCTAAAACCAAAAA
pmm2 genomic sequence (949) CTTTAACAGCAGCTCGTCAAGTGAG
pmm2 splice blocking morpholino (1) ----------GTCAAGTGAG
Consensus (2526) C AC G GCT GTCAAGTGAG
pmm1 genomic (2531) CGATGTATTT--GAAATCTCTTGGC
pmm2 genomic sequence (974) TGAATTAATGCGGAAGGCATTAGCT
pmm2 splice blocking morpholino (11) TGAATTAATGCGGAA----------
Consensus (2551) TGAATTAATGCGGAA C T G

Figure 4.1 Sequence alignment of zebrafish PMM1 and PMM2. (**A**) Black bars denote the four motifs of PMM. Identical residues are boxed in yellow, and conservative changes are boxed in green. (**B**) Alignment of *pmm1*, *pmm2*, and *pmm2* splice blocking morpholino sequences demonstrate that the *pmm2* splice blocking morpholino will not bind to the *pmm1* sequence.

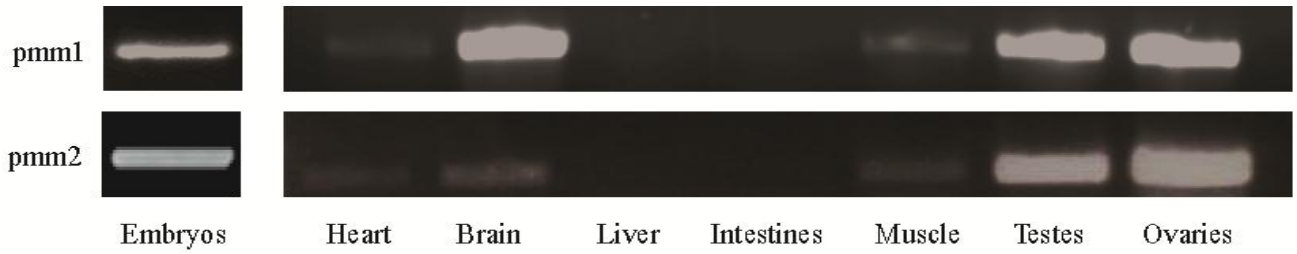

Figure 4.2 Transcripts of *pmm1*and *pmm2* in embryos and adult tissues reveal similar expression patterns. RT-PCR of *pmm1* and *pmm2* transcripts from 4dpf embryos and organs from adult zebrafish.

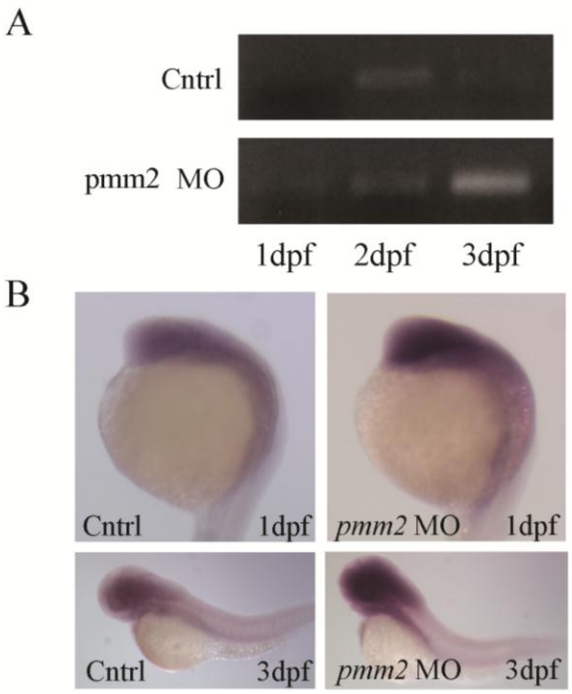

Figure 4.3 *pmm1* transcripts increase in response to *pmm2* knockdown.(**A**) RT-PCR of *pmm1* transcript levels in control and *pmm2* morphants over the timecourse 1-3dpf. (**B**) *In situ* analysis of *pmm1* expression in control and *pmm2* morphant (MO) embryos at 1 and 3dpf.

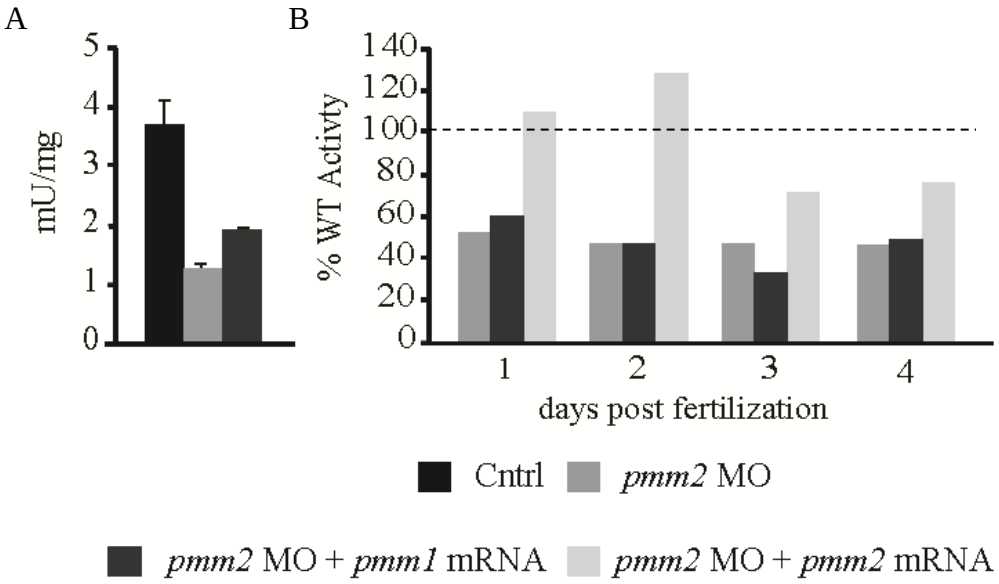

Figure 4.4 *pmm1*overexpression can restore PMM activity in *pmm2* knockdown morphants.(**A**) PMM enzyme activity levels of 3dpf Cntrl, *pmm2* MO, and *pmm2* MO injected with 300pg of *pmm1* mRNA. (**B**) PMM enzyme activity assay over a timecourse of 1-4dpf comparing *pmm2* MO, *pmm2* MO + *pmm2* mRNA, and *pmm2* MO + *pmm1* mRNA. Both mRNA concentrations was set at 200pg, a concentration previously established to restore PMM activity levels in *pmm2* MO. Activity is given as a percent of Cntrl Activity (dashed line).

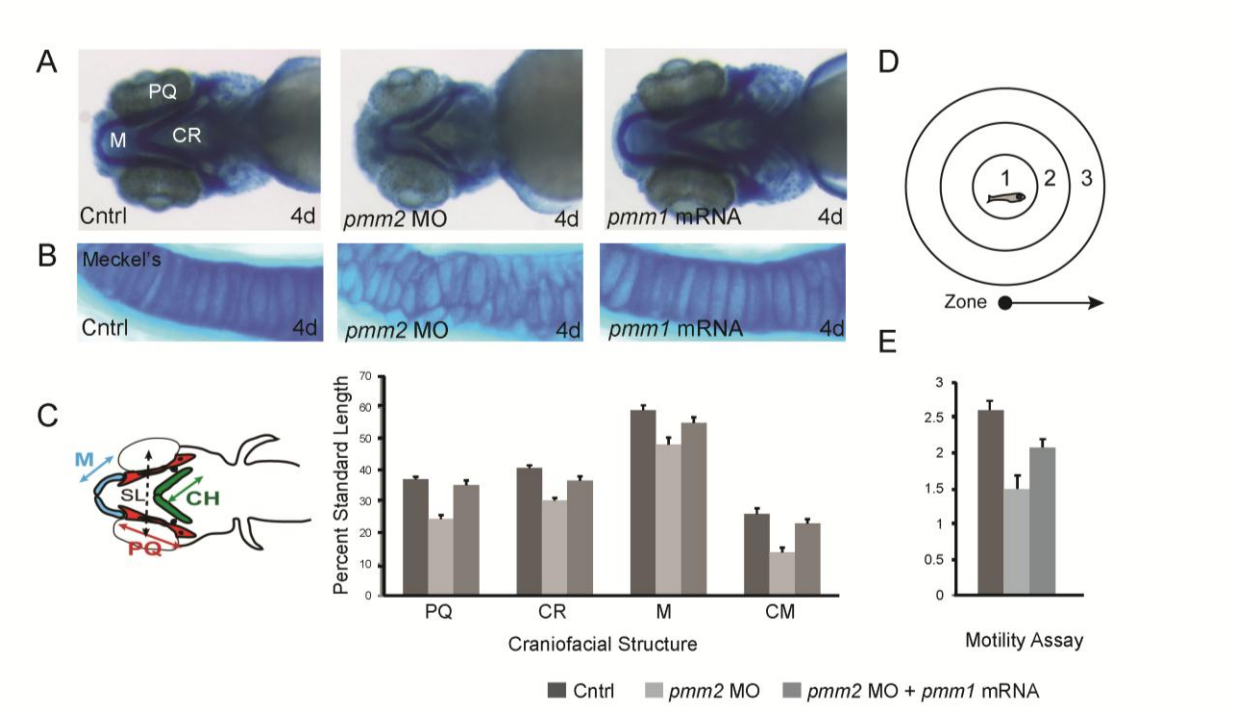

Figure 4.5 *pmm1* mRNA successfully rescues phenotypes seen in *pmm2* morphants. (**A**) Alcian blue stains of 4 dpf control and *pmm2* morphant (MO) embryos revealed altered size and shape of Meckel's cartilage (M), as well as the palatoquadrate (PQ) and certohyal (CH) cartilages. These defects were rescued by co-injection of *pmm1* mRNA. (**B**) 4 dpf WT, *pmm2* morphant (MO), and *pmm1* mRNA rescued embryos were dissected and the cartilages mounted flat. Analysis of these preparations showed morphant chondrocytes were more round and under intercalated compared to WT chondrocytes. This was rescued by co-injection of *pmm1* mRNA. (**C**) The length of individual structures was measured and normalized to a standard length (SL), which was set as the distance between the eyes. Individual cartilage measurements are outlined in the fish schematic. (**D**)) At 3 dpf the swimming behaviors and "escape" responses of control, morphant and *pmm1* mRNA rescued embryos were assessed by placing individual animals in the center of a petri dish marked with 3 concentric rings. Embryos were lightly touched on the head and their behavior and final destination (zone 1, 2 or 3) recorded. For each condition the average "final location" of 100 embryos from 3 experiments is graphed in (**E**).

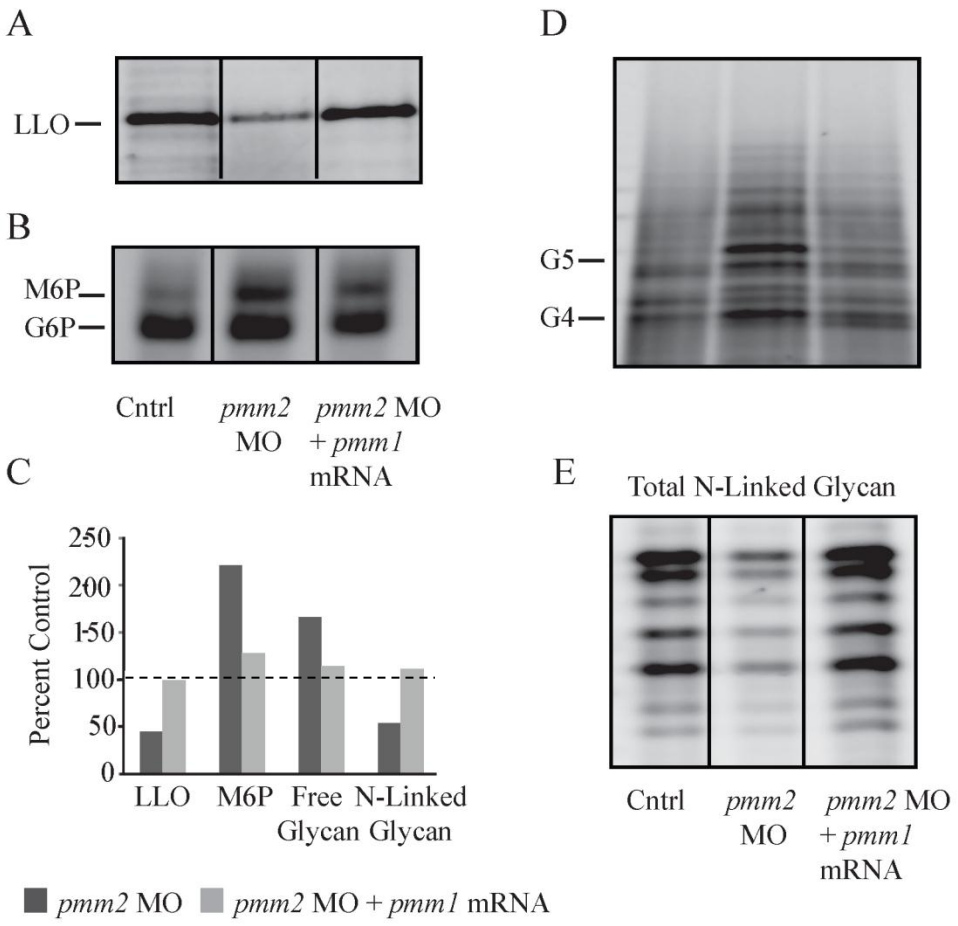

Figure 4.6 FACE analysis of *pmm1*overexpression in *pmm2*morphant background. LLO, M6P, Free Glycan, and Total N-Glycan were measured with FACE techniques from the same samples of zebrafish. Preparations of 200 4dpf embryos were used for each comparison. All measurements were normalized to total protein, which did not vary significantly among the different genetically modified groups of fish. **(A)** Representative FACE images showing LLO glycans (G3M9Gn2) from a single set of control fish, *pmm2* morphants, and *pmm2* morphants coinjected with *pmm1* mRNA. (**B**) Representative FACE gel for sugar phosphates, Man-6-P (M6P) and Glucose-6-P (G6P). (**C**) G3M9Gn2-LLO, M6P, Free Glycan, and total N-glycan measured from FACE analysis. Control levels were arbitrarily set as 100% (dashed line). (**D**) Representative FACE image showing total free glycans from control embryos, *pmm2* morphants, and *pmm1*mRNA *pmm2* morphants. Glucose oligomer standards (G4 – G5) are shown. (**E**) FACE gel showing total N-glycan pools after release from protein fraction from control, *pmm2*morphant, and *pmm2*morphants + *pmm1*mRNA samples.

CHAPTER 5: DISCUSSION AND FUTURE PERSPECTIVES

Hypoglycosylation of Glycoproteins in PMM2-CDG Patients

The Congenital Disorders of Glycosylation (CDGs) are recessive human genetic diseases diagnosed by underglycosylation of serum glycoproteins, and involve defective N-glycosylation due to altered N-glycan assembly, modification, or trafficking. PMM2-CDG would be expected to hinder formation of Man-1-P and GDP-Man, which contributes mannosyl resides to LLO. Therefore, loss of PMM2 activity was predicted to inhibit maturation of the oligosaccharide, resulting in an inadequate supply of mature LLO, accumulation of immature LLO, and subsequent hypoglycosylation of glycoproteins. It is believed that the hypoglycosylation of glycoproteins leads to phenotypes seen in PMM2-CDG patients. However, studies examining specific N-linked glycoproteins from cultured PMM2-CDG fibroblasts found no obvious glycosylation defects.[1, 2] The inconsistencies of *in vitro* analyses emphasized the need for a useful animal model to provide understanding of the systemic aberrations of PMM2-CDG. Thus, a zebrafish model for PMM2-CDG was generated and characterized to provide better understanding of defective glycosylation due to decreased PMM2 activity.

PMM2-CDG Zebrafish Display Decreased N-Glycan Levels

FACE analysis of N-glycan pools in protein fractions from entire zebrafish revealed that decreased Pmm2 activity reduced N-glycan pools to 54% of control. Though specific protein markers have not been fully elucidated, this finding confirms that decreased PMM2 activity

results in hypoglycosylation of glycoproteins. While our data shows clear changes in quantity of total N-glycan pools, it is unclear whether these changes occur in a tissue-specific manner. It is conceivable that certain tissues or cell types are more sensitive to hypoglycosylation than others.[2]

Future Perspectives- Candidates of Hypoglycosylated Glycoproteins in PMM2-CDG Zebrafish

To uncover which tissues in zebrafish and perhaps in patients are most affected by hypoglycosylation, we should further investigate phenotypes of the *pmm2* morphants. The motility defect observed in morphants may correspond to neurological disease seen in PMM2-CDG patients because of the important and dynamic role glycosylation in the nervous system. Identifying specific glycoproteins that are responsible for these neurological phenotypes may be difficult, but the specific attributes may highlight potential candidate genes. Examination of glycoproteins that play important roles in neurogenesis and/or neuronal function may give understanding into the cellular basis for the neurological defect associated with PMM2-CDG. Furthermore, identifying glycoproteins that exhibit hypoglycosylation will help further elucidate the role of glycosylation in the nervous system, and serve as markers for defective glycosylation.

Voltage-Gated Calcium Channels are Associated with Touch Responsiveness

One of the first phenotypes observed in the *pmm2* morphants was lack of touch responsiveness, which may implicate abnormalities in sensory neurons. Sensory neurons relay inputs to interneurons, which then activate motor neurons and induce muscle contractions resulting in locomotion. A recent study suggested that the voltage gated calcium channel 2.1b

(CaV2.1b) is necessary for touch-evoked activation of the locomotor network in zebrafish.[3] The role CaV2.1 within neurons is the conduction of calcium into presynaptic terminals, which is necessary for activity-dependent neurotransmitter release. Given the expression of CACNA1Ab by sensory neurons in zebrafish, researchers suggested that normal CaV2.1b channel activity is necessary for tactile stimuli to reach and activate neurons within the locomotor network.[3] Zebrafish CaV2.1b is heavily N-glycosylated with eight putative N-glycosylation sites. This candidate protein should be investigated to determine if it is abnormally glycosylated and whether it underlies the phenotype see in PMM2-CDG zebrafish. Abnormal glycosylation of CaV2.1b could lead to decreased protein levels, altered activity or resonance at the plasma membrane, possibly resulting in the lack of touch responsiveness observed in *pmm2* morphants.

Glycosylation of the β Subunit of Na^+/K^+-ATPase is Required for Proper Assembly

Another functionally important molecule at the synapse is the enzyme Na^+/K^+-ATPase. The regulatory β-subunits of this ion pump are integral cell surface glycoproteins that contain three N-glycan sites.[4] These subunits play an essential role in the structure and function of the α-subunit, as only assembled subunits in the ER are stably transported to the plasma membrane.[5] Deficient glycosylation of the β subunit leads to folding problems and decreased efficiency in the assembly with the α subunits.[6] Analysis of β subunits during development of the zebrafish central nervous system (CNS) has implicated β3 in the regionalization of the embryonic CNS and in the differentiation of specific neural cell types. The expression pattern of b*eta3* suggests a possible role in mediating cell-cell interactions, either by indirectly affecting intracellular ion concentrations or directly by mediating adhesion.[7] One future avenue of study should be to explore if this protein is hypoglycosylated and its potential role in differentiation of neural cells.

Cell Adhesion Molecules may serve as Hypoglycosylation Markers

Since most cell surface proteins are glycosylated, they are at risk of misfolding and degradation by ER-associated degradation in glycosylation deficient cells. Surface adhesion proteins are heavily N-glycosylated and may serve as important targets and markers for defective glycosylation. Recently, investigators reported intercellular cell adhesion molecule 1 (ICAM-1) was reduced in fibroblasts from 31 CDG patients when compared to normal controls. ICAM-1 is a transmembrane protein with nine occupied N-glycosylation sites. In PMM2-CDG patients' fibroblasts ICAM-1 was barely expressed compared to control cells, but was recovered with complementation of wild-type PMM2 cDNA.[8] Other cell adhesion molecules, L1 and NCAM, are critical for proper development of the CNS, and have been implicated in neurite outgrowth, migration, neuronal growth factor, and differentiation promoter.[9, 10] Human L1 has 21 potential N-linked glycan sites in its ectodomain, and these glycans have been shown to play a primary role in L1- and NCAM-mediated neural adhesion.[8] These cell adhesion molecules are prime candidates as markers for hypoglycosylation, and may play a potential role in the neuronal phenotype observed in the PMM2-CDG zebrafish.

Although the level of residual PMM2 enzyme activity has been correlated with the severity of clinical phenotypes, it is not well known whether the degree of N-glycosylation site occupancy correlates with the severity of the disease.[11] Symptomatically mild CDG cases show only a slight reduction in N-glycans, indicating a small threshold from healthy to pathological conditions.[12] Therefore, the identification of glycoproteins that are hypoglycosylated in CDG cases will help uncover potential mechanisms underlying patient phenotypes and serve as useful markers for defective glycosylation.

Free Oligosaccharides during Protein N-Glycosylation

N-glycans play important roles during the folding and cellular trafficking of glycoproteins. During N-glycosylation, significant amounts of free oligosaccharides are generated in the lumen of the ER.[13] Why free oligosaccharides are produced and how the ER avoids accumulation of these potentially disruptive structures in its lumen is unknown. Although free glycans have no known function in mammalian cells, cellular processes have been discovered that enables them to be catabolized in a specialized manner.

Free glycans are typically transported out of the ER to the cytosol[14]; however, if transport is inhibited or if free glycans remain glucosylated, some N-glycans can be secreted via the Golgi apparatus.[14, 15] Once in the cytosol, free glycans are trimmed to yield $Man_5GlcNAc$. This glycan is then transport into lysosomes by a transport apparatus that primarily recognizes the reducing end of GlcNAc moiety. This transporter shuttles the glycan to the lysosome so that further degradation by lysosomal mannosidases can occur.[16] The resulting mannose and GlcNAc are probably delivered to the cytosol by specific monosaccharide carriers and reincorporated into sugar-containing macromolecules.[17] Whether free oligosaccharides perform unknown function in the cytosol or nuclei of mammalian cells remains to be seen. Although changes in concentration of free glycans in the cytosol could provide information on the level of utilization of the cellular glycosylation pathway.

Free Glycans, the Products of LLO Hydrolysis, are Increased in *pmm2* Morphants

PMM2-CDG morphants displayed ~2 fold increase in free glycans resulting from hydrolysis of the LLO in response to Man-6-P accumulation. These free glycans showed no

qualitative differences in the glycoforms, suggesting that remodeling reactions within the secretory pathway were unaffected. Previous studies confirmed that free glycans were present in the lumenal compartments *in vitro*; however, distinguishing compartments would be difficult in the zebrafish system. [18] If free glycans were found in the cytosol in zebrafish, they may be the result of ER-associated degradation (ERAD) of glycoproteins that failed to fold properly. However, ERAD is not thought to contribute to the free oligosaccharide pool because *pmm2* morphants showed no global increase in markers for ER stress. ER stress may be tissue specific, and could require further analysis to determine which tissues are more sensitive to decreased Pmm2 activity. Nevertheless, free oligosaccharides in the *pmm2* morphants are best explained by increased LLO hydrolysis due to Man-6-P accumulation. The oligosaccharyl transferase (OST) is the likely candidate for the hydrolysis of the LLO because has been found to carry out both hydrolytic and transfer function. It was proposed that, in the absence of sufficient acceptor sequences, the OST can transfer its oligosaccharide onto a water molecule, resulting in the release of the free glycan into the lumen of the ER.[19] Presently it is not known what role these free oligosaccharides play in the ER or cytoplasm of *pmm2* morphant fish after they have been cleaved from their dolichol linkage.

Future Perspectives- Free Glycan Regulation in PMM2-CDG Zebrafish

To investigate the fate of the free glycans present in the *pmm2* morphant zebrafish, we should begin by tracing their possible pathways. The free oligosaccharides are not believed to stay in the lumen of the ER, where they would possible interfere with protein glycosylation and folding. If free glycans were retained in the ER lumen, one would expect ER stress to occur due to the large volume of free glycans found in the *pmm2* morphants. Since qPCR showed no

activation of ER stress components, we believe that the free glycans are exported out of the ER. After leaving the ER, there may be two potential outcomes for free oligosaccharides.

Lysosomal Degradation of Free Oligosaccharides

The first pathway, as mentioned before, is transport out of the ER into the cytosol. Once in the cytosol, removal of a GlcNAc residue and trimming of mannoses should yield $Man_5GlcNAc$, which would be then be transported to the lysosome. After import into the lysosome, lysosomal mannosidases would hydrolyze the free oligosaccharide to monosaccharides. To determine whether free glycans in the zebrafish are being shuttled into this pathway of lysosomal degradation, we could analyze lysosomal trafficking in *pmm2* morphants. It is possible that the large increase in free glycans of *pmm2* morphants could result in dysfunctional lysosomal degradation. Furthermore, hypoglycosylation of lysosomal enzymes could cause cellular misrouting, resulting in targeting of the lysosomal enzymes to the secretory pathway and deficient uptake in the lysosome. In fact, CDG Type I patients display elevated plasma levels of lysosomal enzymes and abnormal lysosomal lamellar inclusions in hepatocytes.[20, 21] Therefore, investigation of free oligosaccharides directed to the lysosomal pathway may give valuable insight into lysosomal function and free glycan regulation in PMM2-CDG zebrafish.

Free Oligosaccharides in the Secretory Pathway via the Golgi

A second possible pathway for the free oligosaccharides observed in *pmm2* morphants is targeting to the secretory pathway via the Golgi apparatus. Glucosylated free oligosaccharides cannot escape from the ER lumen as the transport machinery responsible for shuttling free

glycans into the cytosol does not display specificity for $Glc_3Man_9GlcNAc_2$. [14] ER glucosidase II is responsible for removing glucose residues on oligosaccharide chains to assist in folding of glycoproteins, but it has been shown that accumulation of $Man_{7-9}GlcNAc_2$ in the ER inhibits this glucosidase.[22] . If the non glucosylated free glycans inhibits glucosidase II, yielding glycosylated free glycans in the ER lumen, then these glycans will not be transported to the cytosol. Instead, these glucosylated glycans can be targeted to the Golgi, where they undergo further processing to acquire complex-type structures before secretion into the extracellular space.[15] After secretion, these unconjugated structures could interfere with aspects of glycoprotein function in the extracellular space.

Currently, the composition of free oligosaccharides in the *pmm2* morphants is unknown, though the free oligosaccharides are neutral. Previous work has shown that jack bean mannosidase only partially digested some free glycans, which were produced by LLO hydrolysis due to Man-6-P accumulation.[18] This suggests that some glycans may have glucose, though this assessment is indirect. For example, it is also possible that some free glycans have been modified in the Golgi and have acquired other neutral sugars, such as GlcNAc or galactose. For these reasons, we should consider investigating the presence of free oligosaccharides in the extracellular medium and the composition of the free oligosaccharides in *pmm2* morphants. These potential pathways of free glycans remain unclear, but future studies could provide understanding into the biological roles of free glycans in various cellular processes.

Future Development of Additional CDG Models

Although CDGs have been known for more than 25 years, the pathophysiology of the CDGs remains undetermined. While the genetic and clinical defects of hypoglycosylation that

accompany most CDGs are well characterized, the cellular and developmental changes associated with these diseases are poorly understood. Since most analyses of a patient's disorder is restricted to material such as sera, leukocytes, or fibroblasts, information about the pathology of the disease is limited. In order to gain a deeper understanding and to develop effective therapies for CDG patients, animal models provide opportunities to study the effects of hypoglycosylation in an entire organism. Though mouse models have been generated for PMM2-CDG and MPI-CDG, they have not shown success in mimicking patient phenotypes or glycosylation deficiencies.[23, 24] Zebrafish are a versatile and complementary vertebrate system to study disorders and to evaluate potential therapies because of their high genetic conservation with humans. The ability to carry out reverse genetics using morpholinos make this animal system very advantageous in modeling syndromes that require tunable gene knockdown. In light of these challenges to CDG research and the advantages of the zebrafish system, we generated and characterized zebrafish models for PMM2-CDG.

PMM2-CDG Zebrafish Successfully Mimicked Patient Phenotypes and Uncovered a Novel Pathway of LLO Degradation

A zebrafish model for PMM2-CDG generated via morpholino knockdown of *pmm2* displayed abnormal craniofacial and motility phenotypes representative of those found in CDG patients. Morphants also exhibited altered motor neurogenesis within the spinal cord, a unique finding that may explain neurological defects associated with PMM2-CDG. Most notably, the use of this model revealed a distinctive pathway for LLO degradation due to Man-6-P accumulation that previously had been described *in vitro.*[18] Altering Man-6-P flux into the glycosylation pathway by decreasing MPI activity not only supported the substrate accumulation

degradation mechanism, but also demonstrated that decreased substrates through the N-glycosylation pathway also result in reduced LLO pools.

PMM2-CDG patients display neither accumulating LLO intermediates nor incomplete oligosaccharides on glycoproteins. CDG investigators were once puzzled by these findings, but both can be explained by the Man-6-P accumulation mechanism for LLO hydrolysis. This mechanism may also explain how the phenotypes of PMM2-CDG and MPI-CDG patients differ even though both defects had been thought to affect nucleotide sugar synthesis. Furthermore, overexpression of PMM1 within the PMM2-CDG background revealed that PMM1 can successfully rescue phenotypes and deficient glycosylation profiles of *pmm2* morphants. The role of PMM1 in the glycosylation pathway remains to be clarified, but could prove a potential therapeutic target for PMM2-CDG patients. With a useful animal model for PMM2-CDG finally available, future studies can model other CDGs in zebrafish to further understand the pathophysiology of these complex disorders.

Future Perspectives- Future CDG Zebrafish Models for Potential Therapeutic Testing

Using morpholino-based approaches to decrease activity levels, zebrafish have proven to successfully model CDGs.[25, 26] These investigations have opened the door for future CDG models, and for evaluation of potential therapeutic compounds in the treatment of CDGs. To date, some 50 CDGs have been identified. Though progress has been made in identifying the disorders and diagnosing patients, there has been no progress in providing patients with potential therapies. By further modeling CDG types in zebrafish, we gain not only a unique understanding into the mechanisms of this complex glycosylation pathway, but also a worthwhile opportunity to potentially uncover much needed treatments. Many of these CDG subtypes hold promise for

modeling within the fish and for testing potential therapeutic approaches. Therefore, I believe future investigations should explore three CDG subtypes that are amenable to testing therapeutic agents.

Ketoconazole in Treatment of DPAGT1-CDG

DPAGT1-CDG is caused by a mutation in the gene encoding UDP-GlcNAc: Dolichol Phosphate GlcNAc transferase (DPAGT1), which catalyzes the first sugar transfer of the lipid carrier dolichol-phosphate to generate GlcNAc-PP-Dol.[27] Located in the cytoplasm, this enzyme catalyzes the first step in dolichol-linked oligosaccharide biosynthesis. The gene has shown to be essential by its high degree of sequence conservation among eukaryotes, and by the embryonic lethality of homozygous knock-out mice.[28] DPAGT1-CDG patients display phenotypes including severe hypotonia, seizures, developmental delay, and progressive micocephaly, as well as hypoglycosylation of serum transferrin.[29] Since the first step of oligosaccharide synthesis is compromised, DPAGT1-CDG zebrafish morphants would be predicted to show reduced LLO and N-glycan levels in addition to severe phenotypes. The appeal of modeling this rare CDG in the zebrafish would be the evaluation of ketoconazole to increase substrate flux through this transfer reaction.

Previous studies reported that ketoconazole counteracted effects of tunicamycin.[30] By targeting DPAGT1, tunicamycin inhibits N-glycosylation, thereby inducing ER stress.[31] Ketoconazole redirects farsenyl pyrophosphate, the precursor of dolichol, from the cholesterol biosynthetic pathway through inhibition of CYP51. By interrupting the flow of cholesterol precursors downstream of farnesyl pyrophosphate, ketoconazole redirects them to production of dolichol, and enables cells to overcome the effects of tunicamycin.[30] Ketoconazole treatment

would prove useful in *dpagt1* morphants by increasing dolichol substrates available for GlcNAc transfer. The redirection of substrate flow to dolichol synthesis has already proven successful *in vitro* with cells from another CDG subtype, DPM1-CDG.

Zaragozic Acid Successfully Corrects LLO Profiles of DPM1-CDG Fibroblasts

DPM1-CDG is due to mutations in the catalytic subunit (DPM1) of dolichol phosphate mannose synthase (DPM synthase). DPM synthesizes dolichol phosphomannose (DPM) from GDP-Man and Dol-P on the cytoplasmic face of the ER. DPM then translocates into the ER lumen, where it serves as the mannose donor for the growing oligosaccharide chain. Other glycosylation pathways, such as GPI anchor formation, O-mannosylation, and C-mannosylation, also utilize DPM as a mannose donor. Currently, DPM is on the only known mannose donor in the ER lumen, so reduced levels of DPM could potentially affect other glycosylation pathways as well. Therefore, testing potential therapies in DPM1-CDG morphants could hold promise in correcting other defective glycosylation pathways. One approach is lowering cholesterol synthesis to redirect the flow of polyisoprene precursors to dolichol synthesis through the use of zaragozic acid.

A recent study used DPM1-CDG patient fibroblasts to evaluate zaragozic acid as a potential therapy.[32] Zaragozic acid's inhibition of squalene synthase led to both decreased cholesterol synthesis and stimulation of diverging pathways that resulted in increased formation of dolichol, dolichol-phosphate, and DPM. This treatment decreased accumulation of incomplete LLO intermediates (Man5GlcNAc2-PP-Dol) and correction of LLO patterns. Use of zaragozic acid is similar to ketoconazole since both compounds direct substrates away from cholesterol and towards the dolichol biosynthesis pathway. Both of these potential therapeutic options suggest

that manipulation of dolichol synthesis represent a valid option in developing treatments for glycosylation deficiency. Furthermore, these treatment options in combination with metformin and mannose supplementation may increase substrates available for oligosaccharide synthesis to correct additional Type I CDGs.

Increased Mannose Uptake with Use of Metformin May Correct CDGs due to Defective Mannosyltransferase Activity

Full length LLO consists of nine mannose residues that are added in a stepwise manner by mannosyltransferases both on the cytosolic and lumenal side of the ER. Six mannosyltransferases are responsible for the transfer of mannose from donors to the growing oligosaccharide chain. Each of these mannosyltransferases (ALG1, ALG2, ALG11, ALG3, ALG9, and ALG12) has been associated with a CDG found in patients.[33-40] These CDGs often result in severe phenotypes with death in early infancy, accumulation of incomplete LLO intermediates, and hypoglycosylation of serum transferrin. FACE analysis of zebrafish models for these CDGs would be predicted to show increased levels of LLO intermediates, decreased levels of mature LLO, and decreased N-glycan levels of proteins. These expected glycosylation profiles of morphants would help evaluate potential therapeutic approaches to alleviate the accumulation of LLO intermediates and increased levels of mature LLO and N-glycans.

One such approach is to increased mannose donors available for transfer to the growing oligosaccharide chain. GDP-Man serves as the mannose donor in the cytoplasm for ALG1, ALG2, and ALG11. Increasing cellular mannose uptake may increase GDP-Man levels and result in proper glycosylation of the LLO precursor. In the cell, mannose either comes from extracellular sources or is converted from glucose; however, extracellular mannose has been

found to contribute significantly and preferentially to glycoprotein biosynthesis despite the higher concentration of glucose.[41] Though dietary mannose supplementation could prove beneficial, excess quantities of mannose can cause side effects such as bloating and kidney damage.[42] Thus, improving mannose uptake by cells in addition to mannose supplementation may be a more effective therapy.

Metformin is used to treat type II diabetes due to its ability to stimulate glucose transport activity in skeletal muscle and decrease gluconeogenesis.[43, 44] Previous studies have shown that use of metformin with mannose increased mannose uptake ~2 fold and corrected LLO synthesis and N-glycosylation in PMM2-CDG cells.[45] Therefore, metformin in addition with mannose supplementation may increase GDP-Man levels in order to provide more substrates to the growing oligosaccharyl chain on the cytoplasmic face of the ER. A combination of mannose, metformin, and zaragozic acid may prove advantageous in increasing Dol-P-Man levels, which serves as the mannose donor in the ER lumen. This approach may prove useful for treating CDGs in which ALG3, ALG9, or ALG12 are defective. Conversely, these potential therapeutic strategies may exacerbate deficient glycosylation profiles if precursor accumulation inhibits downstream reactions, just as Man-6-P accumulation resulted in LLO hydrolysis. Nevertheless, evaluating possible therapeutic strategies within CDG models will help in the understanding of these difficult diseases and the N-glycosylation pathway.

REFERENCES

1. Marquardt, T., et al., *Carbohydrate-deficient glycoprotein syndrome (CDGS)--glycosylation, folding and intracellular transport of newly synthesized glycoproteins.* Eur J Cell Biol, 1995. **66**(3): p. 268-73.
2. Dupré, T., et al., *Defect in N-glycosylation of proteins is tissue-dependent in Congenital Disorders of Glycosylation Ia.* Glycobiology, 2000. **10**(12): p. 1277-1281.
3. Low, S.E., et al., *Touch responsiveness in zebrafish requires voltage-gated calcium channel 2.1b.* J Neurophysiol, 2012. **108**(1): p. 148-59.
4. Gloor, S., et al., *The adhesion molecule on glia (AMOG) is a homologue of the beta subunit of the Na,K-ATPase.* J Cell Biol, 1990. **110**(1): p. 165-74.
5. Geering, K., *The functional role of the β-subunit in the maturation and intracellular transport of Na,K-ATPase.* FEBS Lett, 1991. **285**(2): p. 189-193.
6. Beggah, A.T., P. Jaunin, and K. Geering, *Role of Glycosylation and Disulfide Bond Formation in the β Subunit in the Folding and Functional Expression of Na,K-ATPase.* Journal of Biological Chemistry, 1997. **272**(15): p. 10318-10326.
7. Appel, C., et al., *Expression of a Na, K-ATPase beta3 subunit during development of the zebrafish central nervous system.* Journal of Neuroscience Research, 1996. **46**(5): p. 551-564.
8. HE, P., et al., *Identification of intercellular cell adhesion molecule 1 (ICAM-1) as a hypo-glycosylation marker in congenital disorders of glycosylation cells.* Journal of Biological Chemistry, 2012.
9. Hortsch, M., *The L1 Family of Neural Cell Adhesion Molecules: Old Proteins Performing New Tricks.* Neuron, 1996. **17**(4): p. 587-593.
10. Maness, P.F. and M. Schachner, *Neural recognition molecules of the immunoglobulin superfamily: signaling transducers of axon guidance and neuronal migration.* Nat Neurosci, 2007. **10**(1): p. 19-26.
11. Grunewald, S., et al., *High residual activity of PMM2 in patients' fibroblasts: possible pitfall in the diagnosis of CDG-Ia (phosphomannomutase deficiency).* Am J Hum Genet, 2001. **68**(2): p. 347-54.
12. Hulsmeier, A.J., P. Paesold-Burda, and T. Hennet, *N-glycosylation site occupancy in serum glycoproteins using multiple reaction monitoring liquid chromatography-mass spectrometry.* Mol Cell Proteomics, 2007. **6**(12): p. 2132-8.
13. Anumula, K.R. and R.G. Spiro, *Release of glucose-containing polymannose oligosaccharides during glycoprotein biosynthesis. Studies with thyroid microsomal enzymes and slices.* J Biol Chem, 1983. **258**(24): p. 15274-82.
14. Moore, S.E., C. Bauvy, and P. Codogno, *Endoplasmic reticulum-to-cytosol transport of free polymannose oligosaccharides in permeabilized HepG2 cells.* EMBO J, 1995. **14**(23): p. 6034-42.
15. Durrant, C. and S.E. Moore, *Perturbation of free oligosaccharide trafficking in endoplasmic reticulum glucosidase I-deficient and castanospermine-treated cells.* Biochem J, 2002. **365**(Pt 1): p. 239-47.
16. Moore, S.E. and R.G. Spiro, *Intracellular compartmentalization and degradation of free polymannose oligosaccharides released during glycoprotein biosynthesis.* J Biol Chem, 1994. **269**(17): p. 12715-21.
17. Mancini, G.M., C.E. Beerens, and F.W. Verheijen, *Glucose transport in lysosomal membrane vesicles. Kinetic demonstration of a carrier for neutral hexoses.* J Biol Chem, 1990. **265**(21): p. 12380-7.
18. Gao, N., et al., *Mannose-6-phosphate regulates destruction of lipid-linked oligosaccharides.* Mol Biol Cell, 2011. **22**(17): p. 2994-3009.

19. Spiro, M.J. and R.G. Spiro, *Potential regulation of N-glycosylation precursor through oligosaccharide-lipid hydrolase action and glucosyltransferase-glucosidase shuttle.* J Biol Chem, 1991. **266**(8): p. 5311-7.
20. Jaeken, J. and H. Carchon, *The carbohydrate-deficient glycoprotein syndromes: an overview.* J Inherit Metab Dis, 1993. **16**(5): p. 813-20.
21. Grunewald, S., R. De Vos, and J. Jaeken, *Abnormal lysosomal inclusions in liver hepatocytes but not in fibroblasts in congenital disorders of glycosylation (CDG).* J Inherit Metab Dis, 2003. **26**(1): p. 49-54.
22. Bosis, E., et al., *Endoplasmic reticulum glucosidase II is inhibited by its end products.* Biochemistry, 2008. **47**(41): p. 10970-80.
23. Schneider, A., et al., *Successful prenatal mannose treatment for congenital disorder of glycosylation-Ia in mice.* Nat Med, 2012. **18**(1): p. 71-73.
24. DeRossi, C., et al., *Ablation of mouse phosphomannose isomerase (Mpi) causes mannose 6-phosphate accumulation, toxicity, and embryonic lethality.* J Biol Chem, 2006. **281**(9): p. 5916-27.
25. Cline, A., et al., *A Zebrafish Model Of PMM2-CDG Reveals Altered Neurogenesis And A Substrate-Accumulation Mechanism For N-Linked Glycosylation Deficiency.* Mol Biol Cell, 2012.
26. Chu, J., et al., *A zebrafish model of congenital disorders of glycosylation with phosphomannose isomerase deficiency reveals an early opportunity for corrective mannose supplementation.* Dis Model Mech, 2012.
27. Wu, X., et al., *Deficiency of UDP-GlcNAc:Dolichol Phosphate N-Acetylglucosamine-1 Phosphate Transferase (DPAGT1) causes a novel congenital disorder of Glycosylation Type Ij.* Hum Mutat, 2003. **22**(2): p. 144-50.
28. Thiel, C. and C. Korner, *Mouse models for congenital disorders of glycosylation.* J Inherit Metab Dis, 2011. **34**(4): p. 879-89.
29. Wurde, A.E., et al., *Congenital disorder of glycosylation type Ij (CDG-Ij, DPAGT1-CDG): extending the clinical and molecular spectrum of a rare disease.* Mol Genet Metab, 2012. **105**(4): p. 634-41.
30. Harding, H.P., et al., *Bioactive small molecules reveal antagonism between the integrated stress response and sterol-regulated gene expression.* Cell Metab, 2005. **2**(6): p. 361-71.
31. Tsvetanova, B.C., D.J. Kiemle, and N.P.J. Price, *Biosynthesis of Tunicamycin and Metabolic Origin of the 11-Carbon Dialdose Sugar, Tunicamine.* Journal of Biological Chemistry, 2002. **277**(38): p. 35289-35296.
32. Haeuptle, M.A., et al., *Improvement of dolichol-linked oligosaccharide biosynthesis by the squalene synthase inhibitor zaragozic acid.* J Biol Chem, 2011. **286**(8): p. 6085-91.
33. Frank, C.G., et al., *Identification and functional analysis of a defect in the human ALG9 gene: definition of congenital disorder of glycosylation type IL.* Am J Hum Genet, 2004. **75**(1): p. 146-50.
34. Grubenmann, C.E., et al., *ALG12 mannosyltransferase defect in congenital disorder of glycosylation type lg.* Hum Mol Genet, 2002. **11**(19): p. 2331-9.
35. Morava, E., et al., *Defining the Phenotype in Congenital Disorder of Glycosylation Due to ALG1 Mutations.* Pediatrics, 2012. **130**(4): p. e1034-9.
36. Rimella-Le-Huu, A., et al., *Congenital disorder of glycosylation type Id (CDG Id): phenotypic, biochemical and molecular characterization of a new patient.* J Inherit Metab Dis, 2008. **31 Suppl 2**: p. S381-6.
37. Thiel, C., et al., *Improved diagnostics lead to identification of three new patients with congenital disorder of glycosylation-Ip.* Hum Mutat, 2012. **33**(3): p. 485-7.

38. Thiel, C., et al., *A new type of congenital disorders of glycosylation (CDG-Ii) provides new insights into the early steps of dolichol-linked oligosaccharide biosynthesis.* J Biol Chem, 2003. **278**(25): p. 22498-505.
39. Vleugels, W., et al., *Quality control of glycoproteins bearing truncated glycans in an ALG9-defective (CDG-IL) patient.* Glycobiology, 2009. **19**(8): p. 910-7.
40. Westphal, V., et al., *A frequent mild mutation in ALG6 may exacerbate the clinical severity of patients with congenital disorder of glycosylation Ia (CDG-Ia) caused by phosphomannomutase deficiency.* Hum Mol Genet, 2002. **11**(5): p. 599-604.
41. Alton, G., et al., *Direct utilization of mannose for mammalian glycoprotein biosynthesis.* Glycobiology, 1998. **8**(3): p. 285-295.
42. Harms, H.K., et al., *Oral mannose therapy persistently corrects the severe clinical symptoms and biochemical abnormalities of phosphomannose isomerase deficiency.* Acta Paediatr, 2002. **91**(10): p. 1065-72.
43. Mu, J., et al., *A Role for AMP-Activated Protein Kinase in Contraction- and Hypoxia-Regulated Glucose Transport in Skeletal Muscle.* Molecular Cell, 2001. **7**(5): p. 1085-1094.
44. Fryer, L.G., et al., *Activation of glucose transport by AMP-activated protein kinase via stimulation of nitric oxide synthase.* Diabetes, 2000. **49**(12): p. 1978-1985.
45. Shang, J. and M.A. Lehrman, *Metformin-stimulated mannose transport in dermal fibroblasts.* J Biol Chem, 2004. **279**(11): p. 9703-12.

APPENDIX: SUPPLEMENTARY FIGURES

	Total M6P Detected (nomoles)	Total M6P detected (pmoles/embryo)	% of control

Control	3.90 ± 0.20	19.5	100
pmm2 morphants	5.77 ± 0.24	28.0	148

Appendix Table 1. HPAEC analysis of M6P levels in control and *pmm2* morphant embryos. Extracts from 200 4 dpf control and morphant embryos were analyzed using a CarboPac PA20 column as described below. Values represent the average of three separate analyses (± standard deviation). The mannose-6 phosphate standard and the individual samples (control and *pmm2* morphants) were analyzed by HPAEC using a Dionex ICS3000 system equipped with a gradient pump, an electrochemical detector, and an autosampler. The standards and samples (10 µL/injection) were separated using a Dionex CarboPac PA20 (3 x 150 mm) analytical column with an amino trap. Two solvents (A, 100 mM NaOH and B, 1 M sodium acetate in 100 mM NaOH) were used. The elution was performed with a gradient of increasing mobile phase B. Instrument control and data acquisition were accomplished using Dionex Chromeleon software.

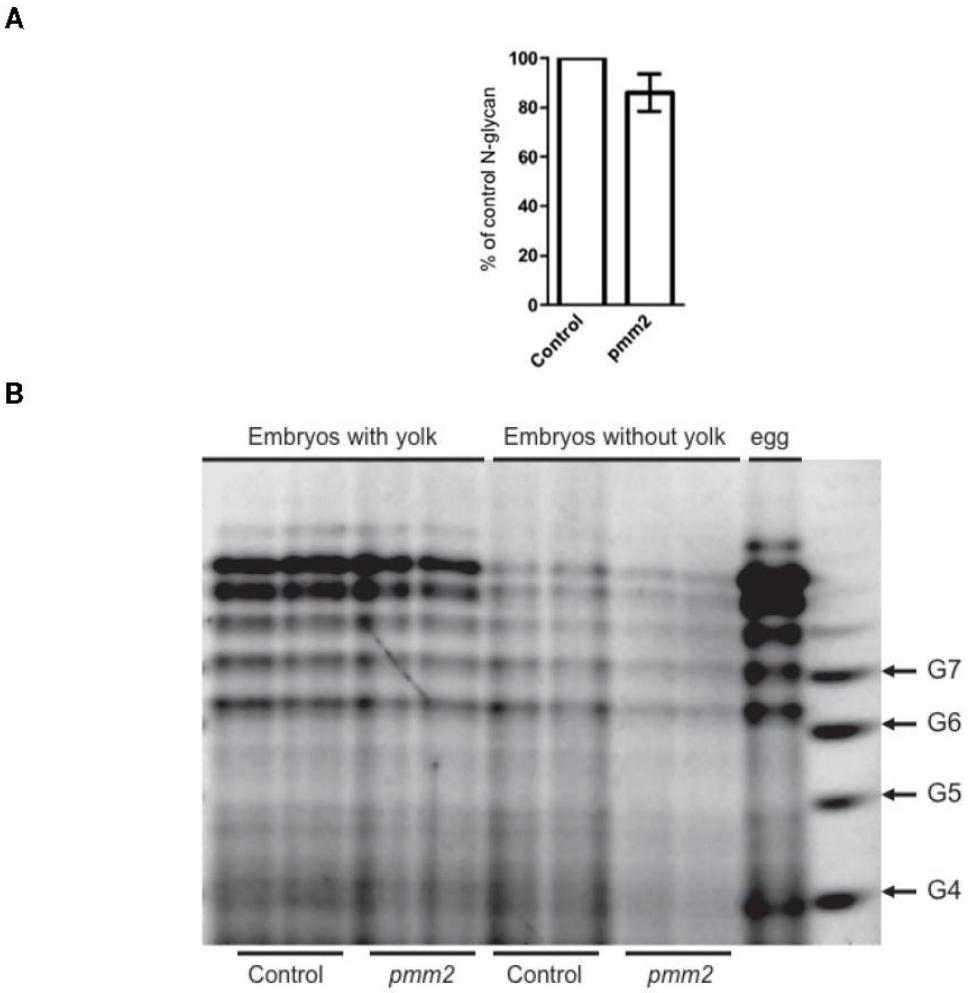

Appendix Figure 1. Quantitation and detection of total N-glycans in embryos with and without yolks. (A) Bar graph depicting the average percentage loss of total N-glycans in *pmm2* morphants (with yolks) in five separate experiments (mean ± S.E.M., $p = 0.068$, t-test). **(B)** FACE gel showing the contribution of the yolk to the total neutral N-glycan pool in 4 dpf embryos. A quantitative bar graph is presented in **Figure 3.1B**. Each lane was loaded with ten embryo or egg equivalents of protein. Total protein in the embryos without yolks was roughly 70% of that found in the embryos with yolks, reflecting the sizable protein contents in the yolk of a 4 dpf zebrafish embryo as well as eggs. Total protein recovered was essentially identical in control and *pmm2* morphant embryos regardless of the absence or presence of yolk. Quantitation of the FACE gel showed that removal of yolk decreased the recovery of Nglycans in control samples by 51%. Thus, the yolk-derived N-linked glycoproteins had a substantial masking effect on the loss of N-glycans in the *pmm2* morphants.

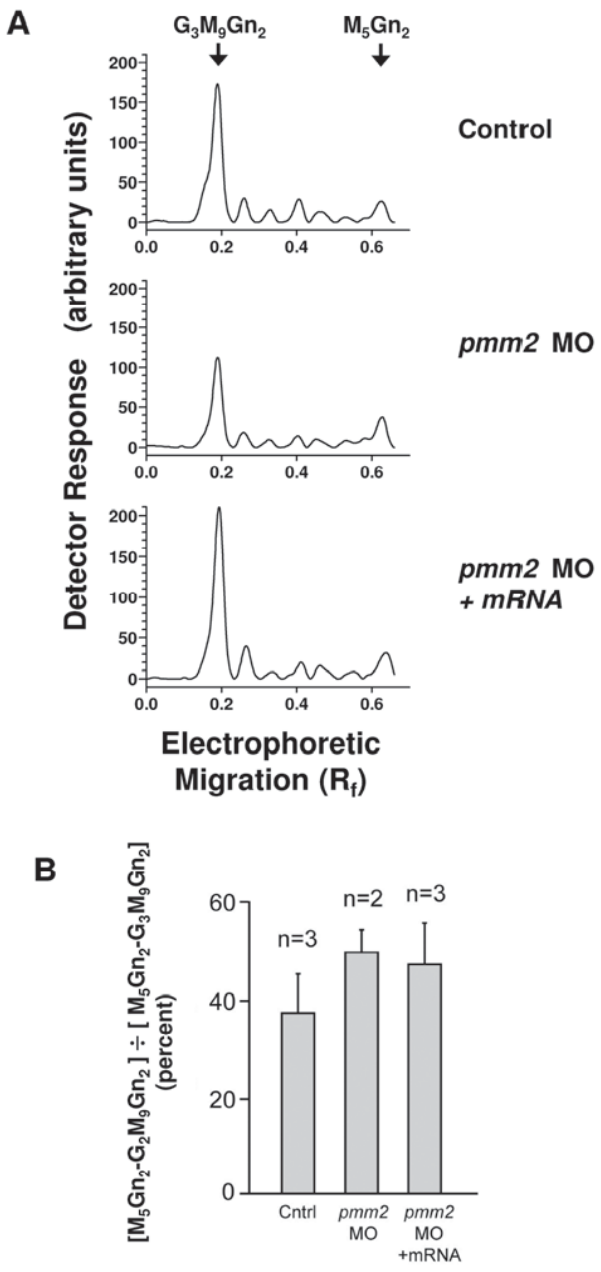

Appendix Figure 2. Detected and quantitation of the M_5Gn_2-$G_2M_9Gn_2$LLO intermediate pool. (A) Line traces of the LLO FACE gels shown in Figure 5C for control, *pmm2* morphants, and *pmm2* morphants rescued with mRNA. **(B)** The percentage of the M_5Gn_2 - $G_2M_9Gn_2$ LLO intermediate pool relative to the full M_5Gn_2 – $G_3M_9Gn_2$ LLO pool (including mature $G_3M_9Gn_2$-LLO) was averaged over 2-3 different experiments, under the same conditions listed for panel A.

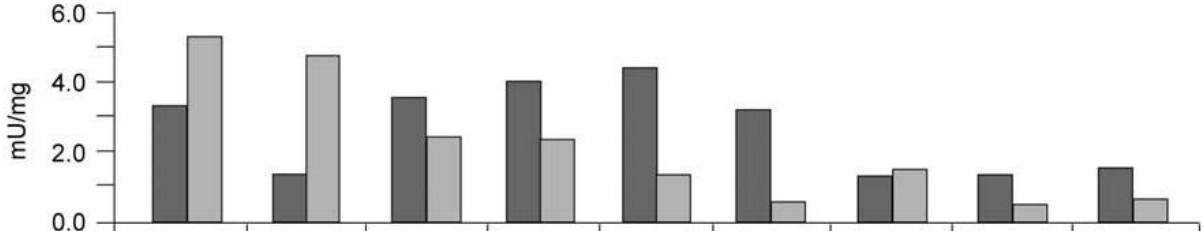

	Cntrl	*pmm2*	*mpi* (.02μM)	*mpi* (.05μM)	*mpi* (.10μM)	*mpi* (.18μM)	*pmm2/mpi* (.02μM)	*pmm2/mpi* (.05μM)	*pmm2/mpi* (.10μM)
Pmm2	3.36	1.20	3.53	4.03	4.38	3.23	1.25	1.30	1.49
Mpi	5.31	4.72	2.38	2.25	1.26	0.48	1.39	0.39	0.52

Appendix Figure 3. Optimization of *mpi* morpholinos. A range of *mpi* morpholino concentrations were injected into control and pmm2 morphant backgrounds, and activities of both Pmm2 and Mpi were measured in embryo lysates as described in Materials and Methods.